5. SITE 538[1]

Shipboard Scientific Party[2]

SITE 538 (HOLE 538)

Date occupied: 0302 hr., 14 January 1981

Date departed: 1806 hr., 14 January 1981

Time on hole: 15.7 hr.

Position: 23°50.98′N; 85°10.26′W

Water depth (sea level; corrected m, echo-sounding): 2820

Water depth (rig floor; corrected m, echo-sounding): 2830

Bottom felt (m, drill pipe): 2882.5

Penetration (m): 6.0

Number of cores: 1

Total length of cored section (m): 6.0

Total core recovered (m): 5.15

Core recovery (%): 86

Oldest sediment cored:
Depth sub-bottom (m): 5.15
Nature: Nannofossil ooze
Age: late Oligocene
Measured velocity (km/s): 1.56

Basement: Not penetrated

Principal results: See Summary section.

SITE 538 (HOLE 538A)

Date occupied: 1806 hr., 14 January 1981

Date departed: 2112 hr., 14 January 1981

Time on hole: 3 days, 3.1 hr.

Position: 23°50.95′N; 85°09.93′W

Water depth (sea level; corrected m, echo-sounding): 2742

Water depth (rig floor; corrected m, echo-sounding): 2752

Bottom felt (m, drill pipe): 2801.0

Penetration (m): 332.5

Number of cores: 36

Total length of cored section (m): 332.5

Total core recovered (m): 137.67

Core recovery (%): 41

Oldest sediment cored:
Depth sub-bottom (m): 268.5
Nature: Limestone
Age: Early Cretaceous (Berriasian-Valanginian)
Measured velocity (km/s): 3.69

Basement:
Depth sub-bottom (m): 268.5–332.5
Nature: Igneous and metamorphic complex
Velocity range (km/s): 5.09
Age: Early Jurassic (~190 Ma): diabase dikes
latest Cambrian (~500 Ma): metamorphic rocks

Principal results: See Summary section.

SUMMARY

Site 538 was the third of three short holes designed to drill through a thin sedimentary section into a high-standing basement block to test the nature, age, and origin of the crust. The site is located on the top of Catoche Knoll, which lies about 25 km northeast of the Campeche Escarpment (Fig. 1). The knoll is a large topographic feature that rises over 750 m above the abyssal floor of the Gulf of Mexico (Fig. 1). Prior to drilling, this knoll was interpreted to be a large, tilted fault block. Two holes were drilled. The first hole was abandoned after only one core was taken because the sediments were too firm to spud safely. The second hole (538A) drilled through a Tertiary and uppermost Cretaceous pelagic cap and a shallow-water Cretaceous limestone sequence; it reached and penetrated 64 m of igneous-metamorphic basement. The results of 538A are summarized in Figure 2 and are discussed below.

Three major lithologic sequences were drilled as follows.

1. foraminiferal-nannofossil ooze, chalk, and limestone (0–211.5 m), late Pliocene to late Albian
2. limestone (211.5–268.5 m), Valanginian
3. gneiss and amphibolite (268.5–332.5 m) with a latest Cambrian metamorphic age (~500 Ma) intruded by diabase dikes of Early Jurassic age (~190 Ma) (Dallmeyer, this volume)

The Upper Cretaceous–Tertiary pelagic sequence consists predominantly of nannofossil-foraminiferal ooze and chalk with scattered graded ash layers. Deposition was interrupted by long periods of erosion and/or nondeposition as indicated by stratigraphic hiatuses and hardgrounds. No clear evidence for turbidites was found. However, within this pelagic sequence an interval of folded Paleocene chalk several meters thick, which oc-

[1] Buffler, R. T., Schlager, W., et al., *Init. Repts. DSDP*, 77: Washington (U.S. Govt. Printing Office).

[2] Richard T. Buffler (Co-Chief Scientist), Institute for Geophysics (formerly Marine Science Institute), The University of Texas at Austin, Austin, Texas; Wolfgang Schlager (Co-Chief Scientist), School of Marine and Atmospheric Science, University of Miami, Miami, Florida (present address: University of Miami, 4600 Rickenbacker Causeway, Miami, Florida 33149); Jay L. Bowdler, Union Oil Company of California, Houston, Texas; Pierre H. Cotillon, Département de Géologie, Université Claude Bernard, 69622 Villeurbanne Cedex, France; Robert B. Halley, Branch of Oil and Gas Resources, U.S. Geological Survey, Denver, Colorado; Hajimu Kinoshita, Department of Geophysics, Chiba University, Chiba 260, Japan; Leslie B. Magoon III, U.S. Geological Survey, Menlo Park, California (present address: U.S. Geological Survey, 3475 Deer Creek Road, Palo Alto, California 94304); Charles L. McNulty, Department of Geology, University of Texas at Arlington, Arlington, Texas; James W. Patton, Marathon Oil Company, Littleton, Colorado; Kenneth A. Pisciotto, Scripps Institution of Oceanography, University of California at San Diego, La Jolla, California (present address: Sohio Petroleum, 50 Fremont Street, San Francisco, California 94105); Isabella Premoli Silva, Istituto di Paleontologia, Università di Milano, Milano, Italy; Otmara Avello Suarez, Oceanological Institute, Havana, Cuba; Margaret M. Testarmata, Institute for Geophysics (formerly Marine Science Institute), The University of Texas at Austin, Austin, Texas; Richard V. Tyson, School of Environmental Sciences, University of East Anglia, Norwich NR4 7TJ, United Kingdom; David K. Watkins, Department of Geology, Florida State University, Tallahassee, Florida.

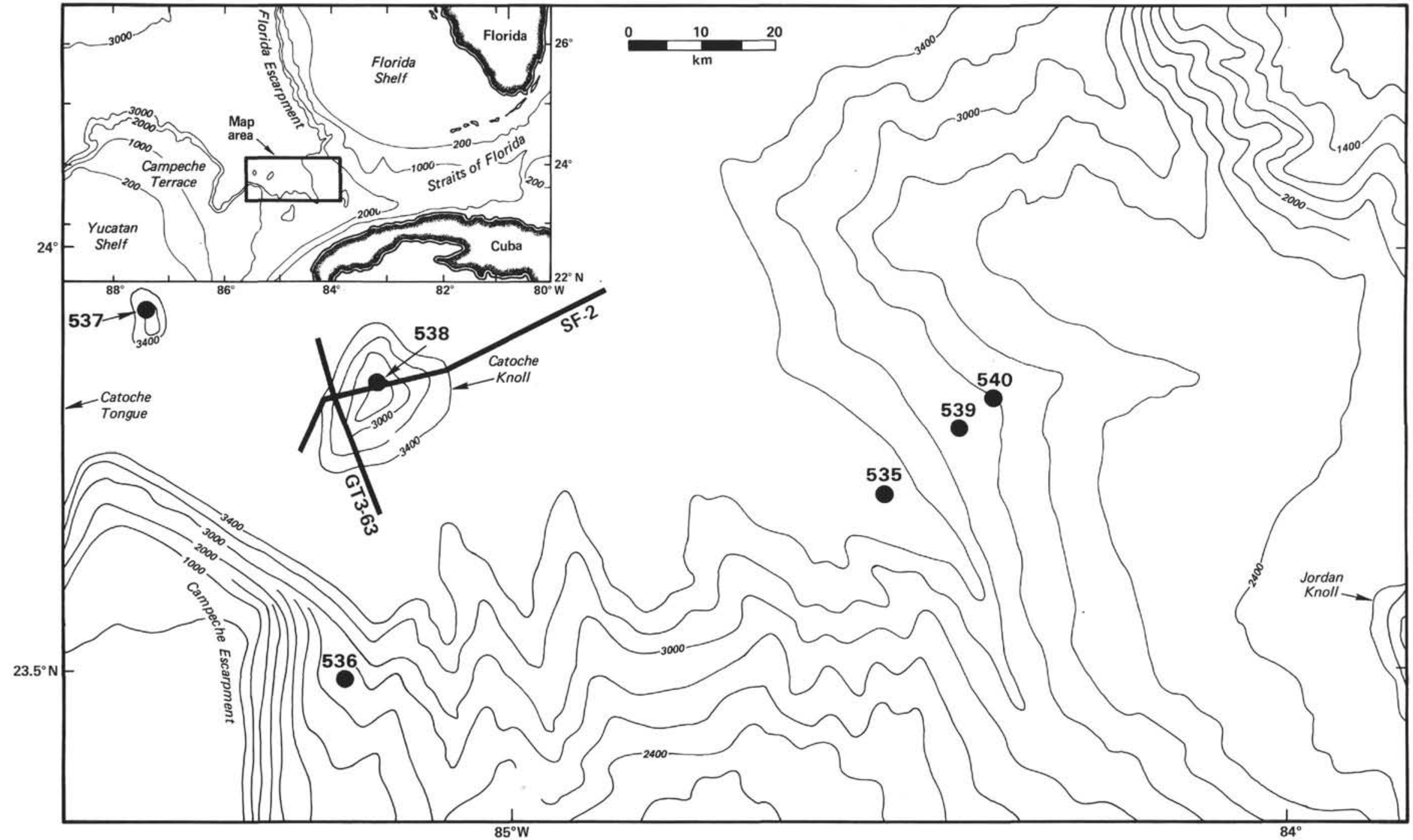

Figure 1. Location map of Leg 77 sites in the western Straits of Florida. Site 538 occurs near the crest of Catoche Knoll.

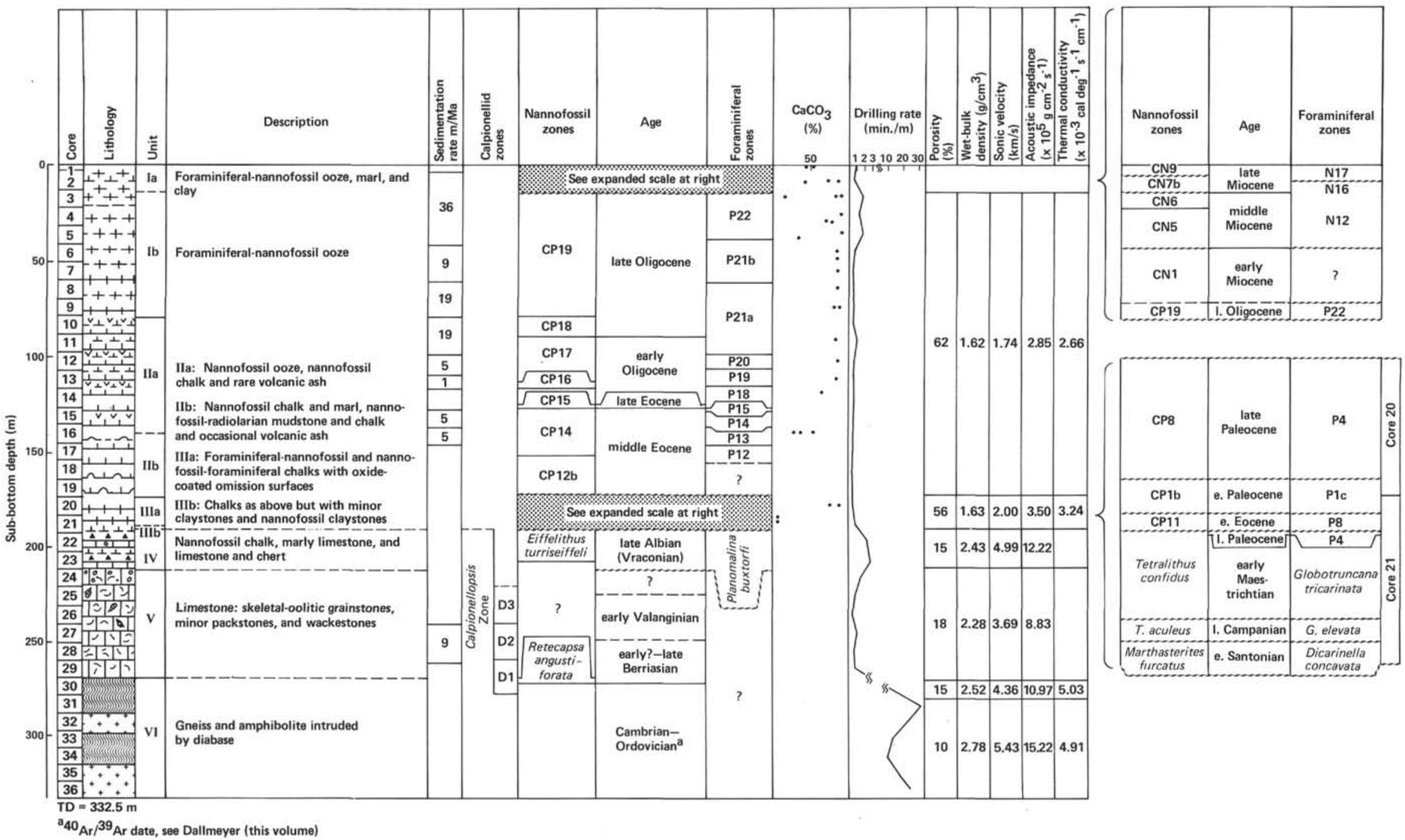

Figure 2. Stratigraphic summary of Hole 538A. See Introduction and Explanatory Notes chapter (this volume) for lithologic symbols. TD = total depth.

curs between Eocene sediments, indicates slumping. Slump folds also occur in the Eocene beds. The knoll must have formed a high hundreds of meters above the abyssal plain throughout the Late Cretaceous and Cenozoic.

Late Cretaceous deposits consist of only a few meters of Santonian, Campanian, and Maestrichtian ooze/ chalk with several hardgrounds and ash layers.

Valanginian limestones that occur below the pelagic sequence resemble those at Site 537. Again, we observed no top or bottom contacts and recovered only 2.7% of the formation in form of isolated fragments. These limestones could be interpreted as *in situ* platform deposits or as platform talus. A thin veneer of Berriasian pelagic chalk occurs on the top of basement. If one assumes that the limestones are *in situ*, this pelagic layer requires either (1) that basement subsided below the photic zone and was later uplifted into this photic zone or (2) that sea level dropped far enough to shift the site into the photic zone.

Basement at Site 538 consists of 64 m of igneous and metamorphic rocks: Cambrian or older gneiss and amphibolite intruded during the Early Jurassic by diabase dikes that are fractured and partly serpentinized. The basement complex as a whole may serve as an example of "transitional" (i.e., attenuated and intruded) continental crust. Crust of this kind, with intermediate density and abnormal velocity, has been postulated for the margins of the Gulf of Mexico.

BACKGROUND AND OBJECTIVES

Site 538 (designated ENA-14A during the planning stages of this cruise) was one of several sites designed to test basement in the southeastern Gulf of Mexico in an area where inferred basement blocks occur near the seafloor and are overlain by only a relatively thin (200–300 m) sedimentary cover. This area occurs along the western part of the deep southeastern Gulf just northeast of the Campeche Escarpment in the vicinity of Catoche Knoll (Fig. 1). A more general discussion of the background and objectives of the basement sites is contained in the Introduction and Explanatory Notes chapter (this volume) and the site chapter, Site 537 (this volume).

Site 538 was drilled on the top of Catoche Knoll, located approximately 25 km northeast of the Campeche Escarpment (Fig. 1). The knoll is a large topographic feature that stands more than 750 m above the surrounding abyssal plain. The site was originally proposed as an alternate to Sites 536 and 537, but it was decided to drill here because the first two basement sites yielded considerably different sections and did not take as long to drill as anticipated.

The site was chosen based on earlier single-channel seismic lines in the area (Bryant et al., 1969) plus more recent University of Texas multichannel lines. The formal site was located where Line SF-2 crosses the crest of the knoll (Fig. 3). The seismic data suggested that the knoll was an uplifted and tilted basement block based on the apparent asymmetry of the blocks and the adjacent sedimentary basins (Fig. 3). The strong reflector at about 4 s was inferred to be basement. Overlying basement is a thin sedimentary section some hundred meters thick that can be subdivided into two sequences separated by a prominent reflector/unconformity. The section above the unconformity was interpreted to be a thin cap of mainly Tertiary pelagic sediments and sedimentary rocks based on previous drilling in the area (Site 96; Worzel, Bryant, et al., 1973). The sequence below the unconformity was thought to consist of older Mesozoic rocks. Although the main objective of this site was to determine the nature, age, and origin of the inferred basement, data about the overlying sedimentary sequences would also provide valuable insights into the tectonic and sedimentary history of this region.

OPERATIONS

Glomar Challenger approached Site 538 (ENA-14A) on a course of about 110°, representing the shortest distance from Site 537. The 3.5-kHz and 12-kHz profilers, air guns, and magnetometer were run underway. The crest of Catoche Knoll was crossed twice and the beacon finally dropped on the northwest flank in 2882.5 m (or 2830 by the precision depth recorder) of water. This position was considered more advantageous than the higher flat top of the knoll because the cover of Tertiary sediments overlying the target reflectors was thinner. Irregular topography made it difficult to precisely determine water depth. The bottom-hole assembly was made up with a F94CK bit and the hole was spudded at 1725 hr. Because the water depth was 53 m deeper than indicated by the precision depth recorder, six water cores were taken before the mudline core was on deck. The core consisted of stiff Tertiary ooze and chalk that could not be drilled without rotating. It was decided that the sediments were too firm to spud in safely. Hole 538 was considered abandoned when the bit cleared the mudline at 1806 hr. Pipe was pulled to 2384 m, and the ship was repositioned over the flat top of a northwest-trending ridge, exactly on Line SF-2. At 0246 hr., 15 January, Hole 538A was spudded in 2801 m of water. Drilling rates were very fast in Tertiary ooze and chalk (22 cores in 21 hr.). At 211.5 m, the bit hit rubbly limestone similar to that encountered previously at Sites 536 and 537. Because this formation tended to cave in, the hole was flushed regularly with guar. Hard basement was encountered at 268.5 m. Because badly fractured formations were plugging the bit and drilling rates were reduced to 225 minutes per core, the hole was abandoned on 17 January at total depth of 332.5 m with 64 m penetration into basement. The bit was unplugged at 1407 hr.; at 2045 hr. pipe was on deck and the ship headed for Site 539. A summary of the coring at Site 538 is included as Table 1.

SEDIMENTOLOGY

The sedimentary sequence at Site 538 is divided into five units summarized in Figure 2 and Table 2 and described below.

Unit I: 0–79.1 m; 538A-1 to 538A-10-1, 60 cm; late Pliocene to late Oligocene

This unit consists predominantly of light-colored foraminiferal-nannofossil and nannofossil-foraminiferal oozes with subordinate amounts of nannofossil ooze,

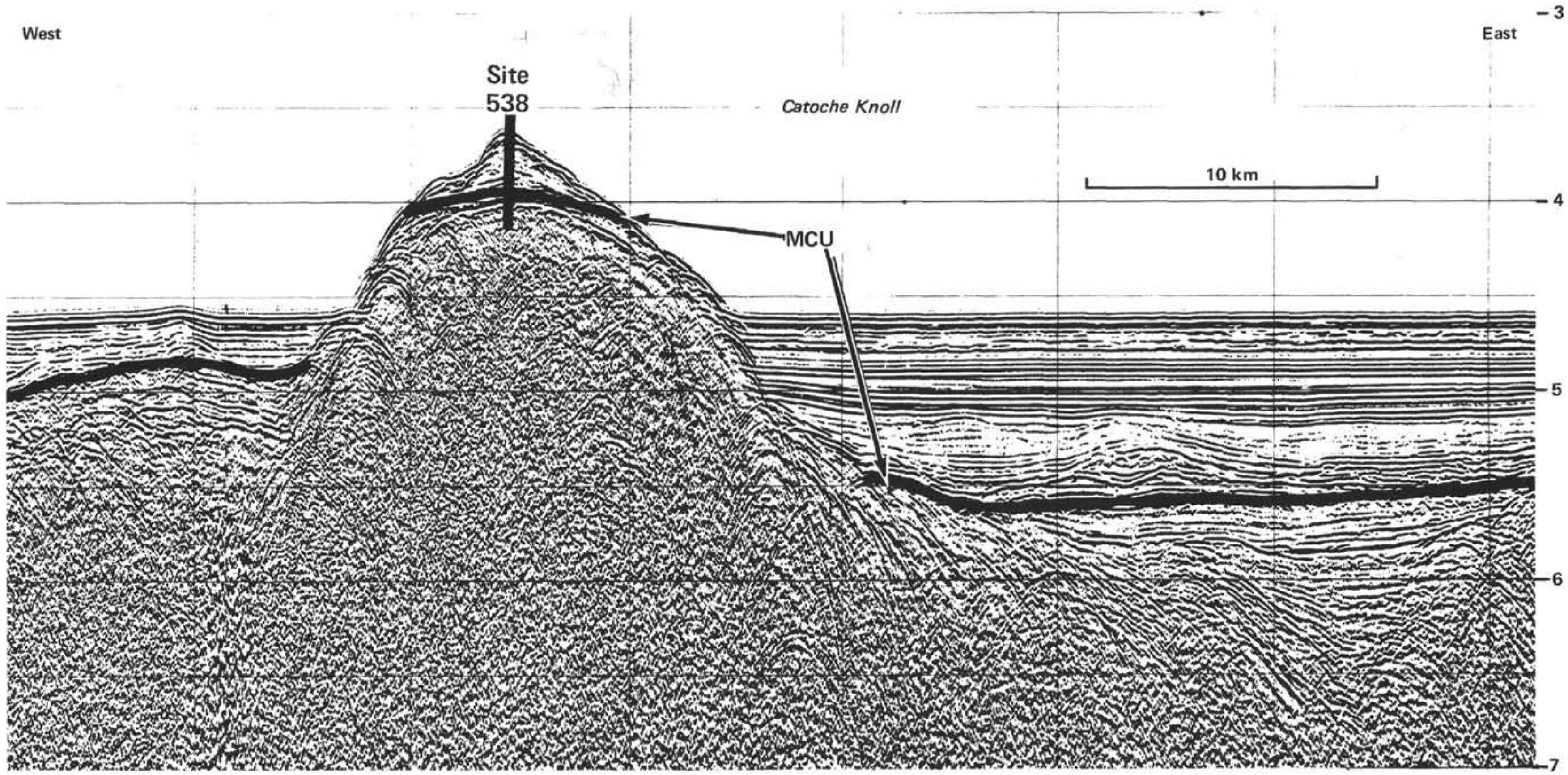

Figure 3. East-west seismic Line SF-2 over Catoche Knoll showing location of Site 538 with thin sedimentary cap over acoustic basement at 4 s. See Figure 1 for location of line. MCU = mid-Cretaceous unconformity.

Table 1. Coring summary, Site 538.

Core	Date (Jan. 1981)	Time	Depth from drill floor (m)	Depth below seafloor (m)	Length cored (m)	Length recovered (m)	Percent recovery
Hole 538							
1	14	1725	2882.5–2888.5	0.0–6.0	6.0	5.15	86
					6.0	5.15	86
Hole 538A							
1	15	0327	2801.0–2803.5	0.0–2.5	2.5	2.41	96
2	15	0422	2803.5–2813.0	2.5–12.0	9.5	3.58	38
3	15	0530	2813.0–2822.5	12.0–21.5	9.5	2.72	29
4	15	0629	2822.5–2832.0	21.5–31.0	9.5	4.97	52
5	15	0727	2832.0–2841.5	31.0–40.5	9.5	2.65	28
6	15	0827	2841.5–2851.0	40.5–50.0	9.5	4.52	48
7	15	0915	2851.0–2860.5	50.0–59.5	9.5	5.73	60
8	15	1013	2860.5–2870.0	59.5–69.0	9.5	3.71	39
9	15	1059	2870.0–2879.5	69.0–78.5	9.5	5.85	62
10	15	1155	2879.5–2889.0	78.5–88.0	9.5	7.14	75
11	15	1248	2889.0–2898.5	88.0–97.5	9.5	2.92	31
12	15	1350	2898.5–2908.0	97.5–107.0	9.5	6.51	69
13	15	1439	2908.0–2917.5	107.0–116.5	9.5	3.95	42
14	15	1544	2917.5–2927.0	116.5–126.0	9.5	1.32	14
15	15	1634	2927.0–2936.5	126.0–135.5	9.5	0.50	5
16	15	1733	2936.5–2946.0	135.5–145.0	9.5	8.85	93
17	15	1831	2946.0–2955.5	145.0–154.5	9.5	9.40	99
18	15	1932	2955.5–2965.0	154.5–164.0	9.5	8.71	92
19	15	2026	2965.0–2974.5	164.0–173.5	9.5	7.54	79
20	15	2129	2974.5–2984.0	173.5–183.0	9.5	7.90	83
21	15	2232	2984.0–2993.5	183.0–192.5	9.5	6.39	67
22	15	2346	2993.5–3003.0	192.5–202.0	9.5	0.94	10
23	16	0320	3003.0–3012.5	202.0–211.5	9.5	0.56	6
24	16	0424	3012.5–3022.0	211.5–221.0	9.5	0.48	5
25	16	0532	3022.0–3031.5	221.0–230.5	9.5	0.15	2
26	16	0630	3031.5–3041.0	230.5–240.0	9.5	0.10	1
27	16	0732	3041.0–3050.5	240.0–249.5	9.5	0.11	1
28	16	0834	3050.5–3060.0	249.5–259.0	9.5	0.19	2
29	16	0952	3060.0–3069.5	259.0–268.5	9.5	0.15	2
30	16	1253	3069.5–3079.0	268.5–278.0	9.5	2.26	24
31	16	1905	3079.0–3088.5	278.0–287.5	9.5	1.97	21
32	16	2352	3088.5–3097.5	287.5–296.5	9.0	8.56	95
33	17	0253	3097.5–3106.5	296.5–305.5	9.0	2.92	32
34	17	0529	3106.5–3115.5	305.5–314.5	9.0	2.80	31
35	17	0923	3115.5–3124.5	314.5–323.5	9.0	5.51	61
36	17	1335	3124.5–3133.5	323.5–332.5	9.0	3.70	41
					332.5	137.67	41

nannofossil marl, and clay. Two subunits are recognized.

Subunit IA. The characteristic feature of this subunit is the presence of nannofossil marls and a single terrigenous clay bed. The top 55 cm consist of yellowish gray foraminiferal nannofossil ooze of which the uppermost 20 cm contains angular fragments of white to very light gray chalk (less than 3 × 2 cm). These chalk fragments are speckled with black manganese and show tubular burrow sections. Below the foraminiferal-nannofossil ooze, the sediments change sharply to 140 cm of greenish gray nannofossil marl (43–53% carbonate and less than 2% quartz), then 160 cm of white, yellowish gray, greenish gray, very light gray, and light greenish gray nannofossil ooze (71% carbonate with only about 1% foraminifers). This sequence is underlain by bluish white foraminiferal-nannofossil ooze (86% carbonate, less than 20% foraminifers), then a 10-cm bed of greenish gray clay (17% carbonate, no foraminifers) that marks the base of the subunit. The sediments, although firm, are highly disturbed by drilling and no primary or biogenic structures are preserved intact.

Subunit IB. This subunit consists of a relatively uniform sequence of bluish white, very pale blue to very light gray, light greenish gray, and white foraminiferal-nannofossil and nannofossil-foraminiferal oozes. Eight carbonate bomb analyses were carried out and averaged 86.6%. The percentage of foraminifers varies from 10–20% in the foraminiferal-nannofossil ooze to 25–40% in the nannofossil-foraminiferal ooze; the remainder of the carbonate content is formed predominantly by coccoliths (often including abundant discoasters). The sediments are generally firm oozes but from Sections 538A-7-1 to 538A-10-1 harder, chalky horizons become more common. The homogeneous nature of the oozes makes it difficult to assess the true extent of drilling disturbance; no primary or biogenic sedimentary structures were observed.

Unit II: 79.1–173.5 m; 538A-10-1, 60 cm to 538A-20-1, 0.0 cm; late Oligocene to middle Eocene

This unit consists predominantly of light-colored nannofossil oozes and chalks with occasional thin beds of altered, sand-sized vitric ashes and, in the lower subunit, nannofossil-radiolarian mudstones, radiolarian-nannofossil chalks, and nannofossil marls. The upper boundary in Unit II is taken at the top of the first ash layer. Two subunits are recognized.

Subunit IIa. This subunit is composed mainly of white to bluish white, or very light gray or light greenish gray, nannofossil oozes and chalks with occasional thin (less than 6 cm) volcanogenic beds (see below). Between Cores 10–13 in Hole 538A, the sediments are generally firm oozes with scattered chalky bands but from Core 14 downward, chalks predominate. Carbonate contents of the oozes and chalks average about 85% (three samples); smear slides indicate that the main carbonate component is nannofossil (or crystalline) calcite. Foraminifers do not exceed 5%. As the ooze/chalk boundary was approached, the proportions of nannofossils estimated in smear slides decreases and the amount of crystalline calcite observed shows corresponding increases. This trend suggests that the lithification of the ooze to a chalk is related to the precipitation of cements that were probably derived from the solution and reprecipitation of nannofossil calcite. Thin layers of indistinctly laminated, very light gray, pale green, or light greenish gray nannofossil chalk and ooze occasionally occur within the more homogeneous sediment (e.g., in Sections 538A-10-4, 538A-11-2, 538A-12-2, 538A-14-1, and 538A-16-3). However, generally sedimentary structures are absent because of a combination of bioturbation, poor color contrasts, and drilling disturbance. Five ash beds were identified in this subunit; they have an average thickness of about 4 cm, are medium gray in color, and have a distinct hyaline appearance reflecting abundant sand-sized volcanic glass shards (average 77% in smear slide). Two of the beds (one in Section 538A-10-5, the other in 538A-12-1) are graded, with sharp bases and burrowed, transitional tops. Although there are only five distinct beds of this material in Subunit IIa, single laminae or irregular burrow-fills rich in volcanic glass are scattered throughout. Some steeply dipping, indistinct laminations occur in the top part of Section 538A-16-3.

Subunit IIb. The boundary between Subunits IIa and IIb is taken as the top of the first pale green nannofossil marly chalk bed. Four of these marly beds occur in Sections 4 and 5 of Core 538A-16, although only one in the

Table 2. Summary of lithologic units of the sedimentary section in Holes 538 and 538A.

Hole	Age	Units and subunits	Lithology	Main colors	Interval (depth)	Thickness (m)	Recovery (%)
538	late Oligocene	I	Nannofossil ooze	White-light gray	538-1-1, 0-6 cm	Unknown	78.3
538A	late Pliocene to late Oligocene	Ia	Foraminiferal-nannofossil ooze, nannofossil ooze, nannofossil marl, and clay	Yellow gray	538A-1 to 538A-3-1, 10 cm (0-21.6 m)	21.6	28.1
		Ib	Foraminiferal-nannofossil and nannofossil-foraminiferal ooze	Light greenish gray-white, blue white, very pale blue	538A-3-1, 10 cm to 538A-10-1, 60 cm (21.6-79.1 m)	57.5	52.9
	late Oligocene to middle Eocene	IIa	Nannofossil ooze, nannofossil chalk, and occasional volcanic ash	White, very light gray, or light greenish gray	538A-10-1, 60 cm to 538A-16-4, 28 cm (79.1-139.8 m)	60.7	43.0
		IIb	Nannofossil chalk, nannofossil marl, nannofossil-radiolarian mudstone, radiolarian-nannofossil chalks, and occasional volcanic ash	Light greenish gray-white, yellow gray	538A-16-4, 28 cm to 538A-20-1, 0 cm (139.8-173.5 m)	33.7	87.0
	middle Eocene to latest Albian	IIIa	Foraminiferal-nannofossil and nannofossil-foraminiferal chalks with manganese and oxide-rich omission surfaces	Very light gray, yellow gray, and very pale orange	538A-20-1, 0 cm to 538A-21-3, 85 cm (173.5-186.9 m)	13.4	87.5
		IIIb	Foraminiferal-nannofossil and nannofossil-foraminiferal chalks with minor claystones and nannofossil claystones; some oxides	White, yellow gray, pinkish gray, and moderate brown	538A-21-3, 85 cm to 538A-21-5, 20 cm (186.9-189.2 m)	2.3	100.0
	latest Albian	IV	Nannofossil chalk, nannofossil marly limestone, limestone, and chert	White, light greenish gray, and light olive gray	538A-21-5, 20 cm to 538A-24-1, 0 cm (189.2-211.5 m)	22.3	7.6
	early Valanginian to Berriasian	V	Skeletal grainstones and minor packstones and wackestones	White grayish orange	538A-24-1, 0 cm to 538A-30-1, 5 cm (211.5-268.55 m)	57.05	2.8
	Basement rocks				268.55 m to total depth (332.5 m)		

latter. The uppermost two of these beds in 538A-16-4 contain thin, light gray layers (less than 0.5 cm), which are rich in volcanic glass at their lower contacts and may be graded. Sections 538A-16-4 and 538A-16-5 also contain bands of dark-colored radiolarian mudstones (less than 15 cm thick): one occurs in 538A-16-4 and is dark yellowish brown (indistinctly laminated and with lighter-colored burrow-fills), and the other two in 538A-16-5 are dusky yellowish brown to black (in part laminated and in part with lighter-colored burrows). These radiolarian mudstones contain about 30% carbonate (mostly mineralic calcite) and up to 40% silica (30% radiolarians, 10% sponge spicules). However, the predominant sediment type from 538A-16-4 through 538A-18-4 is light greenish gray to white nannofossil chalk. Several volcanogenic glassy beds occur between 538A-16-6 and 538A-17-6 (five bands averaging 3.6 cm in thickness) and are identical to those described for Subunit IIa. Only one band (in Section 538A-17-3) has a sharp base, grading, and a burrowed, transitional upper contact. Below Section 538A-18-2, the nannofossil chalk becomes progressively more yellowish gray in color, and in Section 538A-18-5 changes to a yellowish gray radiolarian-nannofossil chalk with approximately 20% radiolarians, 20% nannofossils, and 55% crystalline calcite. Between Sections 538A-19-2 and 538A-19-5 these radiolarian-nannofossil chalks contain scattered, occasional patches and thin disturbed laminae of volcanogenic material. Thin (about 2 mm) lenses of asphalt occur in Sections 538A-18-2 and 538A-19-2, and scattered specks also appear from 538A-18-2 to 538A-19-4, 5 cm. With the exception of some 25° dipping clayey laminae in 538A-17-4, few sedimentary structures were observed in Subunit IIb. Bioturbation and *Planolites* type burrows were only observed in the rare cases where the color contrast between the matrix and burrow-fill was distinct.

Unit III: 173.5–189.2 m; 538A-20-1 to 538A-21-5, 20 cm; middle Eocene to latest Albian

This unit consists predominantly of foraminiferal-nannofossil chalks with lesser amounts of nannofossil-foraminiferal chalk and, in the lower subunit, nannofossil claystones and terrigenous claystones. The unit is characterized by its heterogeneity (both in terms of color and composition) and the presence of manganiferous surfaces or hardgrounds (Fig. 4). The boundary with Unit II is marked by the disappearance of radiolarians and the increase in abundance of foraminifers from trace amounts (less than 1%) to 15–50%. Two subunits are recognized.

Subunit IIIa. The upper part of Unit III is mainly composed of very light gray, yellowish gray, pinkish gray, very pale orange, or grayish orange pink foraminiferal-nannofossil chalks. These sediments contain 78–88% carbonate, 15–20% foraminifers, and 35–80% nannofossils. There are two notable features of this subunit when compared with other parts of the sequence: (1)

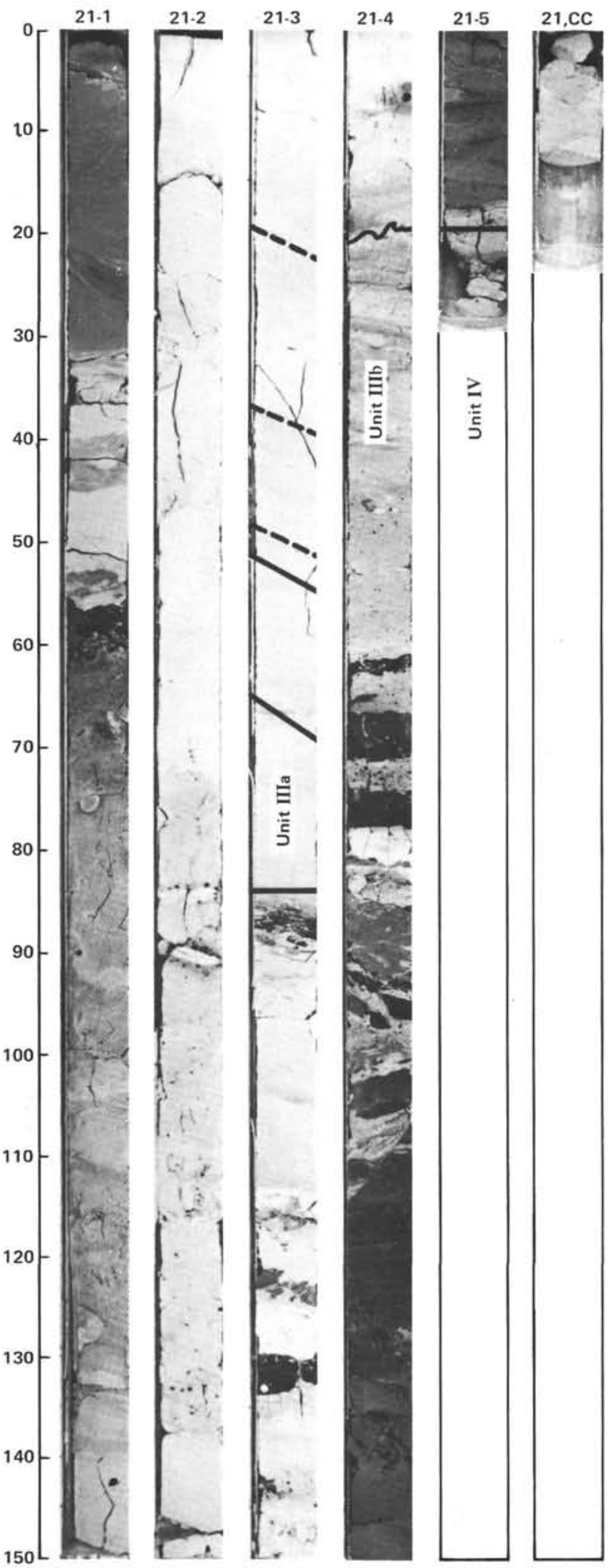

Figure 4. Core 21 illustrates a variety of structures and features characteristic of Units IIIa, IIIb, and IV. Note dark Paleocene chalk with slump fold in 538A-21-1, 0–32 cm; oxide-impregnated hardground (Maestrichtian-Paleocene) in 538A-21-1, 55–60 cm; dipping layers (slumps?) in 538A-21-2, and 538A-21-3, 0–60 cm; and finally a fault in the Albian chalk of 538A-21-4, 105–115 cm. See also the diagram in Figure 6 for further explanation.

conspicuous bioturbation (dominantly unidentified or *Planolites* type) and (2) the occurrence of several distinct hardground horizons (the distribution of these is indicated in Fig. 4). These discontinuities are represented both as irregular bored surfaces (Fig. 5A) or as black manganese-rich crusts (Fig. 5B). The differences in ages across these horizons is usually considerable (Fig. 6; also see Biostratigraphy and the discussion part of this section). Other features indicated on Figures 4 and 6 include the distribution of manganese, microfaulted intervals, and the occurrence of rare, steeply dipping laminae. *Cylindrichnus*(?) or "halo" type burrows were noted in Sections 538A-20-2, 538A-20-4, and 538A-21-1, and a possible aptychus was recorded at 538A-21-2, 146 cm.

Subunit IIIb. The top of this subunit is taken at the first nannofossil claystone bed in Section 538A-21-3. This band is strongly bioturbated (*Planolites*, possible *Chondrites*), contains an unidentified back-filled burrow, is moderate brown in color, and consists of 80% clay and 20% nannofossils. Below this bed the sediments are dominantly white to yellowish or pinkish gray foraminiferal-nannofossil chalks interbedded with several claystone and ash beds (Fig. 4, and the corresponding close-ups Figs. 5C and 5D). The claystones range from dark yellowish brown through olive gray to olive black (bluish where weathered); they contain 60–99% clay, 5–10% nannofossils, and sometimes minor zeolites (less than 15%). Although their contacts are sharp, they usually contain fairly common burrows infilled with lighter-colored sediment from above (Fig. 5C). The ash bands range from light olive gray to light gray in color, have a distinct hyaline appearance, and are composed of 95–98% variably altered volcanogenic glass. Below the prominent microfault in Section 538A-21-4 shown in Figure 5D, there is an interval of pale green claystone that is altered near the fault (down to about 135 cm) to a dusky yellow, light olive brown, and dark yellowish orange color. The base of Unit III is marked by the change to dark nannofossil chalks and lighter-colored chalks and limestones (Fig. 4).

Unit IV: 189.2–211.5 m, 538A-21-5, 20 cm to 538A-24-1, 0.0 cm; latest Albian

Because of poor recovery in this unit (7.6%), few if any original lithologic contacts were preserved in the cores. The lithologies recovered include nannofossil chalks, limestones, marly limestones, and chert, but these may be unrepresentative of the unit as a whole. Because of the poor recovery, the position of the lower boundary of this unit was inferred from a decrease in the drilling rate (Fig. 2).

The nannofossil chalks observed in this unit range in color from white to light greenish or light brownish gray; one darker band in 538A-21-5 contains common phosphatic (fish scale?) debris. The limestones range in color from light gray, light olive gray, yellowish gray, or medium light gray and are variably laminated and banded or bioturbated. They show some moldic porosity (including occasional, small, ammonite molds). Thin sections indicate that these limestones are radiolarian or foraminiferal-radiolarian mudstones and packstones in which the skeletal material is generally recrystallized to sparite. Some of these limestones contain thin lenses of pale green clay similar to that at the base of the overlying unit. The cherts are either black or dark yellow brown to light olive or yellowish gray and some are laminated in part. Intercalated within these limestones and chalks are two intervals of very soft, white calcareous oozes showing well-preserved foraminifer and nannofossil assemblages. The curious lack of cementation in this material contrasts sharply with the rather advanced lithification of the other lithologies observed in the unit.

Unit V: 211.5–268.6 m; 538A-24-1 to 538A-30-1, 5 cm; early Berriasian to Valanginian

Rocks recovered from Unit V consist of white and grayish orange oolitic, skeletal, and oncolitic limestones, most of which are grainstones and packstones. Rare patches of wackestones are scattered throughout samples from the lower two-thirds of the unit. Oolitic limestones occur in the upper third of the unit and consist of well-sorted, medium sand-size ooids and skeletal grains in a fibrous or bladed calcite cement interpreted to be of marine origin. Skeletal grains include echinoderm fragments, composite grains, peloids, and rare benthic foraminifers. Ooid cortices are preserved as concentric micritic laminae with rare dolomite rhombs (about 50 μm on an edge) replacing portions of the ooid coatings. Erosional horizons occur in the oolites, horizontally and evenly truncating grains and cement across the width of a thin section. These horizons are in turn overlain by oolite cemented in a more open-marine environment.

Composite grains and small oncolites (0.5–2 mm) are the characteristic grains below the oolitic limestone, with echinoderms, coral, peloids, and foraminifers forming the majority of other grain types. Unusual but distinctive grains in this oncolitic facies include echinoderm spine fragments and trocholinid foraminifers. Cement is again common, and wackestone fills both pockets and borings in the specimens. Calpionellids are rare. The cement encloses layers of peloids, which may form geopetal surfaces and, in some instances, display reverse grading.

Porosity is estimated to be between 10 and 20%, derived mainly from dissolution of originally aragonitic grains. Microspar or blocky calcite apparently also replaced some aragonite. Primary pore space is largely filled with cement, although patches of preserved primary porosity exist throughout the unit.

At the base of the unit, a chalk crust, 1–2-mm thick, coats the surface of the underlying metamorphic basement rock. The crust contains coccoliths, nannoconids, and nannoconid debris, but is composed primarily of fine calcite silt of indeterminate origin.

Discussion

The oldest sediments recovered in Hole 538A were the limestones of Unit V and the thin pelagic chalk on the uppermost piece of basement. Although the very poor recovery of this unit (about 3%) places considerable constraints on the elucidation of the early geologic history at this site, sufficient data are available to propose two alternative sequences of events.

The material from the lower two-thirds of Unit V, the oncolite facies, is similar in facies and age to that of Unit II at Site 537. As with that material, this sediment is probably derived from an open-marine part of a carbonate platform (upper forereef or deeper platform terrace). Like the material from Site 537, it is possible that the oolitic, oncolitic, and skeletal limestones at Hole 538A have been redeposited in deeper water.

The oolitic limestone from the top of Unit V is also a sediment characteristic of carbonate platform margins. Such facies often occur just a few kilometers bankward of the shelf margin or, more infrequently, on bank interiors characterized by low sedimentation rates. The oolite represents a more shallow-water facies than the underlying oncolite facies. We found no evidence of distinct clast margins in the recovered material, which would suggest that these rocks are resedimented clasts of shallow-water limestone. Distinct layers of pelagic sediment are absent from recovered rocks of Unit V. Such layers are characteristic of Unit III at Site 536, present both within and between core segments of shallow-water debris.

Although pelagic sediment layers seem to be absent from the unit, planktonic skeletal material is scattered throughout the interval, as might be expected on a isolated knoll in the deep southeastern Gulf of Mexico. In particular, scattered planktonic foraminifers and calpionellids occur in areas of fine-grained matrix and are incorporated in the coatings of oncolites. Calpionellids, which occur in all cores, suggest the unit is Berriasian to Valanginian in age and the probable occurrence of three calpionellid zones in sequence supports the *in situ* origin of the unit.

In Hole 538A, the contact between oolite and oncolite facies is gradational over several tens of meters. Thin sections from Cores 25 through 28 contain both oncolites and ooids. Oolitic limestone occurs as deep as Core 28 and oncolites occur as shallow as Core 25, but the unit is clearly an oolitic limestone at the top and an oncolitic limestone at the base. The gradation between these facies suggests one continuous unit, not two units with a hiatus between them.

Although it is unlikely that Unit V is redeposited platform talus, the possibility cannot be eliminated. Intercalated layers of soft pelagic sediment may occur in the unit but were not recovered. It is possible that the rocks recovered were redeposited in deep water as clasts and that these clasts have never been firmly cemented. Redeposition would have to be periodic, so that biostratigraphic stages were not mixed. (For further discussion, see Schlager et al., this volume).

The preferred interpretation of Unit V is that it was deposited in place, on a raised basement block. Deposition commenced with pelagic sediment, the pelagic crust, on a surface swept free of any preexisting sediment by currents or by slumping or faulting, perhaps during the uplift of the block. The sediments on the block record deposition in decreasing water depth. The chalk was prob-

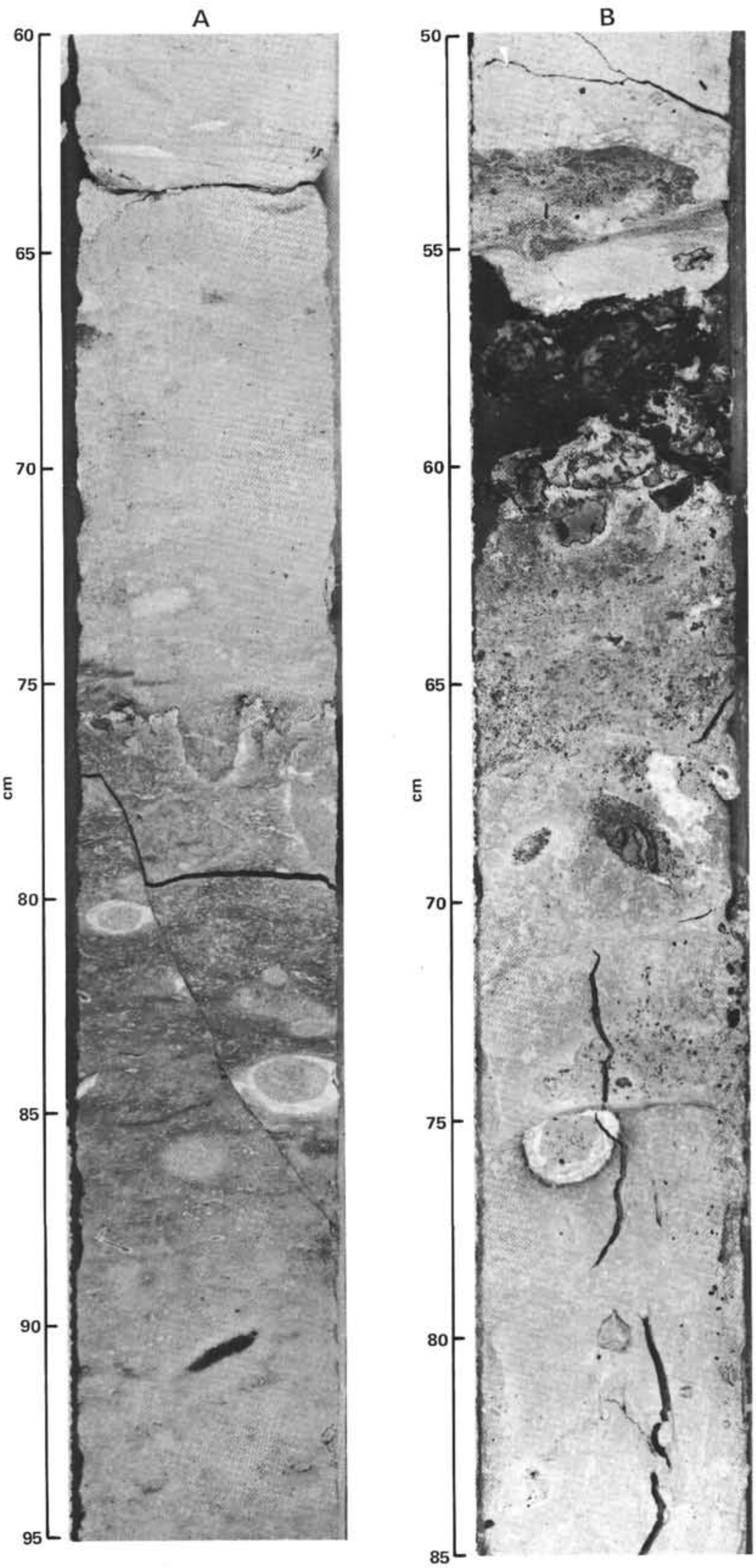

Figure 5. Details of sedimentary structures and features in Unit III. Scales in cm. A. 538A-20-2, 60–95 cm; irregular, bored surfaces and burrows in Unit IIIa. B. 538A-21-1, 50–85 cm; manganese-rich crust at 538A-21-1, 56–59 cm, Unit IIIa. C. 538A-21-4, 50–85 cm; interbedded dark claystone at 75–78 cm and foraminiferal-nannofossil ooze at 78–85 cm, Unit IIIb. D. 538A-21-4, 85–120 cm; interbedded chalk, ash, and claystone faulted over green claystone, Unit IIIb.

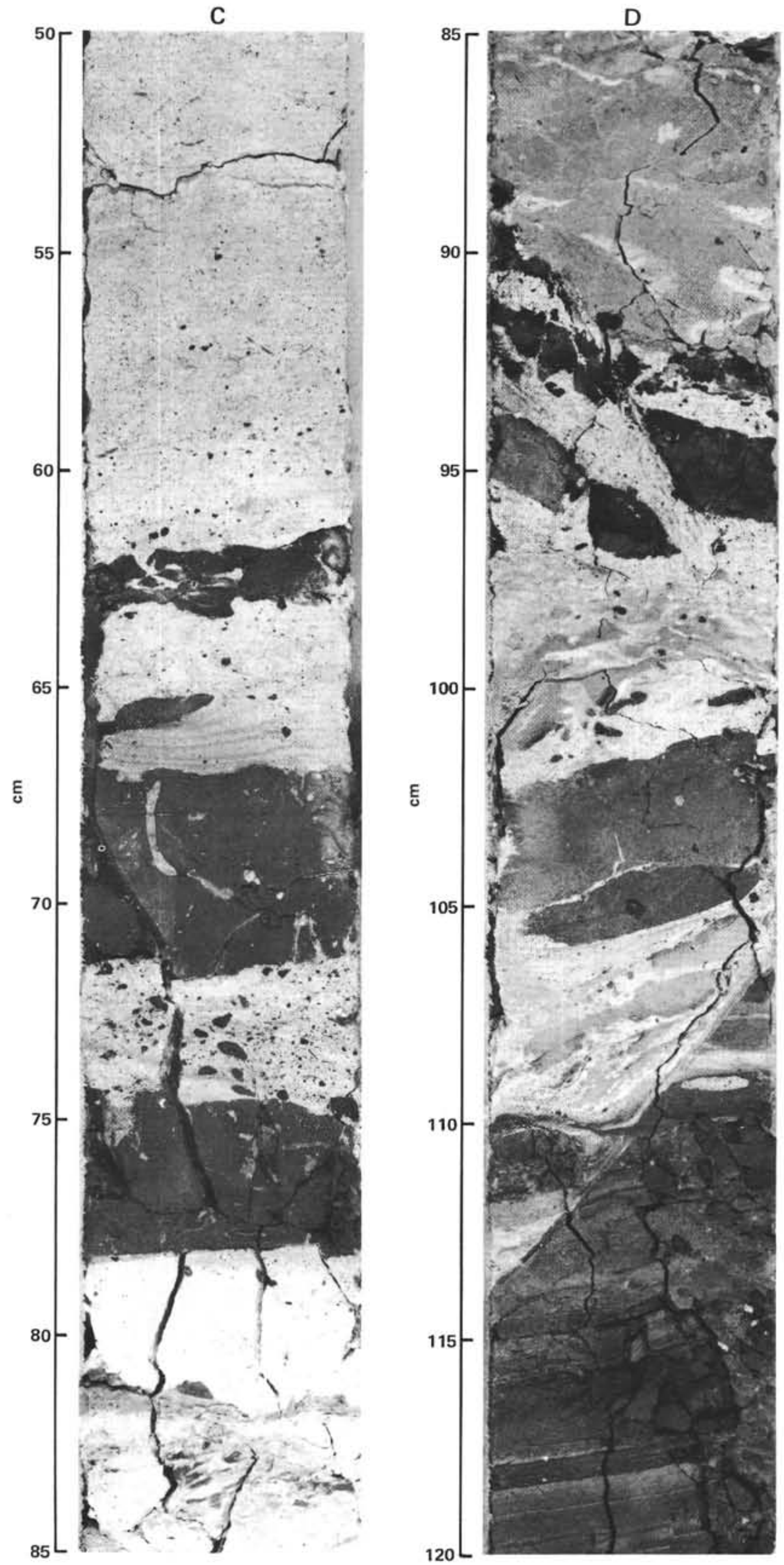

Figure 5. (Continued)

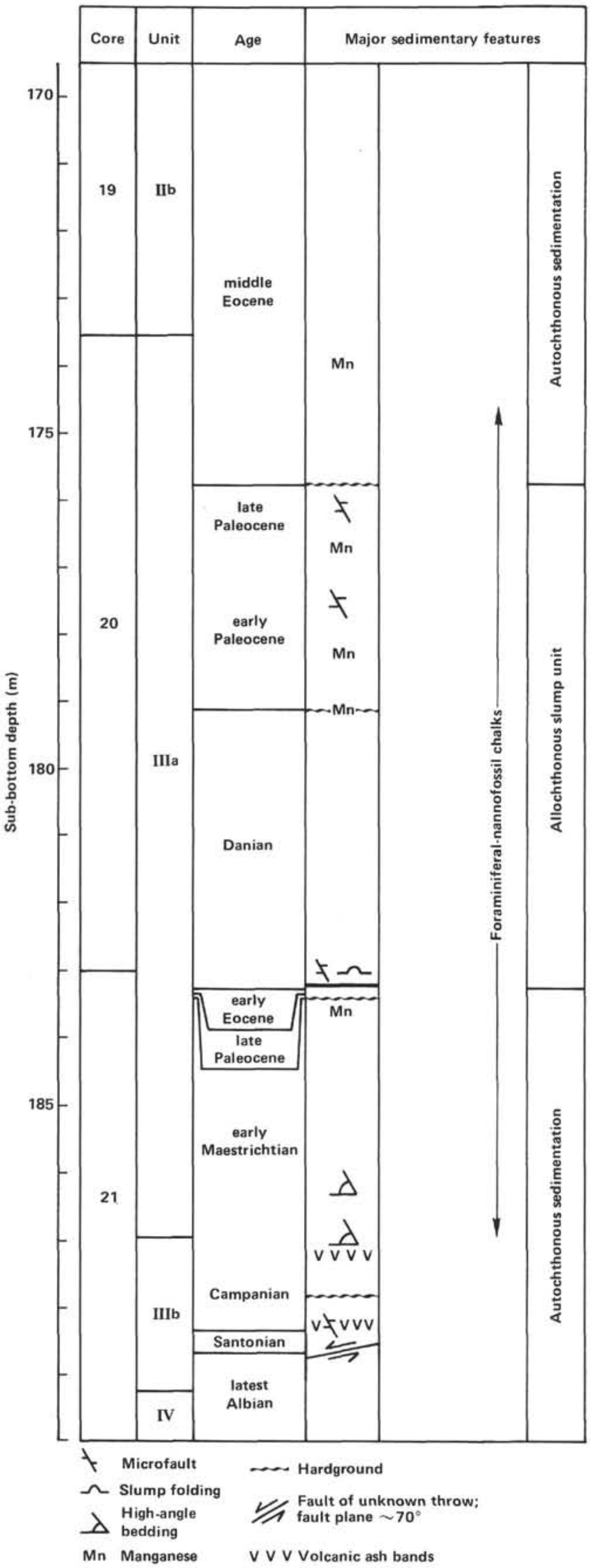

Figure 6. Detailed interpretative section showing ages and principal sedimentary features of Units IIb, III, and IV, Hole 538A.

ably deposited in bathyal depth, the oncolite facies probably in the depth range of 50–200 m, followed by the oolite (which may represent deposition in as little as a few meters of water). Shoaling water may have resulted from continued relative uplift of the basement block, sea level fall, or a combination of the two. Sometime in the Valanginian, the block was submerged more deeply, resulting in nondeposition or erosion.

During the late Albian, the pelagic sediments of Unit IV were deposited. Poor recovery hinders the interpretation of this unit. The change from the oolitic grainstones at the top of Unit V to the chalks, limestones, and cherts of Unit IV occurred at some point within the Valanginian through Albian interval. Depending on whether the platform hypothesis or the talus hypothesis is correct, this transition may represent either: (1) drowning of a shallow-water platform and transition to a relatively deeper, more pelagic environment, or (2) rapid decline of sediment influx from platforms into the deep basin. This decline may have been caused by drowning or backstepping of carbonate platforms, or it may be related to a change in the topography of the seafloor.

Unit IV is late Albian in age, and this implies a considerable hiatus between Unit IV and the underlying Valanginian limestones of Unit V. The unit consists of two suites of lithologies. Light, massive limestone and darker-laminated, hard limestone; dark carbonaceous marl; and black chert compose the dominant group (nearly identical with coeval rocks at Site 540), and represent sediments in an advanced stage of diagenesis. Two short sections of very soft, white carbonate ooze, on the other hand, appear to have undergone hardly any diagenesis at all and show no transitions to the limestone lithologies. Well-preserved biota in both lithologic groups clearly indicate the same age. The alternation of these lithologies in one core is very puzzling. In the North Atlantic, unlithified, white Albian ooze has been recovered from shallow positions on the continental slope, for instance the Blake Nose (Benson, Sheridan, et al., 1978; Sites 390, 392), whereas dark sediments, normally lithified, occupy the abyssal areas below 3200 m. Tucholke, Vogt, and others (1978) postulated a body of stagnant deep water to explain this facies pattern. Catoche Knoll may have been located near a similar boundary of water masses. Short-term fluctuations of this boundary could explain the change from white ooze to darker, laminated, carbonaceous sediment and back to white ooze. To explain the difference in lithification, depositional environment and sediment facies must play an important role during burial history in controlling the progress of diagenesis.

Unit III appears to be a pelagic sequence composed predominantly of foraminiferal-nannofossil chalks, but it is complicated by the presence of several omission surfaces and a major slump unit (see Figs. 4 and 5). The base of Subunit IIIb is marked by pale green and yellowish (altered) claystones of latest Albian age separated from the overlying chalks, interbedded ashes, and dark claystones by a conspicuous fault. Despite the sharp change in lithology across this fault, detailed biostratigraphic sampling indicates that sediments of latest Albian age occur on both the upthrown and downthrown sides, although the overlying sediment is mainly Santonian and Campanian in age (see Fig. 6). The evident stratigraphic hiatus is not, therefore, produced by the faulting (which is probably small scale), and the Cenomanian to Coniacian interval appears to have been lost by erosion and/or nondeposition. The same is partly true for the Santonian and Campanian intervals, which are both abbreviated and incomplete (see Biostratigraphy section).

The dark mudstones in the Santonian-Campanian probably represent altered, fine-grained volcanic ashes. The mudstone layers exhibit bored surfaces, and one appears to correspond with the Maestrichtian/Campanian boundary and another with the Campanian/Santonian contact.

An additional interesting feature of Unit III is the presence of apparently "shallow-water" foraminifers in the Campanian foraminiferal-nannofossil chalks. Some of this material is coeval with the matrix and has not been reworked from older, Unit V type sediments exposed elsewhere. It may indicate that the site, although raised above the surrounding seafloor, was still within reach of turbidity currents.

At the top of the lower Maestrichtian interval in Core 538A-21, there is a manganese-encrusted omission surface which is capped by a thin layer of lower Eocene chalk, suggesting condensing and loss of the upper Maestrichtian and Paleocene sections. However, above the 25 cm of lower Eocene chalk there is an approximately 7.2-m thick section of Paleocene sediment topped by a hardground and overlain by lower middle Eocene chalk. This reversal of stratigraphic order indicates that slumping has taken place (see Fig. 4), and this is supported by the deformation of the lowest ± 30 cm of the allochthonous unit. Several important points are evident:

1. In the autochthonous sequence at Hole 538A there was either minimal deposition during the Paleocene or most Paleocene sediment was removed by slumping.
2. The slump took place between the early and early middle Eocene, at which time the slumped sediment must have been relatively cohesive.
3. Prior to displacement, the omission surface at the top of the slump unit may have merged laterally with the one at its base.

Schlager and others (this volume) consider this slump to have been triggered by tectonics rather than sediment loading.

Unit II is a fine-grained pelagic deposit that contains two particularly interesting features; these are the apparent episode of a higher radiolarian productivity during the middle Eocene (Subunit IIb) and the thin, sand-grade, vitric ash beds. When not disturbed by bioturbation or drilling, several of the ash beds reveal sharp bases, grading, and bioturbated transitional upper contacts. Because we observed no evidence for traction current deposition (e.g., winnowed sand layers, ripple cross lamination) in these beds, we believe that they were produced by the settling out of volcanogenic particles deposited from atmospheric ash clouds rather than deposition from turbidity currents.

Unit I is also a purely pelagic deposit, although the upper subunit is less pure, containing marls and even a clay layer. The latter lithologies may suggest an increase in the amount of suspended clay materials entering the basin. At least two of the more clayey bands contain a small amount of sand-size quartz grains (less than 2%) and it is possible that the top of the knoll was not totally beyond the influence of large turbidity currents at this time. The Tertiary pelagic sequence in Hole 538A is capped by a chalky hardground of late Pliocene age.

BIOSTRATIGRAPHY

Summary

Most of the biostratigraphic data at Site 538 have been collected from Hole 538A, which penetrated 267 m of sediments ranging in age from Holocene to late to early(?) Berriasian and resting on older metamorphic and igneous basement rocks. Sediments recovered in Hole 538 add some information only about the uppermost part of the sedimentary sequence.

Sedimentologically, five discrete units have been recognized at this site. The upper four units are predominantly pelagic in origin (ooze and chalk), whereas the fifth unit is mainly composed of skeletal-oolitic limestone in which pelagic sediments are a minor component.

Biostratigraphically, the pelagic sequence that represents the bulk of the sediments recovered at Site 538, can be subdivided into specific intervals, characterized by peculiar composition or preservation of the biota. In very few cases do these intervals coincide with main changes in lithology.

These biostratigraphic intervals are as follows (from top to bottom):

1. The uppermost interval, about 20 m thick, corresponds to the uppermost part of Lithologic Subunit Ia (Core 538-1; 538A-1 to 538A-2-2, 10 cm) and is characterized by large hiatuses marked sometimes by indurated crusts (top of Core 538-1) or by questionable glauconitic ash layers (538A-1,CC). The ages of the recovered sediments are late Pliocene (Hole 538: nannofossil Zone CN12a, foraminiferal Zone MPL4); early Pliocene (Hole 538: Zones CN10c, b; MPL2); late Miocene (Hole 538A: Zones CN9 and CN7b; N17–N16); and middle Miocene (Hole 538A: Zones CN5–CN6; N12). Except for the upper Pliocene assemblages, all other planktonic foraminiferal faunas, and in some cases nannofloras, are affected by dissolution.
2. The second interval (538-2,CC; 538A-2-2, 11 cm through 538A-11) is characterized by a continuous sequence of upper Oligocene sediments deposited at a rate of 19–36 m/Ma. However, lower rates of sedimentation (9 m/Ma) are reported between 28 and 26 Ma in Zone P21b. In this specific interval, planktonic foraminiferal faunas are dissolved to varying degrees. Such an event can be correlated with an important cooling event on a global scale.
3. The next lower interval (47.5 m thick), from Cores 538A-12 through 538A-16 (most of Unit IIa), ranges in age from early late Oligocene through early middle Eocene and is characterized by a period of low depositional rates, interrupted by discrete hiatuses that appear not

to exceed 2-Ma duration. The biozones represented in this interval are: foraminiferal Zones P20–P18 and nannofossil Zones CP17–CP16 in the Oligocene; foraminiferal Zone P15 and nannofossil Zone CP15 in the upper Eocene; foraminiferal Zones P14–P13 and nannofossil Zone CP14 in the middle Eocene.

4. The interval from Core 538A-17 through 538A-20-2, 75 cm—about 30 m thick—(Unit IIB) is characterized by predominant radiolarians. The entire interval is within the 1-Ma long nannofossil Zone CP12b of early middle Eocene age. The abundant of radiolarians in this interval (they are scarce in other parts of this sequence) is in our opinion a reflection of the high biogenic silica production similar to that at Site 537 as well as at many other oceanic areas during the middle Eocene (e.g., Horizon A in the western North Atlantic).

5. About 30 Ma of the geologic history of the area is represented by only 12.45 m from 538A-20-2, 75 cm to 538A-21-4, 110 cm (Unit III). The sequence is characterized by large hiatuses frequently marked by conspicuous hardgrounds. The youngest sediments recorded in the interval are of early Eocene age (*Morozovella aragonensis* Zone P8; *Discoaster lodoensis* Zone CP11). They are overlain abruptly by about 6 m of sediments of late Paleocene age. This stratigraphic repetition is interpreted as a slump that took place in late early Eocene, approximately 51–49 Ma. Other sediments recorded in the sequence are: (1) upper Paleocene, just below the hardgrounds at the bottom of the lower Eocene sediments in 538A-21-1, 58–63 cm associated with some volcanic glass and exotic lithotypes; (2) lower Maestrichtian (538A-21-1, 62 cm to 538A-21-2, 125 cm), beginning just below the mentioned hardgrounds; (3) lower upper Campanian (538A-21-2, 126 cm to 538A-21-4, 75 cm), separated by a hiatus of at least 1 Ma from the lower Maestrichtian; (4) lower Santonian in 538A-21-4, 78–110 cm.

This interval contains the longest record of the Upper Cretaceous sediments ever recovered in this area of the Gulf of Mexico, and it contains the youngest influx of reefal, shallow-water debris from the Early Cretaceous carbonate platform, as well as neritic benthic forms of late Campanian age that display affinities to similar forms in Texas. Reworked and displaced material occurs at the bottom of the recovered upper Campanian pelagic sediments. The lowermost interval—22 m thick, corresponding to Unit IV, from 538A-21-1, 110 cm through Core 23—spans the whole *Planomalina buxtorfi* Zone of latest Albian, whose duration is about 2 Ma. Hard limestones in between the nannofossil chalk and marly limestones are dominated by radiolarians, but foraminifers are poorly preserved and sparse.

Unit V, the lowest sedimentary unit overlying the metamorphic and igneous rocks (Core 538A-24 through 538A-30-1, 0–4 cm) consists primarily of oolitic, skeletal, and oncolitic limestones with pelagic limestone as a minor component. However, the latter lithotype contains age-diagnostic calpionellids. Based on the occurrence of the various species belonging to this pelagic fossil group, the limestone sequence can be dated as early Valanginian to late-early(?) Berriasian.

Foraminifers and Calpionellids

Hole 538

The 6 m (Core 1) of nannofossil ooze (Unit I) recovered in Hole 538 range in age from late Pliocene to late Oligocene, and the sequence is characterized by important hiatuses.

The uppermost 53 cm in Section 538-1-1 contain a rich planktonic foraminiferal fauna of late Pliocene age. The concurrence of *Globorotalia puncticulata* and *Sphaeroidinellopsis* ssp. in the absence of *G. margaritae* allows us to attribute this interval to Zone MPL4.

The color change at 538-1-1, 54 cm coincides with a hiatus of less than 1 Ma. At this level, a rich, moderately preserved planktonic foraminiferal fauna of early Pliocene age occurs. The assemblage, belonging to Zone MPL2 and characterized by *G. margaritae* associated with *Globigerina nepenthes*, occurs through 538-1-4, 10 cm. Faunas become progressively more dissolved downwards. At 538-1-4, 10 cm, another abrupt change in both color (bluish) and lithology (more chalky) corresponds to another hiatus—one of about 20 Ma. In fact the remainder of Core 538-1 contains a diversified assemblage of the *G. angulisuturalis* Zone (= P22) of late Oligocene age.

Hole 538A

On the basis of the fossil content, the sequence recovered at this hole can be subdivided in two parts: (1) an upper portion consisting dominantly of foraminiferal-nannofossil ooze or nannofossil chalk, rich in planktonic organisms, but characterized by large hiatuses (Units I through IV) and (2) a lower unit (Unit V) of mainly oolitic, skeletal, and oncolitic limestone with minor pelagic limestone.

In Core 1, the first sediments encountered are already late Miocene in age and are indurated at their top. According to the nannoplankton data (foraminifers were not processed in this interval), most of Core 1 belongs to the upper Miocene Zones N17 through N16. The core catcher sample contains a largely mixed assemblage of different ages, which includes upper Miocene Zone N17 elements (dominant), middle Miocene forms possibly belonging to Zone N12, and some undifferentiated upper Oligocene forms. Planktonic foraminiferal faunas are partially dissolved. Some glauconite grains also occur.

Most of Core 2 contains a middle Miocene Zone N12 assemblage, but it bottoms in upper Oligocene sediments of the *Globigerina angulisuturalis* Zone (= P22). The same zonal assemblage occurs in Cores 3 through 5. Cores 6 through 7 yield a rich assemblage attributable to the upper part of the *Globorotalia opima* Zone (= P21b), characterized by the concurrence of the zonal marker with *Globigerina angulisuturalis*. The lower part of the *G. opima* Zone (= P21a) is represented in Cores 8 through 11. It is within this interval that sediments are more lithified (Unit II). The next older zone, *G. ampliapertura* Zone (= P20), occurs apparently only in Core 12. Core 13 contains a planktonic foraminiferal assemblage characteristic of the upper part of the *Pseudohas-*

tigerina micra/Cassigerinella chipolensis Zone (= P19), whereas Core 14, core catcher excluded, seems to contain the lower part of the same zone (= P18), which represents the lowermost zone of the lower Oligocene. Thus, the Oligocene sequence appears to be almost complete in Hole 538A. Planktonic foraminiferal faunas are well preserved in the upper part of the Oligocene but display a progressive deterioration downwards because of dissolution effects. The environment change implied would account for the clearly low rate of sedimentation of the lower portion.

A hiatus probably occurs in Core 14 and spans the Oligocene/Eocene boundary and part of the upper Eocene. However, poor recovery (less than one section) prevents a definite conclusion. Sample 538A-14,CC belongs to the lower upper Eocene *Globigerinatheka semiinvoluta* Zone (= P15).

Cores 15 and 16 yielded relatively well-preserved faunas of the upper middle Eocene *Truncorotaloides rohri* and *Orbulinoides beckmanni* Zones (= P13, P14), respectively. Core 17 contains a planktonic assemblage of lower middle Eocene *Hantkenina aragonensis* Zone. Thus, the middle part of the middle Eocene is missing at Hole 538A. Radiolarians from Core 17 downwards become predominant, and preservation of planktonic foraminifers progressively deteriorates, so no specific age assignment on the basis of foraminiferal content can be made for Cores 18 to 20. Nannofossil assemblages suggest that the whole interval has the same age as Core 17.

A conspicuous hardground at 538A-20-2, 76 cm is the sedimentary expression of a hiatus of about 7 Ma, spanning the whole lower Eocene and the uppermost Paleocene (*Morozovella velascoensis* Zone = P5). The hardground truncates sediments containing a planktonic foraminiferal fauna of the upper Paleocene *Planorotalites pseudomenardii* Zone (= P4). The same zonal assemblage is recorded in most of Core 20 through 538A-20-2, 112 cm. The bottom part of Core 20 and the uppermost 32 cm of 538A-21-1, contain rich planktonic faunas of the lower Paleocene "*Subbotina*" *pseudobulloides* Zone (P1c). Manganese coating marks a hiatus of more than 6 Ma. The lower Paleocene pink chalk rests unconformably on 25 cm of whitish foraminiferal chalk of the lower Eocene *M. aragonensis* Zone (= P8). Consequently, the upper and lower Paleocene strata are interpreted as a slump formed sometime after the *M. aragonensis* Zone (early Eocene) and before the middle Eocene.

The 25 cm of lower Eocene sediments lie upon an irregular, manganese-rich burrowed surface or hardground (4 cm thick). Elements of the hardground are a chalky sediment, now manganese impregnated, of late Paleocene age (*P. pseudomenardii* Zone), fragments of altered volcanic glass, clay minerals, chert, and other rock fragments. No Upper Cretaceous microfaunas occur in that layer. A very irregular and indurated upper surface of the grayish foraminiferal-nannofossil chalk that underlies the Mn-rich hardground may represent a second hardground. This lower unit, encountered at 538A-21-1, 62 cm, contains a rich foraminiferal assemblage attributable to the lower Maestrichtian *Globotruncana tricarinata* Zone; the same assemblage is recorded through 538A-21-2, 125 cm. At that level, no lithologic break occurs to account for the absence of the upper Campanian *G. calcarata* Zone, *G. subspinosa* Zone, and possibly the top part of the *G. elevata* Zone. The planktonic faunas are older than these zones or parts of zones and can be attributed to a generalized medial part of the *G. elevata* Zone, still of Campanian age. The same assemblage continues downwards as far as 538A-21-4, 75 cm. The allochthonous benthic foraminiferal faunas contain forms indicating a lower bathyal environment. Some omission surfaces in this interval have been suggested by sedimentologic observations, but the poor resolution of planktonic foraminifers prevents the detection of such minor hiatuses.

The lower part of the upper Campanian sediments recovered in 538A-21-4, 10–75 cm is much coarser than the overlying chalk. This layer contains fragments of altered ash layers, neritic benthic foraminifers of late Campanian age, shallow-water skeletal debris of Early Cretaceous age, and finally an early Santonian planktonic foraminiferal assemblage. The allochthonous material is very abundant at 538A-21-4, 72–75 cm and at 538A-21-4, 53 cm. It decreases gradually upwards to 538A-21-4, 29 cm, where it is a minor component. This suggests that this upper Campanian interval may contain originally graded turbidites with shallow-water material that was largely destroyed by burrowing and are thus not recognizable in the cores.

A rich, diversified planktonic fauna occurs in 538A-21-4, 78–110 cm. The assemblages contain several specimens of *Dicarinella concavata* and of various species of *Marginotruncana*. The concurrence of those forms dates this interval as early Santonian within the *D. concavata* Zone. The allochthonous benthic foraminiferal assemblages are characteristic of a dominantly lower bathyal environment; however, shallow-water Lower Cretaceous benthic foraminifers and debris also occur within this interval.

Another hiatus and possible hardground occurs at 538A-21-4, 110 cm. The underlying yellowish to green claystones are barren. In 538A-21-5, 18–23 cm, a light brownish gray nannofossil chalk contains only a very large amount of fish debris. Rich and well preserved, planktonic foraminiferal faunas of the uppermost Albian *Planomalina buxtorfi* Zone, occur in several layers from the core catcher sample of Cores 21 through 23. The benthic foraminiferal assemblages are characteristic of the middle bathyal zone. The most prominent species belong to the genera *Praebulimina, Ellipsoidella, Osangularia*, and *Gaudryina*. Shallow-water benthic foraminifers are mixed in the assemblages. Fish debris is a relatively common component of the residues.

The limestone (Unit V) recovered at Hole 538A contains two different assemblages: (1) a shallow-water assemblage from a carbonate platform very similar in aspect as well as in biogenic components to that recovered in limestones at Site 537; (2) a pelagic assemblage constituted by calpionellids (Cores 538A-25 through 538A-30-1, 0–4 cm).

The shallow-water material of Core 24 has the same composition as underlying cores and as the material recovered at Site 537 in the same stratigraphic position. The major difference is that, at Site 538, biogenic components, such as *Trocholina*, occur mainly as nuclei of ooids, whereas in the deeper cores they are mainly found as separate sediment particles. We believe that *Trocholina* in Core 24 are reworked from older parts of a shallow-water sequence.

Besides the shallow-water components, the interval from Core 538A-25 through 538A-30-1, 0–4 cm contains several layers with abundant calpionellids (see 538A-27-1, 4–5 cm). Based on their occurrence, this interval can be dated as a succession of three biozones, ranging from early Valanginian (Core 25) to possibly early Berriasian (Core 30) at the bottom. Specifically, Cores 25 and 26 can be attributed to Subzone D3 of calpionellid Zone; Cores 27 and 28 to Subzone D2 on the basis of the occurrence of *Calpionellopsis simplex*, the zonal marker; and finally Cores 29 and 30 to Subzone D1, which straddles the upper/lower Berriasian boundary, on the basis of the occurrence of *Calpionella elliptica* and the absence of the former index species. The shallow-water assemblages are very monotonous.

Calcareous Nannofossils

Hole 538

Core 1 recovered an approximately 520-cm sequence of pelagic calcareous oozes ranging in age from late Pliocene to late Oligocene. In addition, a small amount of soupy, brown, calcareous ooze was recovered washed along the liner in 538-1-1, 0–120 cm. This soupy material contains a mixture of Neogene and Upper Cretaceous nannofossils with species of the *Emiliania huxleyi* Zone (CN15—late Pleistocene through Holocene) most abundant. Interval 538-1-1, 0–53 cm contains assemblages with *Discoaster tamalis, D. surculus, D. brouweri*, and *Ceratolithus rugosus*. This interval is assigned to the *D. tamalis* Subzone (CN12a) of late Pliocene age. Separated from this interval by a sharp lithologic break are nannofossil oozes of the *Amaurolithus tricorniculatus* Zone (CN10) of early Pliocene age. This lower Pliocene interval (from 538-1-1, 54–55 cm to 538-1-4, 8–9 cm) contains *D. asymmetricus, D. surculus*, and *A. tricorniculatus*. The core interval from 538-1-4, 10–11 cm through 538-1,CC contains an assemblage of the *Sphenolithus ciperoensis* Zone (CP19) of late Oligocene age. Species present include *S. ciperoensis, S. moriformis*, and *Cyclicargolithus abisectus*.

Hole 538A

Drilling in Hole 538A penetrated approximately 267 m of Tertiary and Cretaceous sediments before entering older metamorphic and igneous rocks. Cores 1 through 21 (partim) contain Tertiary sediments, and Cores 21 (partim) through 30 (partim) contain Cretaceous sediments.

The interval from Core 538A-1 through 538A-2-3, 20 cm contains sediments of Miocene age. Core 1 is topped by a hardground developed in upper Miocene sediments. The interval 538A-1-1, 0–27 cm contains *Discoaster quinqueramus, Amaurolithus primus*, and *A. delicatus*, indicating the upper Miocene *D. quinqueramus* Zone (CN9). Samples from the interval between 538A-1-1, 28 cm and 538A-1-2, 63 cm contain *D. hamatus, Catinaster calyculus*, and *D. neohamatus*. This interval is assigned to the *C. calyculus* Subzone (CN7b) of late Miocene age. The core catcher of Core 1 contains *C. coalitus* but lacks both *D. hamatus* and *C. calyculus*, indicating the *C. coalitus* Zone (CN6) of middle Miocene age. The interval from the top of Core 538A-2 to 538A-2-2, 10 cm contains *Reticulofenestra pseudoumbilica, Triquetrorhabdulus rugosus*, and *D. exilis*, but does not contain *Sphenolithus heteromorphus* nor *C. coalitus*. This association indicates the *D. exilis* Zone (CN5) of middle Miocene age. The interval from 538A-2-2, 11 cm through 538A-2-3 contains *Cyclicargolithus floridanus, D. deflandrei*, and *T. carinatus*, but lacks both *S. belemnos* and *S. ciperoensis*. This indicates that this interval is in the *T. carinatus* Zone (CN1).

The interval from 538A-2,CC through 538A-9 contains an upper Oligocene assemblage that includes *S. ciperoensis, C. abisectus*, and *C. floridanus*. This interval is assigned to the *S. ciperoensis* Zone (CP19). The interval between the top of Core 538A-10 and 538A-10-5, 3–4 cm contains *S. distentus* and *S. predistentus* but lacks *S. ciperoensis*. This interval is assigned to the *S. distentus* Zone (CP18) of late Oligocene age. The interval from 538A-10-5, 22–23 cm through 538A-13-3 contains *S. predistentus* but lacks *S. distentus, R. umbilica*, and *R. hillae*, indicating the *S. predistentus* Zone (CP17) of early Oligocene age. Both 538A-13,CC and 538A-14-1 contain *S. predistentus, R. umbilica*, and *R. hillae*, indicating the *Helicopontosphaera reticulata* Zone (CP16) of early Oligocene age. Some Eocene species, such as *D. barbadiensis* and *D. saipanensis*, occur as very rare, badly dissolved, or overgrown elements of these assemblages.

The core catcher of 538A-14 contains a well-preserved assemblage that includes *D. barbadiensis* and *D. saipanensis* but lacks *Chiasmolithus grandis*, indicating the *D. barbadiensis* Zone (CP15) of late Eocene age. The interval from 538A-15 through 538A-17-5 contains *C. grandis* and *R. umbilica;* this association indicates the *R. umbilica* Zone (CP14) of middle Eocene age. The interval from 538A-17-6 through 538A-20-2, 75 cm contains *Nannotetrina quadrata* and *Rhabdosphaera inflata*, indicating the *R. inflata* Subzone (CP12b) of early middle Eocene age. A beautifully expressed hardground at 538A-20-2, 75 cm separates the overlying lower middle Eocene sediments from the underlying strata.

The interval from 538A-20-2, 75 cm through 538A-21-1, 57 cm contains a biostratigraphic succession of nannofossil assemblages that reveals structural complications in what appears to be a lithologically simple sequence. The interval from 538A-20-2, 75 cm through 538A-20-4, 111 cm contains assemblages typical of the *D. multiradiatus* Zone (CP8) of late Paleocene age. A hardground at 538A-20-4, 111 cm separates this upper Paleocene strata from the underlying sequence. The interval from 538A-20-4, 114 cm through 538A-21-1, 31 cm contains nannofossils of the lower Paleocene (Danian) *Cruciplacolithus tenuis* Subzone (CP1b). A sharp lithologic boundary at 538A-21-1, 32 cm separates this Danian interval from the underlying strata. The structural complications are evident if the sediments immediately below this boundary are considered. The nannofossils in this sediment include *D. barbadiensis* and *D. lodoensis* but lack *D. sublodoensis, Nannotetrina quadrata*, and *Reticulofenestra umbilica*, indicating the *D. lodoensis* Zone (CP11) of early Eocene age. Thus, the Paleocene block lies between two interval of Eocene sediments. Slumping of the Paleocene block is a probable explanation for this situation. Slumping would have taken place during the early Eocene to early middle Eocene.

The lower Eocene sediments (538A-21-1, 32–57 cm) lie on a prominent hardground. The sediments below this hardground are Cretaceous. The interval from 538A-21-1, 60 cm through 538A-21-3, 123 cm contains a rich assemblage that includes *Tetralithus gothicus, T. trifidus*, and *T. aculeus*, indicating a late Campanian to early Maestrichtian age. The interval from 538A-21-3, 127 cm through 538A-21-4, 78 cm contains *T. gothicus* and *T. aculeus* without *T. trifidus;* this indicates a middle to late Campanian age. The interval 538A-21-4, 80–110 cm contains nannofossils of the *Marthasterites furcatus* Zone of Coniacian to early Santonian age. A high angle fault (extending from 538A-21-4, 105–114 cm) is present in the core. Sediments containing nannofossils of the *Eiffellithus turriseiffeli* Zone (late Albian to early Cenomanian) occur on both sides of the fault. In the hanging wall, upper Albian to lower Cenomanian sediments occur at 538A-21-4, 112–114 cm. In the footwall, sediments of late Albian to early Cenomanian age occur at 538A-21-4, 105–114 cm (the entire length of the footwall). These ages suggest that the fault is a minor one; it may have little displacement and resulted in little or no loss of section. Sediments of the *E. turriseiffeli* Zone occur from 538A-21-4, 105 cm through 538A-23-1, 40 cm (in the footwall of the fault). Sediments within this interval include hard limestones, softer marls, and calcareous clays, and (from 538A-23-1, 33–40 cm) a nannofossil ooze. The occurrence of nannofossil ooze underlying hard nannofossil limestone in this short sequence is somewhat curious. Preservation of nannofossils throughout this interval is excellent.

The sediments between 538A-23-1, 41 cm and 538A-30-1, 6 cm are limestones with no significant nannofossil assemblages. No age can be assigned to this interval using nannofossils. A thin layer of nannofossil limestone occurs at 538A-30-1, 6–7 cm, lying directly on metamorphic rock. The sparse, moderately preserved assemblage of nannofossils recovered from this sediment indicates an early Berriasian through Valanginian age. Species present include *Retecapsa angustiforata, Rucinolithus wisei, Parhabdolithus asper*, and *Lithraphidites carniolensis.*

SEDIMENTATION RATES

Thirty-three cores were recovered from Hole 538A. The majority of the sedimentary record is punctuated by hiatuses, which make it difficult to compute accurate sedimentation rates. However, two intervals, middle Eocene and Oligocene, are relatively complete. These two intervals have been chosen for the calculation of sedimentation rates.

Core 538A-2 through 538A-13-3 contain an Oligocene section (Fig. 7), which is apparently continuous. The lowermost Oligocene and the Eocene/Oligocene boundary were not recovered. Cores 14 through 17 of Hole 538A apparently contain a continuous sequence of the middle Eocene. A list of the biostratigraphic data employed to define each of the sediment accumulation boxes is given below.

Figure 7 box	Biozone	Sedimentation rate (m/Ma)
1	lower *Globigerina ciperoensis* Zone, P22	36
2	upper *Globorotalia opima* Zone, P21a	9
3	middle *G. opima* Zone, upper P21a; base of box defined by the bottom of *Sphenolithus ciperoensis* Zone (CP19)	19
4	lower *G. opima* Zone, lower P21a	19
5	lowest *G. opima* Zone and *Globigerina ampliaperta* Zone, P20	5
6	*Cassigerinella chipolensis* Zone, upper P19; base of box defined by bottom of *S. predistentus* Zone (CP17)	1
Hiatus		
7	*Truncorotaloides rohri* Zone, P14	5
8	*Orbulinoides beckmanni* Zone, P13	5

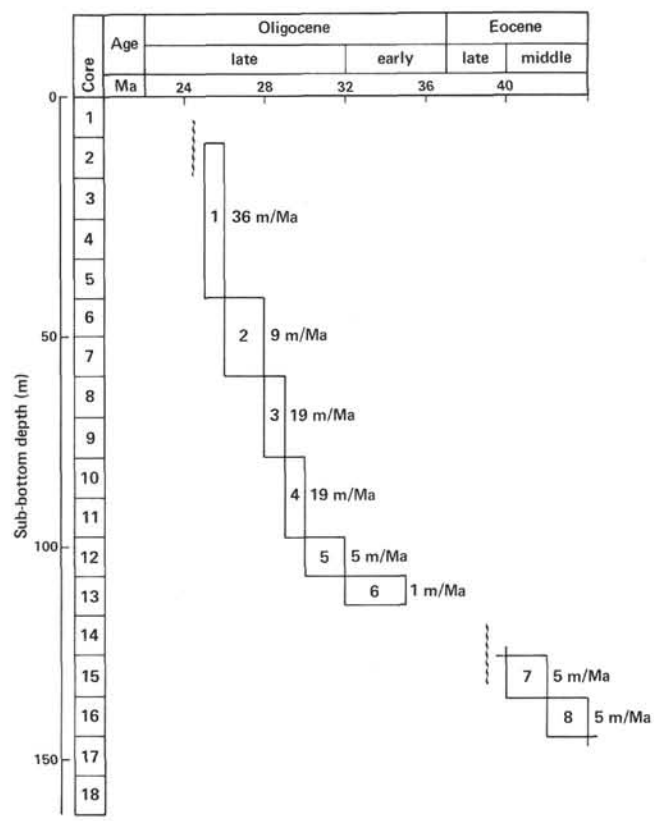

Figure 7. Oligocene and middle Eocene sedimentation rate curves for Site 538. Data from Hole 538A. Numbered boxes give the depth and age ranges of zones described in the text. Wavy lines indicate hiatuses.

The sedimentation rate is low for the middle Eocene and early Oligocene intervals (Cores 16 through 12). The rate increases three-fold for the early late Oligocene (Fig. 7). This increase is even more marked in the later portion of the late Oligocene (Cores 2 through 5). The sedimentation rate increases markedly after 30 Ma and this age corresponds with a significant global sea level lowstand (Vail et al., 1977). The increased rates for the section younger than 30 Ma could reflect the subsequent sea level rise and establishment of a suitable pelagic depositional environment, one perhaps favored by a combination of increased productivity and sediment preservation.

IGNEOUS AND METAMORPHIC PETROLOGY

The igneous and metamorphic rocks underlying the sedimentary sequence in Hole 538A include gneiss and amphibolite intruded by diabase dikes. The diabase dikes allow convenient separation of this complex into four lithologic units. These are illustrated in Figure 8 and discussed below.

Unit I: Cores 30 to 31

Gneiss and amphibolite are the principal rock types of Unit I. A distinct interval of altered diabase within this sequence permits further separation into three subunits.

Subunit Ia (538A-30-1, 5 cm to base of core). Dark gray, variably mylonitic, felsic gneiss with a steeply dipping fabric composes this subunit. The contact of this gneiss with the overlying limestone was apparently recovered in 538A-30-1 (piece 2), where several fragments of fractured, partly brecciated, and calcite-cemented gneiss are coated with a thin veneer of white, chalky nannofossil limestone. The uppermost piece is coated on two sides with this limestone; the underlying fragment has only a thin coating at its top surface. The gneiss is fine-grained to coarse-grained with a porphyritic texture. Protomylonitic textures are locally developed. Quartz is the most abundant mineral (about 50%), forming irregular and elongate crystals up to 2 mm long with sutured contacts. Feldspars (about 20%) occur as large (up to 3 mm) porphyroblasts of orthoclase, as smaller interstitial groups of perthitic orthoclase-albite, and as granular crystals (0.1–0.05 mm) of albite. Some orthoclase is zoned. Greenish brown pleochroic biotite is common (about 5%) in the gneiss as small (0.1–0.05 mm), platy crystals aligned parallel to apparent shear zones. Locally, biotite is completely replaced by chlorite. Sphene occurs as small (0.1–0.3 mm, but can be up to 1 mm), idioblastic grains, some with opaque minerals in their cores. Opaque minerals are cubic or subhedral (about 0.1–0.5 mm) and randomly distributed. A large pink calcite vein cuts this gneiss in 538A-30-1.

Subunit Ib: (538A-31-1, 0–105 cm). This subunit includes a thin interval of green, very fine-grained, altered diabase that grades downcore to dark green, severely altered diabase with calcite veins. The diabase consists of small (0.01–0.02 mm) plagioclase laths (about AN_{45-55}) with subophitic to intersertal intergrowths of pyroxene and interstitial glass, the latter two completely altered to green clay. Small (0.01–0.1 mm) skeletal and cubic crystals of magnetite occur along the edges of plagioclase laths.

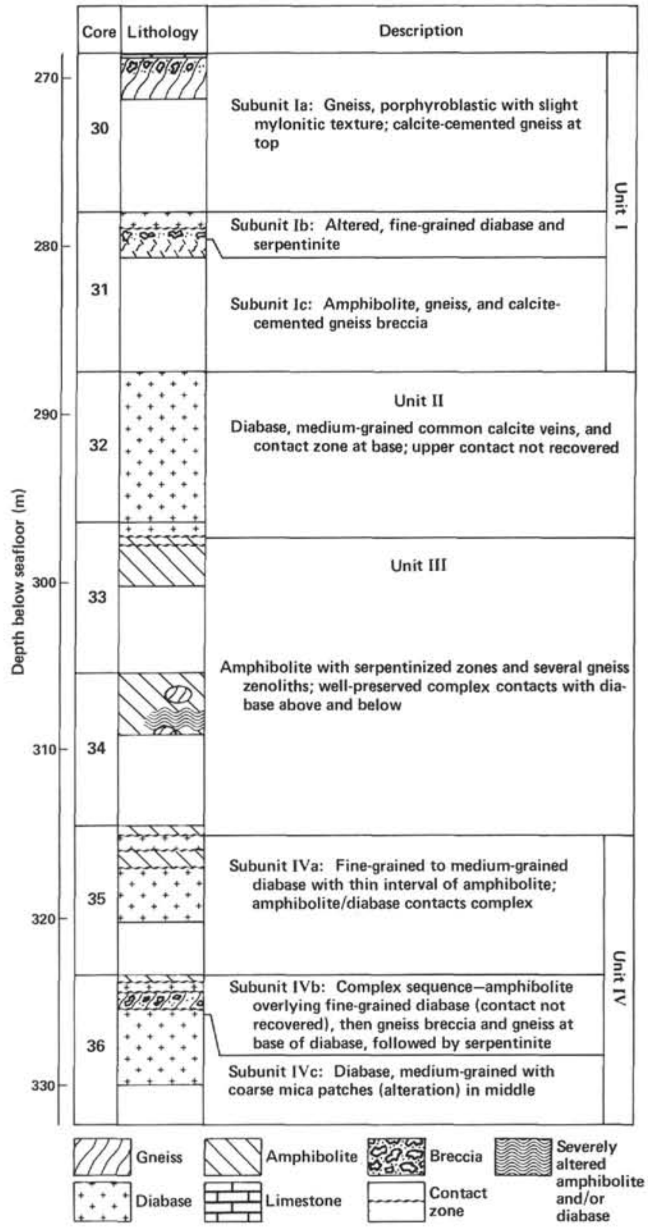

Figure 8. Summary of igneous and metamorphic rocks at Hole 538A.

Subunit Ic (538A-31-1, 105 cm to base of core). This lower subunit is a complex association of gneiss and amphibolite. At the top a calcite-cemented gneiss breccia occurs. Below this is dark gray green amphibolite interlayered in the middle of Section 538A-31-2 by several pieces of gneiss with a steeply dipping fabric. The gneiss is texturally and compositionally identical to that in Subunit Ia. The amphibolite has an ophitic to subophitic texture and consists of about equal proportions of idioblastic green hornblende and xenoblastic plagioclase with minor sphene (less than 1%) and no opaque minerals. The hornblende is strongly pleochroic and has good cleavage and an extinction angle of about 16°. Plagioclase crystals (about AN_{40}) are slightly larger than the hornblende and partly sericitized. Sphene occurs as small (about 0.2 mm) xenoblastic crystals associated with the hornblende. We observed only a faint lineation in thin sections of this amphibolite. However, some fragments at the base of Core 31 have a strong steeply dipping fabric, parallel to the gneiss.

Unit II: Top of Core 538A-32 to 538A-33-1, 120 cm

Medium gray to dark gray, fine-grained to medium-grained diabase with abundant calcite vein makes up Unit II. It has an ophitic to subophitic texture and consists of plagioclase (55%), pyroxene (40%), interstitial glass (about 5%; completely altered to green clay), minor biotite (less than 1%), and opaque minerals (about 5%). Plagioclases (about An_{30-65}) are zoned, lath-shaped crystals (1–2 mm long) with common Carlsband and albite twins. Pyroxene is mostly normal euhedral augite (0.2–1.2 mm) with $Z \wedge C \sim 40°$, $2V \sim 60°$ and a positive optic sign. One hundred twins occur in the larger euhedral crystals. Green clay, probably a replacement of glass, occurs in interstices between plagioclase and augite crystals. Small, platy, green brown, pleochroic biotite crystals are associated with this clay. Opaques (magnetite?) form skeletal and interstitial, granular crystals up to 0.5 mm across. The upper contact of this diabase with Unit I is a drilling break. The lower contact with amphibolite of Unit III is a wide alteration zone of 538A-33-1, 10–110 cm. Abundant calcite veins cut this zone. A diabase sample from the middle of this zone shows relict biotite, plagioclase laths, and augite crystals, the latter apparently pseudomorphed by calcite. The lowest piece (538A-33-1, 110 cm) has a relict metamorphic fabric.

Unit III: 538A-33-1, 120 cm through Base of Core 538A-34

Green to medium gray and dark gray, fine-grained, variably altered amphibolite forms the bulk of Unit III. It is texturally and compositionally similar to amphibolite described in Subunit Ic except that it contains up to 5% opaque minerals and the hornblendes are more altered. The hornblende is green, strongly pleochroic with ragged terminations. It occurs as ophitic to subophitic intergrowths with plagioclase and as inclusions in some large plagioclase crystals. Plagioclase crystals (about An_{30-45}) are about 0.2–0.4 mm across and twinned (albite mostly, but Carlsbad for larger crystals). Opaque minerals are irregular or subhedral (0.1–0.2 mm) occurring mostly in the centers of hornblende crystals. A well-developed linear fabric is evident in thin section.

Enclaves of felsic gneiss occur locally in Unit III. The best examples are in 538A-34-2 and 538A-34-3, where complete gradations from gneiss to amphibolite can be seen. Relatively unaltered gneiss is similar to that in Unit I. Several pieces (e.g., piece 6 in 538A-34-3) have protomylonite to mylonite textures, with large 1–2 mm porphyroblasts of fractured feldspar (orthoclase and perthitic orthoclase-albite) and an interstitial "fluxion" foliation defined by ribbons of recrystallized quartz and biotite. Epidote (less than 1%) is present as small (0.1-mm) broken grains along the fluxion surface. Soft, dark green severely altered amphibolite and/or diabase(?) is common in 538A-34-2.

Unit IV: Top of Core 35 through Core 36

Fine-grained to medium-grained diabase forms most of Unit IV. It is texturally and compositionally similar to that of Unit II. The occurrence of variably altered amphibolite and gneiss breccia in the top of Core 36 permit a threefold division of this unit.

Subunit IVa: Core 35. This subunit consists of fine-grained to medium-grained, calcite-veined diabase and a thin interval of amphibolite and common calcite veins. The diabase is composed of plagioclase, augite, biotite, opaque minerals, and green clay (altered interstitial glass). It is texturally and mineralogically similar to that of Unit II. A 2-cm thick "lens" of pink feldspar (and quartz?) occurs in this diabase at 538A-35-1, 45 cm.

The amphibolite is dark gray and medium-grained to coarse-grained. It is highly altered green clay, particularly near its lower contact with the diabase. The contacts between these rocks are steep, complex, and extensively veined with calcite.

Subunit IVb (top of Core 538A-36 to 538A-36-2, 55 cm). Amphibolite, diabase, and gneiss breccia make up this subunit. The amphibolite occuring at the top of Section 538A-36-1 is dark gray and macroscopically similar to the amphibolite of Unit III. No thin sections were taken, so it is not possible to compare it further with those Unit III rocks. The contact with the underlying diabase is a drilling break. This diabase is dark gray and very fine-grained with abundant calcite veins. It contains plagioclase, augite, biotite, opaques, and green clay. It is similar in mineralogy and texture to the diabase of Unit II and Subunit IVa. The basal contact of this diabase with the underlying gneiss breccia is obscured by drilling breaks but appears to be gradational; the last few pieces of diabase in 538A-36-1 have a faint gneissose fabric. In addition, fragments of diabase occur in the gneiss breccia. The lowest member of Subunit IVb is a gneiss breccia consisting of gneiss and some diabase fragments (up to 3 cm across) in a calcite cement. Severely altered amphibolite and/or diabase forms the base of this member and the transition to the underlying diabase.

Subunit IVc (538A-36-2, 55 cm to base of core). The dark gray, medium-grained diabase of this subunit is similar to but slightly coarser-grained than the diabase of Subunits IVa and IVb and of Unit II. A zone of alteration containing large (0.5–1 mm) white crystals of mica occurs in 538A-36-3. This mineral is probably muscovite despite the low 2V ($\sim 15°$); it is too hard for talc and the wrong paragenesis for phlogopite(?). Calcite veins are also common in this diabase.

Interpretation

The igneous and metamorphic suite penetrated at Catoche Knoll records a complex history of metamorphism and igneous intrusion. The gneiss and amphibolite of this sequence are, in part, interlayered. Mineral assemblages within both the gneiss and amphibolite are characteristic of middle to upper amphibolite grades of metamorphism. The high grade minerals are aligned into well-defined foliations suggesting that growth occurred during a regional, deep-seated metamorphic event. Later mylonitic fabrics are locally superimposed on the gneiss-amphibolite sequence but are not developed on the diabase dikes. The dikes also show no evidence of metamorphism and are not foliated. Both the metamorphic suite and the dikes are variably affected by low-temperature hydrothermal and/or deuteric alteration. Alteration products occur as unfoliated, pseudomorphic replacements.

Together, textural and mineralogy characteristics of the basement terrain suggest the following history.

1. regional middle to upper amphibolite grade metamorphism (protoliths uncertain) concomitant with penetrative deformation
2. uplift and cooling of the metamorphic terrain
3. local development of high-strain ductile fabrics
4. intrusion of diabase dikes
5. low-temperature alteration

GEOCHEMISTRY

Organic Geochemistry

The techniques used to analyze the organic geochemistry of rocks and sediments on Leg 77 are described in the introductory chapter of this volume. Eleven rock samples were taken from Cores 16 through 22 at Hole 538A for Rock-Eval analysis. From the Rock-Eval data, two CHN and carbonate bomb samples were selected. Unit I, upper Pliocene to upper Oligocene foraminiferal-nannofossil ooze, was not sampled because it was much too light-colored to contain any organic material. Three samples were taken from Unit II, upper Oligocene to middle Eocene nannofossil ooze and chalk, as there were several dark gray intervals in Section 538A-16-5. Seven samples were analyzed from Unit III, a series of different lithologies of middle Eocene to latest Albian age. Unit IV, late Albian nannofossil chalk, was sampled once. Unit V and basement were not sampled because the lithologies were not suitable; the former unit is a skeletal-oolitic limestone and the latter unit is composed of igneous and metamorphic rocks.

Except for the first two samples from Unit II, all other samples give no indication of volatile (S_1) or pyrolyzable (S_2) hydrocarbons (Fig. 9 and Table 3). The two samples from 538A-16-5 (25–26 cm and 60–61 cm) are dark gray nannofossil ooze with S_2 values of 4.5 and 2.1 mg HC/g rock, respectively. The S_2 peak temperature of the two samples is below 435°C, and thus they are immature. The production index is below the minimum value for generated hydrocarbons or for "live" oil shows. Organic and carbonate carbon analyses were carried out on the first two samples to determine the type of kerogen in these rocks. The organic carbon values are 3 and 2 wt.%, respectively. The hydrogen index is low (150 and 105), and the oxygen index is high (80 and 96). Type III kerogens, when they are this low in hydrogen content (0.75 H/C), are generally gas "prone." However, these rocks contain 2–3 wt.% organic carbon so they may yield some oil as well as gas at maturity. Car-

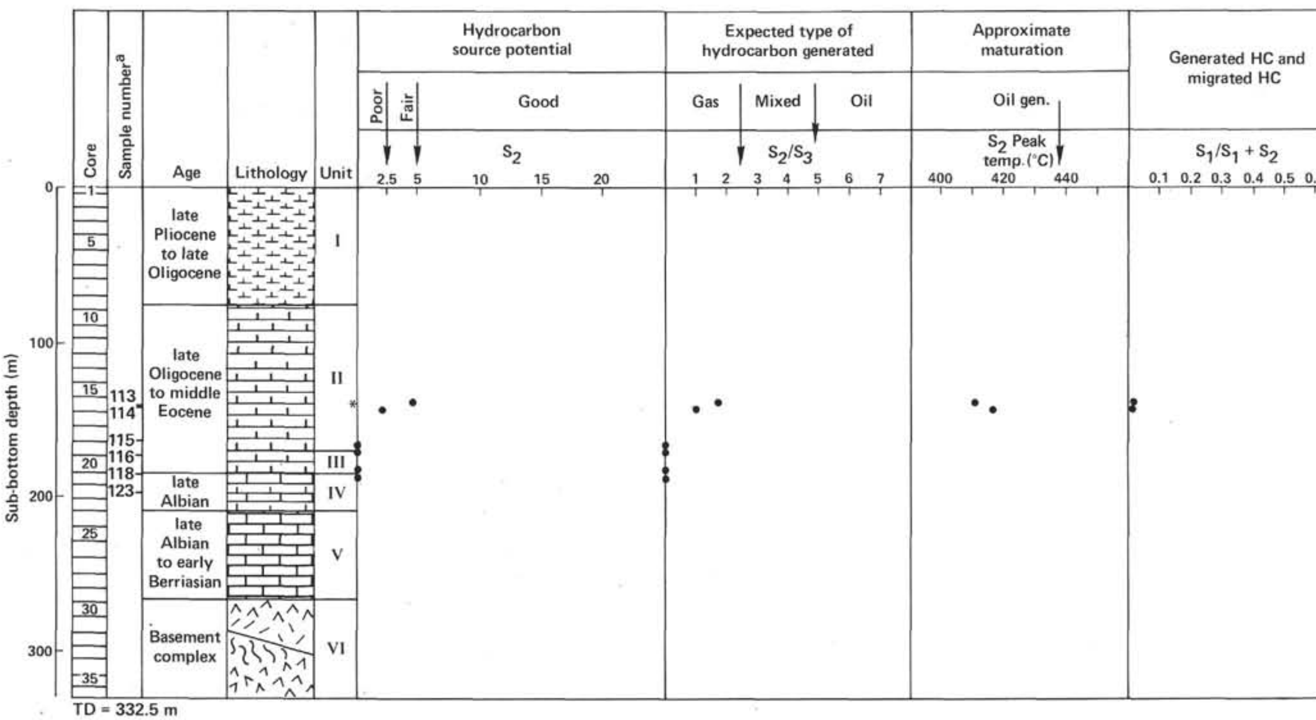

Figure 9. Organic geochemistry summary, Hole 538A (after Clementz et al., 1979). TD = total depth. * denotes asphalt. See Introduction and Explanatory Notes chapter (this volume) for lithologic symbols.

Table 3. Summary of organic geochemistry data, Hole 538A.

Sample no.	Core-Section (interval in cm)	Sub-bottom depth (m)	S_1	S_2	S_2/S_3	S_2 peak temp. (°C)	$\frac{S_1}{S_1 + S_2}$	Organic carbon (wt. %)	CO_3 carbon (wt. %)	Hydrogen index mg HC / g OC	Oxygen index mg CO_2 / g OC
113	16-5, 25-26	141.75	0.24	4.5	1.7	410	0.05	3	52	150	80
114	16-5, 60-61	142.10	0.19	2.1	1.0	415	0.08	2	12	105	96
115	19-2, 14-15	165.64	0	0	0	0					
116	20-1, 53-55	174.03	0	0	0	0					
117	20-2, 132-134	176.32	0	0	0	0					
118	20-5, 116-118	180.66	0	0	0	0					
119	21-1, 14-15	183.14	0	0	0	0					
120	21-3, 7-8	186.07	0	0	0	0					
121	21-4, 69-70	188.09	0	0	0	0					
122	21-5, 5-6	189.05	0	0	0	0					
123	22-1, 38-39	192.88	0	0	0	0					

bon in carbonate for Sample 538A-16-5, 25-26 is 52 wt.%, a marl, whereas that for Sample 538A-16-5, 60-61 is 12 wt.%, a shale (Table 3).

Asphalt was disseminated throughout Core 16 (135.5-141.5 m) as small particles or, in a few cases, as small blebs (1-3 mm). The asphalt did not fluoresce under the fluoroscope but did fluoresce when cut with 1,12,2-tetrachloroethane. There was no oil stain in the host nannofossil chalk, and the dark intervals sampled for the Rock-Eval were not involved.

An explanation for the asphalt in Core 16 may be that in the late Oligocene to middle Eocene, oil or asphalt from a seep near Site 538 settled out of the water column and became incorporated into the sediment on the seafloor. An alternative explanation might be a large oil spill from an Eocene supertanker.

Inorganic Geochemistry

Six samples for carbonate bomb analyses were taken from Hole 538 and 25 samples were taken from Hole 538A. The results are tabulated in Table 4 and are shown on the summary figure (Fig. 2). The analyses generally confirm the petrographic evidence. No interstitial water samples were taken at Hole 538, but four samples were taken at 538A. The results are tabulated on Table 5. The results are typical of many deep-sea sections. Salinity, pH, alkalinity, and chlorinity do not vary significantly with depth. Calcium increases slightly and magnesium decreases somewhat with depth, a pattern common to many deep-sea sites.

Table 4. Carbonate content of selected samples from Holes 538 and 538A.

Hole	Core-Section (interval in cm)	$CaCO_3$ (%)	Hole	Core-Section (interval in cm)	$CaCO_3$ (%)
538	1-1, 25-26	82	538A (cont.)	6-1, 70-71	89
	1-2, 51-52	83		7-2, 61-62	86
	1-2, 137-138	78		8-2, 60-61	84
	1-3, 88-89	76		9-2, 5-6	81
	1-4, 4-5	60		9-2, 60-61	88
	1-4, 40-41			11-2, 60-61	82
				12-2, 60-61	86
				13-2, 60-61	86
538A	1-1, 80-81	43		16-4, 32-33	30
	1-2, 63-64	53		16-4, 89-90	38
	2-1, 24-25	42		16-5, 23-24	53
	2-1, 85-86	71		20-2, 105	88
	2-2, 80-81	86		20-4, 138-140	78
	3-1, 3-4	17		21-4, 76-77	4
	3-1, 94-95	90		21-4, 146-147	6
	3-2, 30-31	85			
	4-2, 80-81	90			
	5-1, 81-82	90			

Table 5. Summary of interstitial water analyses, Hole 538A.

Measurement	Surface	538A-2-1, 144-150 cm	538A-7-3, 144-150 cm	538A-12-4, 114-120 cm	538A-17-6, 144-150 cm
pH	8.25	7.43	7.45	7.42	7.38
Alkalinity (meq/l)	2.53	2.29	2.60	2.69	2.64
Salinity (‰)	37.3	36.4	36.6	36.3	36.6
Calcium (mmol/l)	10.61	11.03	12.92	13.78	14.26
Magnesium (mmol/l)	54.96	51.45	49.91	48.7	49.2
Chlorinity (‰)	20.52	19.71	19.68	19.64	19.64

PALEOMAGNETISM

Danian

At Hole 538A, a 2.1-m section of Danian chalk was recovered from 538A-20-4 through 538A-20-6. It is sandwiched between Eocene rocks and topped by a hardground, implying that it was lithified at the time of slumping. There was apparently little tilting during slumping, because the bedding is nearly horizontal and the foraminiferal zones are in correct stratigraphic sequence. Magnetic polarity determinations should, therefore, be correct, although there may be a slight inclination error. Eleven oriented minicores were taken at 15-25 cm intervals within the Danian section in order to magnetically correlate this sequence with Site 536, where a complete section through the Cretaceous/Tertiary boundary was sampled.

Low intensities made it necessary to measure the samples with a cryogenic magnetometer at the University of Texas, Galveston Geophysics Laboratory. All samples were demagnetized at 50, 100, and 200 Oe, followed by thermal demagnetization at 220, 300, 400, 500, and 550°C. Two samples had a single component of magnetization, and in all other samples two components could be clearly identified from orthogonal vector diagrams. In the latter case, the less stable component was always of normal polarity.

The reversal stratigraphy, derived from the more stable component cannot be unequivocally correlated with the Danian reversal pattern until more detailed paleontologic data are available. The occurrence of two foraminiferal zones (*"Subbotina" pseudobulloides* and *Globorotalia trinidadensis*) in the sample interval necessitates that the reversal pattern includes Anomaly 28. Two possible correlations are shown in Figure 10. One makes use of the observation that Anomaly 27 may consist of a triplet (Gubbio section, Roggenthen and Napoleone, 1977). Additional sampling may help determine the correct correlation. Magnetically this section cannot be correlated with an equivalent section at Site 536.

Basement

The basement complex at Hole 538A (Cores 30 through 36) consists of gneiss and amphibolite intruded by diabase dikes. Low-temperature hydrothermal and/or deuteric alteration locally affects rocks of the basement complex, so sampling was concentrated in unaltered intervals. Twenty-one oriented minicores were taken from the diabase, and five were collected from the amphibolite. Shipboard measurements included initial susceptibility and natural remanent magnetization (NRM). To avoid the effect of the ship's 1-Oe field on any viscous component in the samples, demagnetization was not conducted onboard. Further work was done in the magnetically shielded room at the Galveston Geophysics Laboratory.

Shore-based NRM measurements agreed well with shipboard measurements. After pilot studies, all samples were demagnetized at four or five levels between 50 and 400 Oe, and further demagnetization at 100-Oe intervals was performed on selected samples to a maximum of 700 Oe. The samples behaved very systematically upon demagnetization. Component #1, which is normal in all but two cases, is usually removed by demagnetization to 100 to 200 Oe. Component #2 is a stable component evident at higher demagnetization steps. The stable inclination and other measured parameters are listed in Table 6 and plotted in Figure 11. The magnetic mineralogy of the basement complex is discussed in a separate paper in this volume.

The five amphibolite samples are readily distinguished from the diabase by their low NRM intensities and low susceptibilities. Four of the five samples have a low positive inclination. The negative inclination of the one sample (538A-33-2, 81 cm) may be due to remagnetization during the intrusion of the overlying diabase. A thermoremanent magnetization (TRM) acquired in this manner would also explain the extremely high mean demagnetizing field (MDF) of that sample.

The magnetic parameters provide constraints on any model of diabase intrusion. The diabase from Core 32 differs significantly from that of Core 35 in its polarity, average inclination, Q_n, and NRM intensity. The Q_n and intensity differences can be explained by a different cooling rate, which would result in a different grain-size distribution. The opposite polarities suggest that the intrusions occurred after the end of the Permian Kiaman Interval, which was a period of constant reverse polarity lasting most of the Permian. The difference in inclinations (23.5 versus 37.5°) would suggest north-south block tilting or latitudinal motion between the time of the two intrusions.

The polarities of the diabase in Core 36 present a confusing picture. Each sample was from a different piece and could, therefore, represent a separate diabase dike whose contacts were not recovered. Alternatively, one could call upon a reversely magnetized intrusion adjacent to the drill hole to remagnetize the two middle samples, 538A-36-1, 89 cm and 538A-36-2, 86 cm.

The paleolatitude (σ) of a site is related to magnetic inclination (I) by:

$$\tan \sigma = \tfrac{1}{2} \tan I.$$

The average inclination of the basement rocks at Hole 538A (20.6°) is significantly different from that of the sedimentary rocks of Leg 77 (about 40°). It is tempting to interpret this as evidence of "plate motion." Alternatively, one could assume Catoche Knoll was part of the North American Plate and use the paleolatitude to determine the age of the intrusions. Unfortunately, neither of these approaches can be employed without first cor-

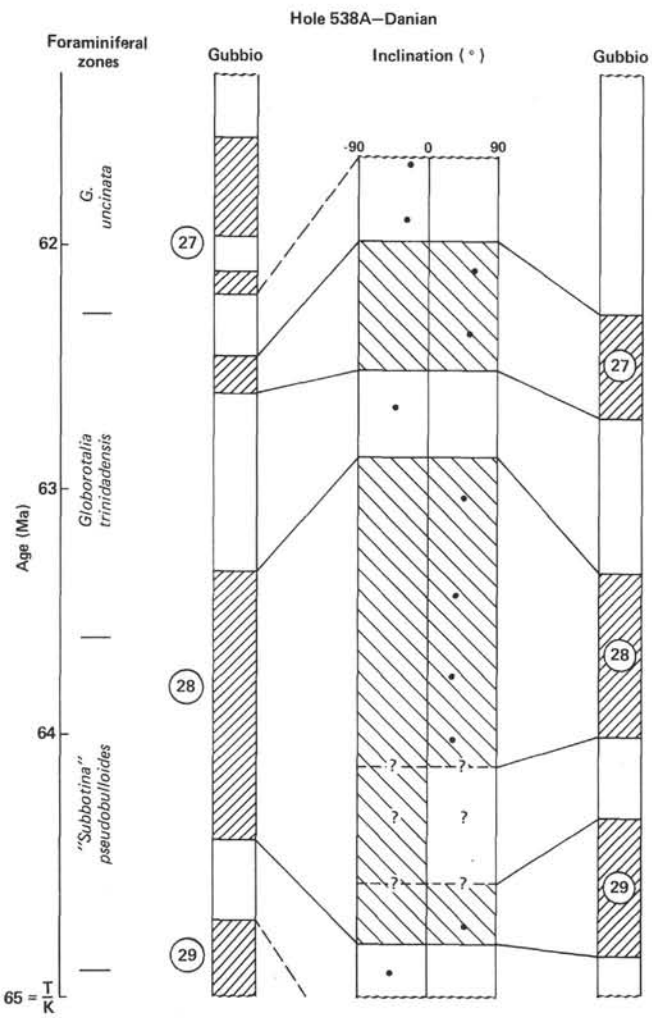

Figure 10. Paleomagnetic results for Hole 538A showing several possible correlations with the Gubbio section (Roggenthen and Napoleone, 1977) and related foraminiferal zones. Circled numbers are marine magnetic anomalies. T = Tertiary; K = Cretaceous.

Table 6. Summary of paleomagnetic data for basement rocks, Hole 538A.

Core-Section (depth in section in cm)	Rock type	Sub-bottom depth (m)	NRM Intensity ($\times 10^{-4}$ emu/cm^3)	NRM Incl. (°)	Stable incl. (°)	MDF (Oe)	Susceptibility ($\times 10^{-4}$) emu/cm^{3}Oe)	Q_n
31-1, 12	Diabase*	278.12	3.06	18.8		325	15.9	0.41
31-1, 23	Diabase*	278.23	2.31	21.1	−21.2	187	21.1	0.23
32-1, 21		287.71	7.33	3.3	−23.0	404	33.6	0.47
32-1, 85		288.35	7.70	−7.0	−27.0	400+	28.1	0.59
32-1, 132		288.82	9.67	−2.2	−33.4	400	32.5	0.64
32-2, 30		289.30	6.72	11.2	−13.3	418	33.2	0.43
32-2, 106		290.06	8.42	−18.3	−25.4	400	31.1	0.58
32-3, 70	Diabase	291.20	5.83	5.4	−22.4	400+	32.4	0.38
32-4, 16		292.16	9.33	28.5		358	32.6	0.61
32-5, 33		293.83	7.07	−10.9	−20.7	353	29.7	0.51
32-5, 141		294.91	6.30	17.9	−21.4	343	20.5	0.66
32-6, 77		295.77	7.03	5.5	−25.3	408	35.0	0.43
32-7, 25		296.75	8.50	3.3	−17.4	246	35.3	0.51
33-2, 81		298.81	0.014	4.2	−15.0	700+	0.67	0.04
33-3, 52		300.02	0.137	25.9	3.0	271	1.32	0.22
34-1, 31	Amphibolite	305.81	0.097	56.3	12.5	156	0.91	0.23
34-1, 40		305.90	0.111	47.9	19.6	196	1.06	0.22
34-1, 70		306.20	0.169	35.3	6.1	305	1.20	0.30
35-1, 14	Diabase*	314.64	3.88	18.8	11.8	194	11.4	0.73
35-3, 146		318.96	17.3	53.6	37.2	177	31.5	1.17
35-4, 18		319.18	19.5	45.3	37.2	314	37.0	1.13
35-4, 94		319.94	31.0	46.1	38.1	254	37.3	1.78
36-1, 57	Diabase	324.07	23.8	24.8	15.5	192	43.5	1.17
36-1, 89		324.39	22.2	8.7	−4.1	178	41.1	1.15
36-2, 86		325.86	6.86	−1.2	−20.8	265	38.4	0.38
36-3, 21		326.71	2.21	46.1	18.0	369	11.5	0.41

Note: NRM = natural remanent magnetization; Inc. = inclination; MDF = mean demagnetizing field; Q_n = Königsberger ratio (H = 0.468 Oe); * = moderately altered.

recting for any tilting that has occurred since the time of the intrusions. Seismic sections from the southeastern Gulf of Mexico indicate that during rifting, tilting of basement blocks was a widespread phenomenon. Indeed, the inclination difference between the diabase in Core 32 and that in Core 35 suggest that Catoche Knoll did tilt. Unfortunately, the seismic lines do not provide sufficient information to correct the inclination data from Hole 538A for possible tilting.

PHYSICAL PROPERTIES

Sonic velocity, density, porosity, thermal conductivity and Torvane shear strength measurements were conducted at Site 538. Continuous GRAPE was run for sediment cores only. The results are listed in Table 7 and are shown graphically in Figure 12. Five groups of samples, each with a significantly different physical properties and lithologies can be distinguished (Table 8). A discussion of these groupings and of vertical trends of these properties follow.

The sonic velocity of unconsolidated nannofossil ooze of Group A reflects only the horizontal component. The sonic velocity values of this group are distributed mostly between 1.5 and 1.7 km/s and they show little change with depth. At the bottom of Group A, where sediments consist of homogeneous nannofossil chalks, the velocity value shows a small but rapid increase by about 0.3 km/s (Fig. 13). This small velocity increase correlates with the boundary of Lithologic Units II and III. Therefore, the section can be divided at this boundary into A (Lithologic Units I and II) and B (Unit III). Below Unit B, there is a sharp change in the acoustic values associated with the change in the lithofacies from Unit III to Unit IV (Fig. 13). An additional acoustic boundary correlates with the lithologic boundary between Units IV and V (base of Group C) (Fig. 13).

Most of the limestones of Group D are highly fragmented and, hence, their orientations could not be determined. The velocity values along vertical and horizontal directions are not differentiated for these samples and they are treated as identical. A low velocity layer is clearly observed in this portion.

The basement rocks have markedly higher velocities than any of the overlying sedimentary units and are easily distinguished (Fig. 13).

The density and porosity distribution showed an abrupt change at around 190 m sub-bottom depth in Hole 538A (Fig. 12). Density increases sharply and porosity decreases at this position. These changes correspond to the boundary between Lithologic Units III and IV. The density and porosity principally reflect increasing lithification and diagenesis of the carbonate section.

The Torvane shear strength and the thermal conductivity data show considerable scatter and general increases with depth. Scatter of the Torvane data is probably caused by the disturbance of cores due to drilling. Scatter of the thermal conductivity might reflect poor contacts between sample surface and the flat probe face. The effect is evidently more pronounced as the sample becomes harder (refer to 270–326 m sub-bottom depth in Fig. 12).

SEISMIC STRATIGRAPHY

Site 538 was drilled on the top of Catoche Knoll, which is located about 25 km northeast of the Campeche Escarpment (Fig. 1). The knoll is a large topographic feature that rises over 750 m above the surrounding abyssal seafloor. The seismic data suggest that the knoll is an uplifted and tilted basement block, based on the apparent asymmetry of the block and the possible synrift sediments filling basins between the blocks. This relationship can be seen on regional seismic Line SF-2 (Fig. 3).

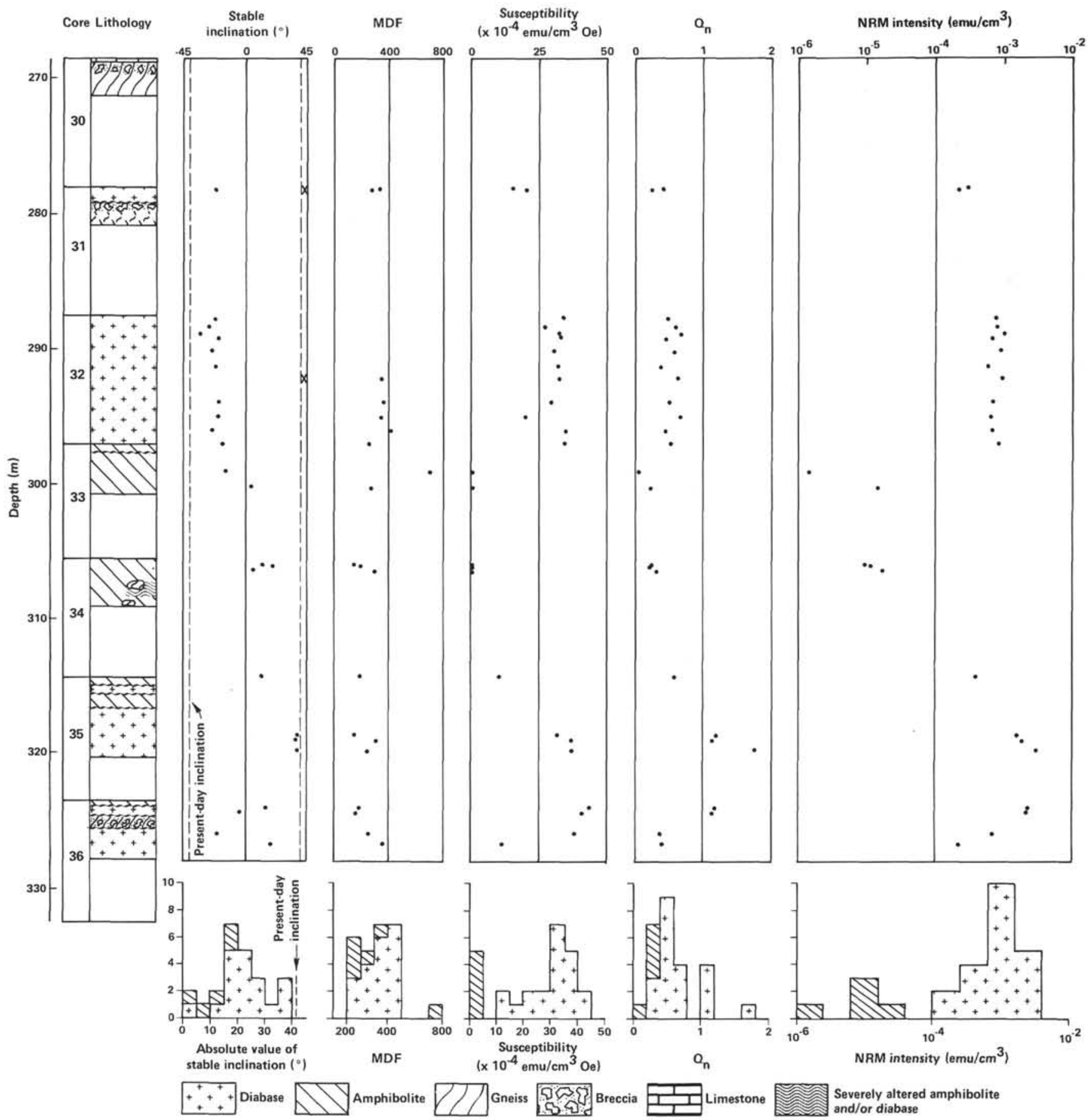

Figure 11. Paleomagnetic summary of basement rocks at Hole 538A. MDF = mean demagnetizing field; Q_n = Königsberger ratio; NRM = natural remanent magnetization.

Single-channel seismic profiles published by Bryant and others (1969) clearly showed the relationship atop Catoche Knoll i.e., an acoustic basement block overlain by a relatively thin sediment cover. More recent multichannel seismic lines shot across the knoll by the University of Texas (SF-2 and GT3-63, Figs. 3 and 14), also show the same relationships.

Line GT3-63 cuts across the western flank of the knoll and shows only a thin sediment cover (Fig. 14), whereas Line SF-2 cuts across the top of the knoll and shows a more complete sedimentary section (Fig. 3). Figure 3 shows the regional setting of the knoll along Line SF-2, whereas Figure 15 shows a more detailed blowup of the site.

The sedimentary section overlying the knoll consists of two main seismic sequences. This subdivision is quite obvious on the earlier single-channel lines of Bryant and others (1969), as well as on the multichannel Line SF-2 (Fig. 15). The two sequences are separated by a strong prominent reflector. Prior to drilling, the upper relatively

Table 7. Summary of physical properties for Holes 538 and 538A.

Core-Section (interval in cm)	Depth (m)	Sonic velocity (km/s) H	Sonic velocity (km/s) V	2-minute GRAPE Wet-bulk density (g/cm^3) H	2-minute GRAPE Wet-bulk density (g/cm^3) V	2-minute GRAPE ϕ (%)	Gravimetrics Wet-bulk density (g/cm^3)	Gravimetrics ϕ (%)	Gravimetrics Water content (%)	Acoustic impedance ($\times 10^5$ g cm^{-2} s^{-1}) vertical	Tor-vane shear strength (kPa)	Thermal conductivity ($\times 10^{-3}$ cal·deg^{-1} cm^{-1} s^{-1})	Lithology
Hole 538													
1-1, 120-122	1	1.549					1.57			2.43	7.13		
1-2, 120-122	3	1.542					1.57			2.42	12.07	2.73	Nannofossil ooze
1-3, 120-122	4	1.519					1.58			2.40	21.07		
1-4, 25-27	5	1.648					1.74			2.87	16.91	2.59	
Hole 538A													
1-1, 140-143	1	1.555					1.55			2.41	27.77	2.70	
1-2, 55-58	2	1.532					1.57			2.41	42.13	2.57	
2-1, 129-132	4	1.544					1.55	69	44	2.40	18.67		
2-2, 125-128	5	1.563					1.64	65	40	2.56	8.14	2.92	
3-1, 60-63	13	1.527					1.63	65	40	2.49	11.49		
3-2, 60-63	14	1.539					1.63	65	40	2.51	20.11	2.67	
4-1, 127-130	23	1.500					1.67	62	37	2.51	13.41		
4-3, 127-130	25	1.555					1.66	63	38	2.58	16.28	2.56	
5-1, 127-130	32	1.549					1.65	62	37	2.56	16.66		
5-2, 95-98	33	1.600					1.68	61	36	2.69	39.26	2.79	Carbonate ooze
6-1, 130-133	42	1.587					1.67	62	37	2.65	35.91	2.80	
6-3, 110-113	45	1.561					1.70	60	35	2.65	27.29		
7-1, 110-113	51	1.614					1.64	61	37	2.65	22.03	2.86	
7-3, 105-108	54	1.544					1.56	65	42	2.41	35.43		
8-1, 43-46	60	1.606					1.63	63	38	2.62	23.46	2.65	
8-3, 56-59	63	1.552					1.57	64	41	2.44	22.98		
9-1, 120-123	70	1.568					1.63	63	39	2.56	24.89		
9-4, 115-118	75	1.625					1.66	61	37	2.70	32.56	1.90	
10-1, 135-138	80	1.644					1.65	60	36	2.71	17.24		
10-5, 88-90	85	1.617					1.63	63	38	2.64	25.85		Nannofossil ooze
11-1, 125-127	89	1.538					1.60	65	41	2.46	22.98	2.77	
11-2, 125-127	91	1.708					1.62	67	42	2.77	22.02		
12-1, 130-133	99	1.654					1.62	62	38	2.67	22.98	3.07	
12-3, 135-138	102	1.673							39				Chalk
12-5, 30-32	104	1.563					1.63	62	38	2.54	19.13		Ooze
13-1, 125-128	108	1.712	1.711	1.77		55.5	1.77	55	31	3.03		2.92	
13-3, 75-78	111	1.687	1.694	1.69		60.3	1.68	61	36	2.86			Chalk
14-2, 14-17	118	3.295	2.906	2.02		40.6	1.96	38	20	5.70		2.73	
15-1, 42-45	126	1.524					1.66	62	37	2.52		2.37	
16-2, 5-8	137	1.656	1.651	1.61		65.1	1.60	64	40	2.64		3.08	Nannofossil chalk
16-4, 147-150	141	1.657	1.669	1.59		66.3	1.56	66	42	2.61			
16-5, 60-61	142	3.349	2.960	2.05		41.5	1.90	31	16	5.62			Chert
17-2, 145-148	148	1.757	1.666				1.60	64	40	2.67		2.78	
17-5, 5-8	151	1.662	1.709	1.67		61.5	1.62	62	38	2.77			
18-2, 10-13	156	1.648	1.643	1.48		72.8	1.46	70	48	2.40		2.37	
18-4, 5-8	159	1.631	1.645	1.45		74.6	1.42	72	51	2.34			
18-6, 0-3	162	1.650	1.575	1.50		71.6	1.45	70	49	2.28			Chalk
19-1, 70-73	165	1.648	1.648	1.50		71.6	1.51	65	43	2.49		1.96	
19-4, 118-121	170	1.698	1.681	1.44		75.2	1.46	69	47	2.45			
20-1, 147-150	175	2.033	1.991	1.82		52.5	1.79	52	29	3.56			
20-2, 147-150	176	1.821	1.801	1.91		47.2	1.84	50	27	3.31			
20-4, 117-120	179	2.001	2.002	1.69		60.3	1.68	60	36	3.36		3.24	
21-1, 10-13	183	2.027	2.065	1.74		57.3	1.74	57	33	3.59		3.23	Limestone
21-3, 5-8	186	1.864	1.892	1.50		71.6	1.90	47	25	3.60			Chalk
21-5, 5-8	189	1.660	1.641	1.58		66.9	1.57	67	43	2.58			
22-1, 27-30	193	4.709	4.822	2.54		9.6	2.52	11	4	12.15			Limestone
22-1, 75-78	193	5.267	5.126	2.60		6.0	2.52	10	4	12.92			
23-1, 20-23	202	5.694	5.674	2.61		5.4	2.44	15	6	13.85			Chalk
23-1, 45-48	202	4.809	4.565	2.46		14.3	2.44	16	6	11.14			
24-1, 35-37	212	3.688		2.15		32.8	2.25	23	10	8.30			
24-1, 63-65	212	4.463		2.48		13.1	2.45	15	6	10.93			
25-1	221	4.493		2.40		17.9	2.36	18	8	10.60			
26-1	231	3.565					2.26	25	11	8.06			Limestone
27-1	240	3.491		2.32		22.7	2.29	25	11	7.80			
28-1	250	3.710		2.26		26.3	2.32	23	10	8.61			
29-1	259	3.986		2.23		28.1	2.28	23	10	9.09			
30-1, 135-138	270	4.738	4.567	2.52		10.7	2.58	10	4	11.78		5.03	Gneiss
30-2, 60-63	271	4.337	3.728	2.44		15.5	2.48	14	6	9.23			
31-1, 18-21	278	4.192	4.081	2.65		13.3	2.54	17	7	10.36			Diabase
31-1, 135-139	279	5.046	4.546	2.50		11.9	2.52	16	6	11.46			Breccia or gneiss
31-2, 47-50	280	3.948	4.643	2.55		18.7	2.51	17	7	11.65			Altered amphibole
31-2, 82-85	280	5.055	4.572	2.62		14.9	2.48	18	7	11.34			Gneiss
31-2, 125-128	281	6.582	6.394	2.86		2.1	2.86	4	1	18.29			Altered amphibolite
32-1, 50-53	288	6.399	6.372	2.99		<0	2.96	4	1	18.86		4.40	
32-3, 50-53	291	6.154	6.009	2.90		0	2.93	5	2	17.60			Diabase
32-6, 50-53	296	6.160	6.180	2.96		<0	2.95	4	1	18.23			
33-1, 80-83	297	3.618	3.394	2.45		23.5	2.40	23	10	8.16		5.96	
34-1, 50-53	306	5.995	6.125	2.89		0.5	2.81	6	2	17.21		5.13	Diabase (serpentine)
35-1, 110-113	316	4.723	4.802	2.71		10.1	2.70	13	5	12.97		4.03	Diabase
35-2, 10-13	316	5.001	4.952	2.66		12.8	2.65	16	6	13.12		6.50	
36-1, 50-53	324	5.078	5.211	2.89		0.5	2.83	9	3	14.75			
36-2, 94-97	326	4.480	4.838	2.71		10.1	2.69	14	5	13.01		3.44	Diabase with quartz veins

Note: H = horizontal; V = vertical; ϕ = porosity.

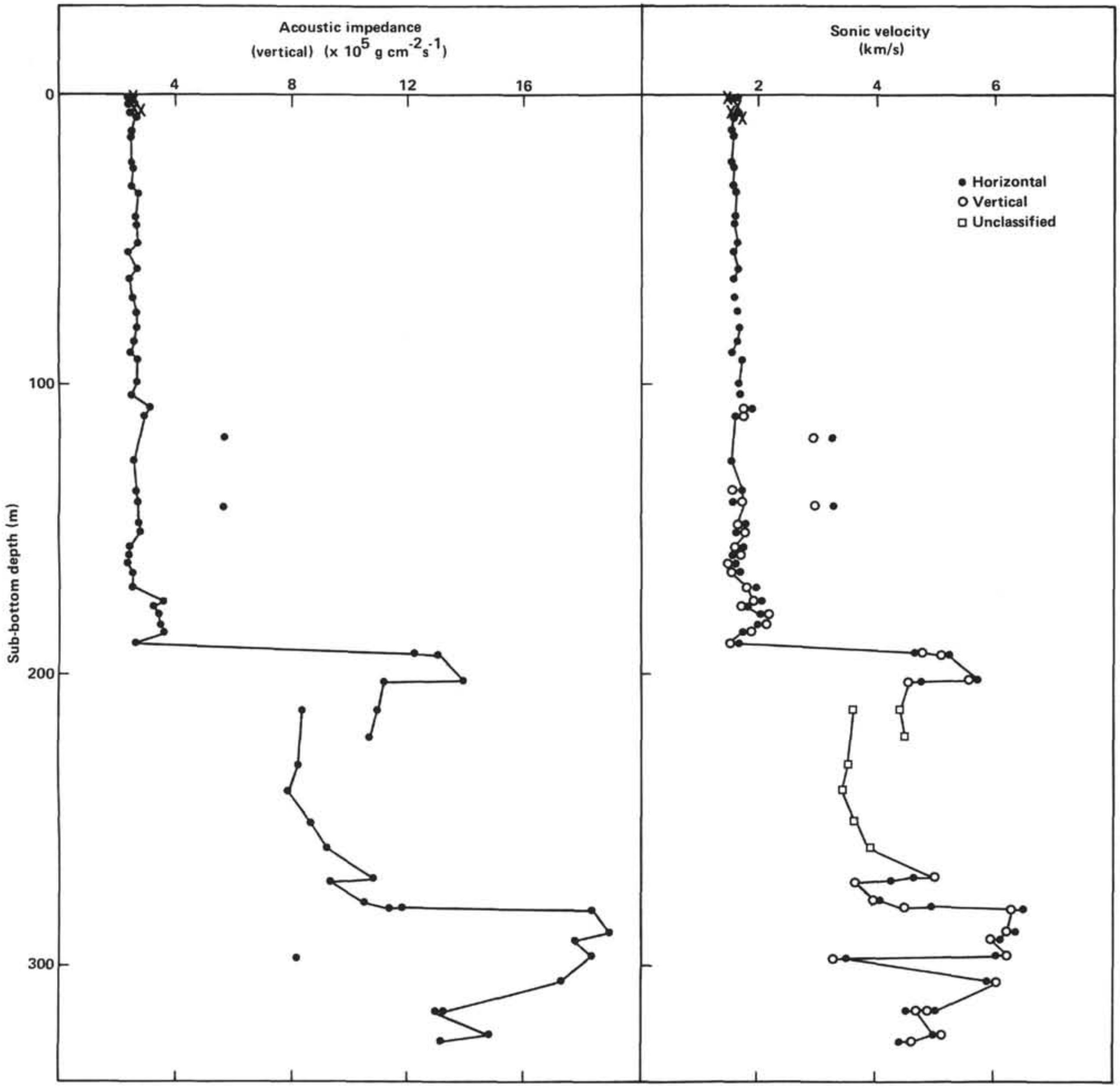

Figure 12. Profiles of selected physical properties, Hole 538A. x's are data from Hole 538 (all horizontal); all other data are from Hole 538A. See Table 7.

transparent sequence was thought to represent mainly Tertiary pelagic sediments, whereas the lower sequence was thought to represent older Mesozoic rocks. The acoustic basement reflector was interpreted to be the top of the crystalline basement and was the main objective of the site.

The final drill site for Hole 538A was located almost exactly along SF-2 at the crest of the knoll (Fig. 15). Drilling at the site penetrated three major lithologic groups as follows: (1) 189 m of ooze and chalk of Miocene through Late Cretaceous age (Lithologic Units I–III); (2) 79 m of deep-water limestone underlain by skeletal-oolitic limestone, both of Early Cretaceous age (Lithologic Units IV–V); and (3) 64 m of igneous-metamorphic basement. Average sonic velocities and calculated acoustic impedances show marked increases at the boundaries between Lithologic Units III and IV (chalk to limestone) and also at the basement (Fig. 16). These changes should produce strong reflectors. These boundaries were converted to two-way traveltime using the measured average velocities (Table 8 and Fig. 16) and were plotted on the seismic section beginning at a water depth of 2801 m (based on 1500 m/s) (Fig. 15). There is a good correspondence between the boundaries and the two strong reflectors on the section. The upper reflection, therefore, is correlated with the major change from Upper Cretaceous-Tertiary ooze and chalk to Lower Cretaceous limestones, whereas the lower reflectors or acoustic basement is correlated with the igneous-metamorphic basement.

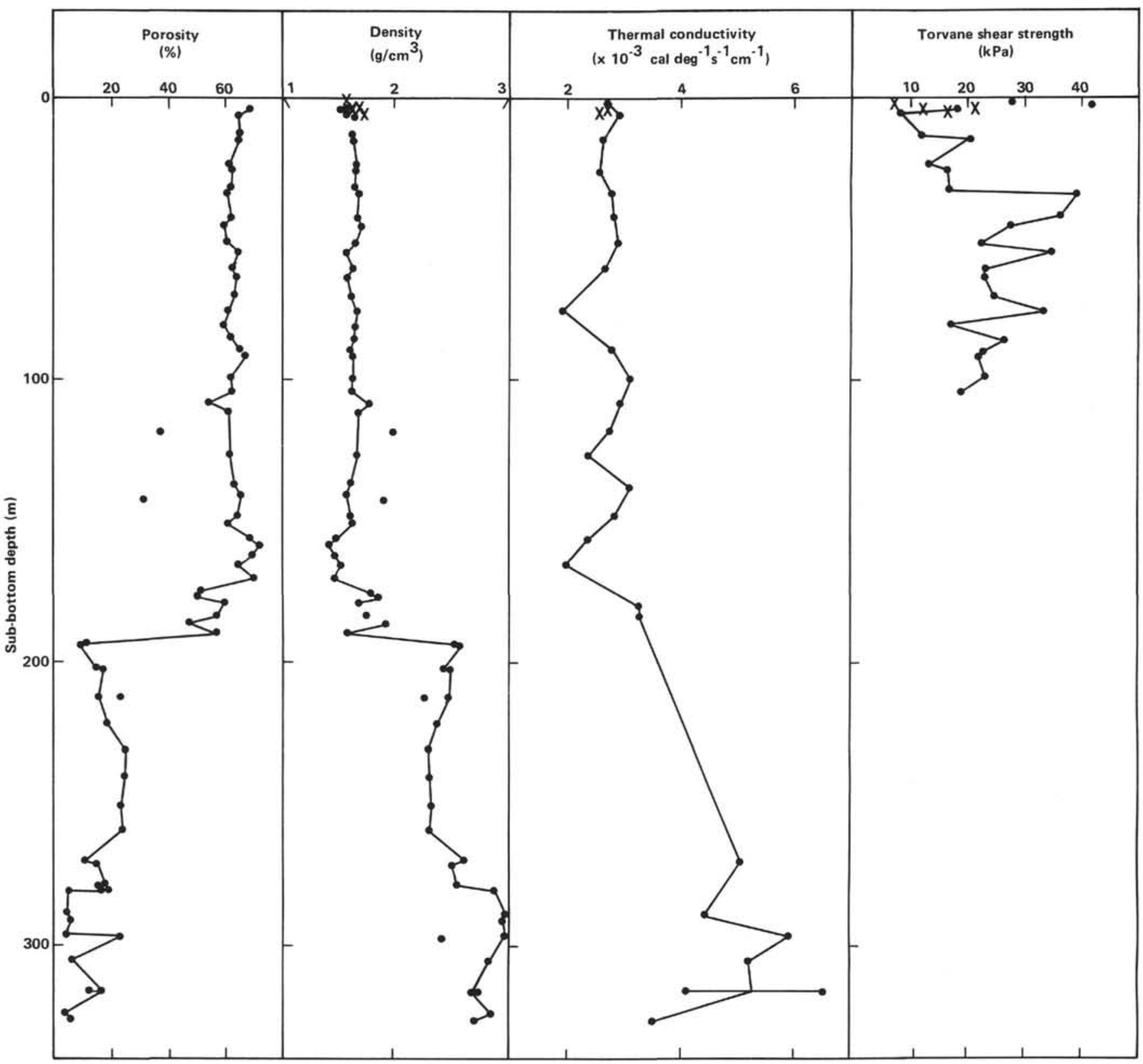

Figure 12. (Continued).

Table 8. Groupings of physical properties, Hole 538A.

Group	Sub-bottom depth (m)	Number of samples	Wet-bulk density (g/cm^3)	Porosity (%)	Acoustic velocity[a] Vert. (km/s)	Acoustic velocity[a] Horiz. (km/s)	Sonic impedance[a] ($\times 10^5$ g cm^{-2} s^{-1})	Thermal conductivity ($\times 10^{-3}$ cal deg^{-1} s^{-1} cm^{-})	Lithology
A	0–171	43	1.62	62	1.74	1.76	2.85	2.66	Units I and II; carbonate ooze and chalk
B	172–189	6	1.63	56	2.00	2.01	3.50	3.24	Unit III; chalk
C	190–211	6	2.43	15	4.99	5.08	12.22		Unit IV; chalk, limestone
D	212–269	5	2.28	18	3.69		8.83		Unit V; limestone
E	270–326	16	2.67	12	5.03	5.09	13.63	4.93	Basement; gneiss, amphibolite, and diabase

[a] Correction applied according to Boyce (1976).

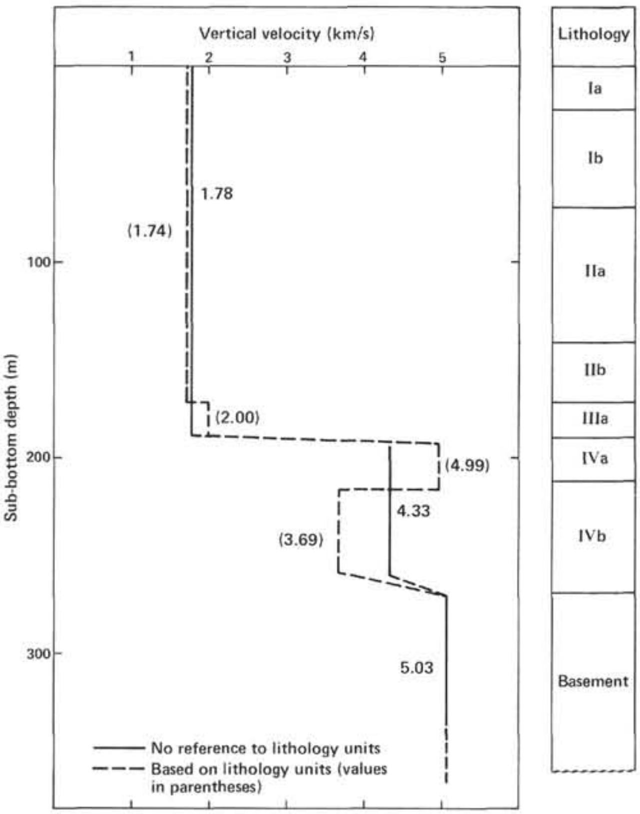

Figure 13. Vertical velocity groupings and corresponding lithologic units, Hole 538A.

The seismic unit in between the two reflectors is tentatively correlated with the skeletal-oolitic limestone (Unit V). A cross section across the knoll using the average velocities from the cores shows that the top of the seismic unit is relatively flat, but the unit thickens considerably along both flanks of the knoll. This supports the hypothesis that this unit was deposited *in situ* as a shallow-water carbonate platform on top of a raised basement block.

CONCLUSIONS

The conclusions concerning this site are given in the Summary section earlier in this chapter.

REFERENCES

Antoine, J., and Ewing, J., 1963. Seismic refraction measurements on the margins of the Gulf of Mexico. *J. Geophys. Res.*, 68:1975–1996.

Benson, W. E., Sheridan, R. E., et al., 1978. *Init. Repts. DSDP*, 44. Washington (U.S. Govt. Printing Office).

Bryant, W. R., Meyerhoff, A. A., Brown, N. K., Furrer, N. A., Pyle, T. E., and Antoine, J. E., 1969. Escarpments, reef trends, and diapiric structures, eastern Gulf of Mexico. *Am. Assoc. Pet. Geol. Bull.*, 53:2506–2542.

Roggenthen, W. M., and Napoleone, G., 1977. Upper Cretaceous-Paleocene magnetic stratigraphy at Gubbio, Italy. IV. Upper Maestrichtian-Paleocene magnetic stratigraphy. *Geol. Soc. Am. Bull.*, 88:378–382.

Tucholke, B. E., Vogt, P. R., et al., 1979. *Init. Repts. DSDP*, 43: Washington (U.S. Govt. Printing Office).

Vail, P. R., Mitchum, R. M., Jr., and Thompson, S., III, 1977. Seismic stratigraphy and global changes in sea level. *In* Payton, C. E. (Ed.), *Seismic Stratigraphic Applications to Hydrocarbon Explorations:* Tulsa, Oklahoma (Am. Assoc. Pet. Geol.), AAPG Mem. 26:49–212.

Worzel, J. L., Bryant, W., et al., 1973. *Init. Repts. DSDP*, 10: Washington (U.S. Govt. Printing Office).

Date of Initial Receipt: July 22, 1983
Date of Acceptance: July 22, 1983

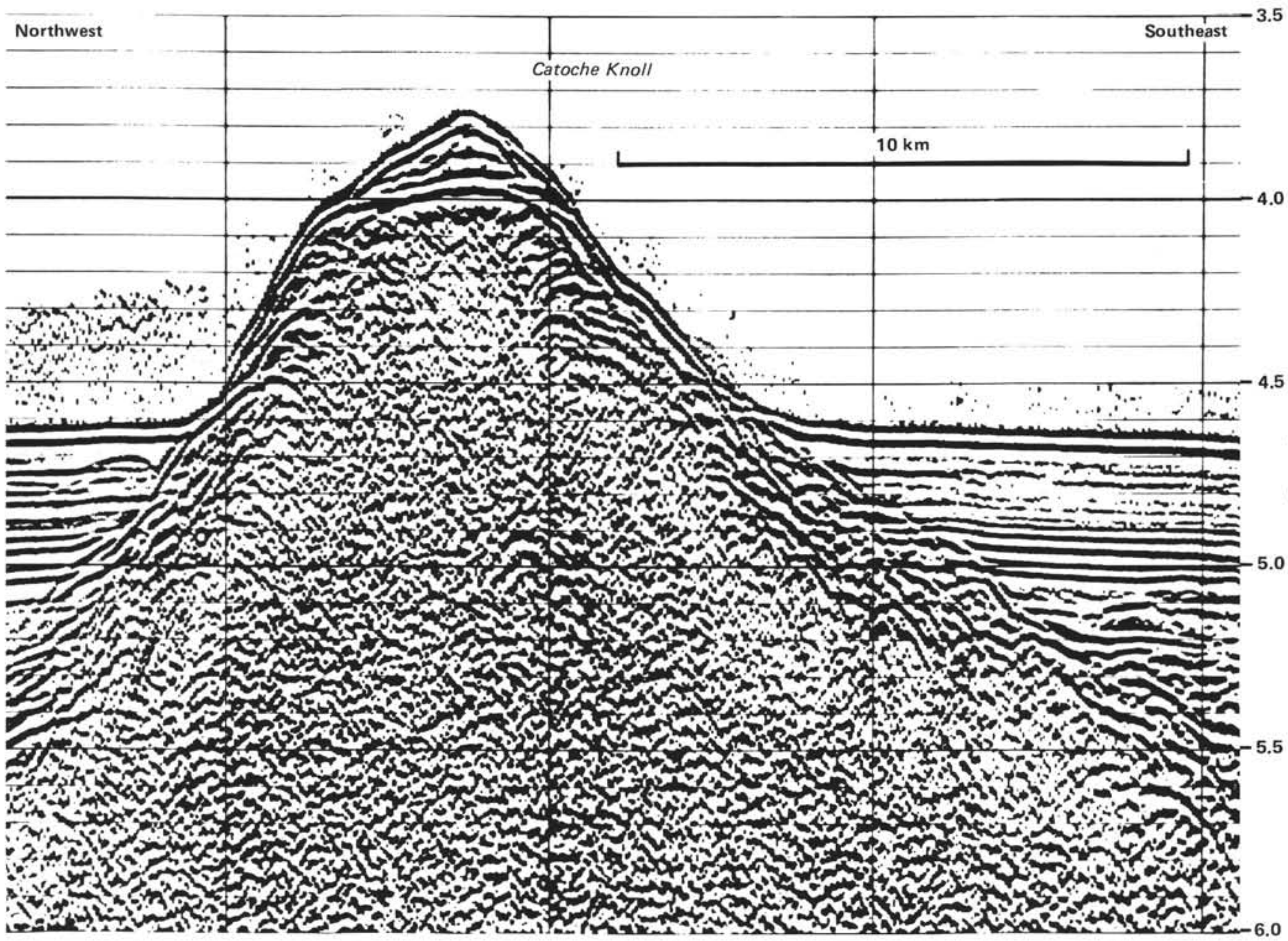

Figure 14. Northwest-southeast seismic Line GT3-63 across the western flank of Catoche Knoll showing sedimentary cover over acoustic basement (see Fig. 1 for location).

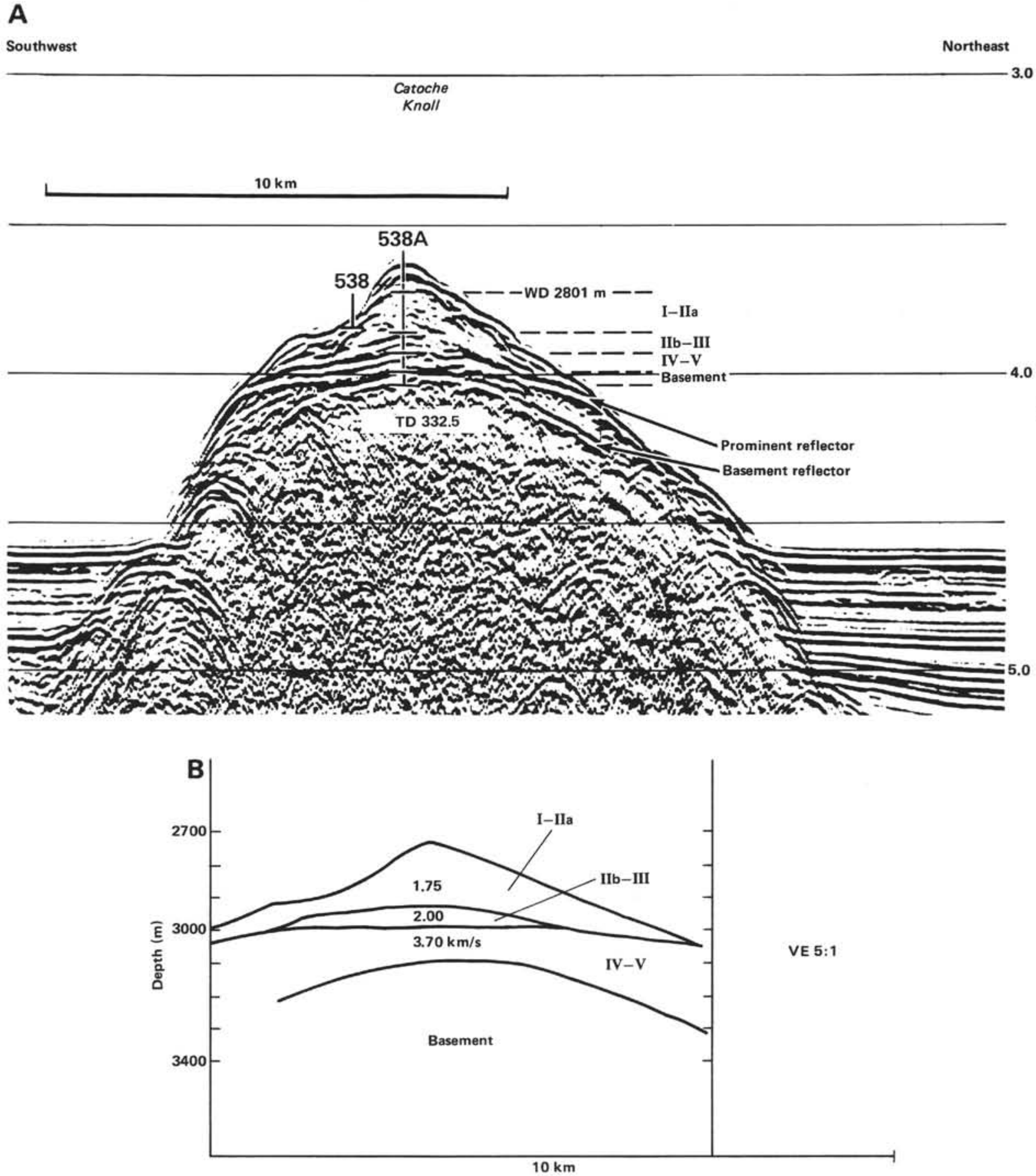

Figure 15. A. Enlarged portion of seismic Line SF-2 (Fig. 2) showing correlation of seismic stratigraphic units with lithologic units drilled at Hole 538A. WD = water depth; TD = terminal depth. B. Depth section showing major seismic units, lithologic units, and average velocity from cores used for depth conversion. VE = vertical exaggeration.

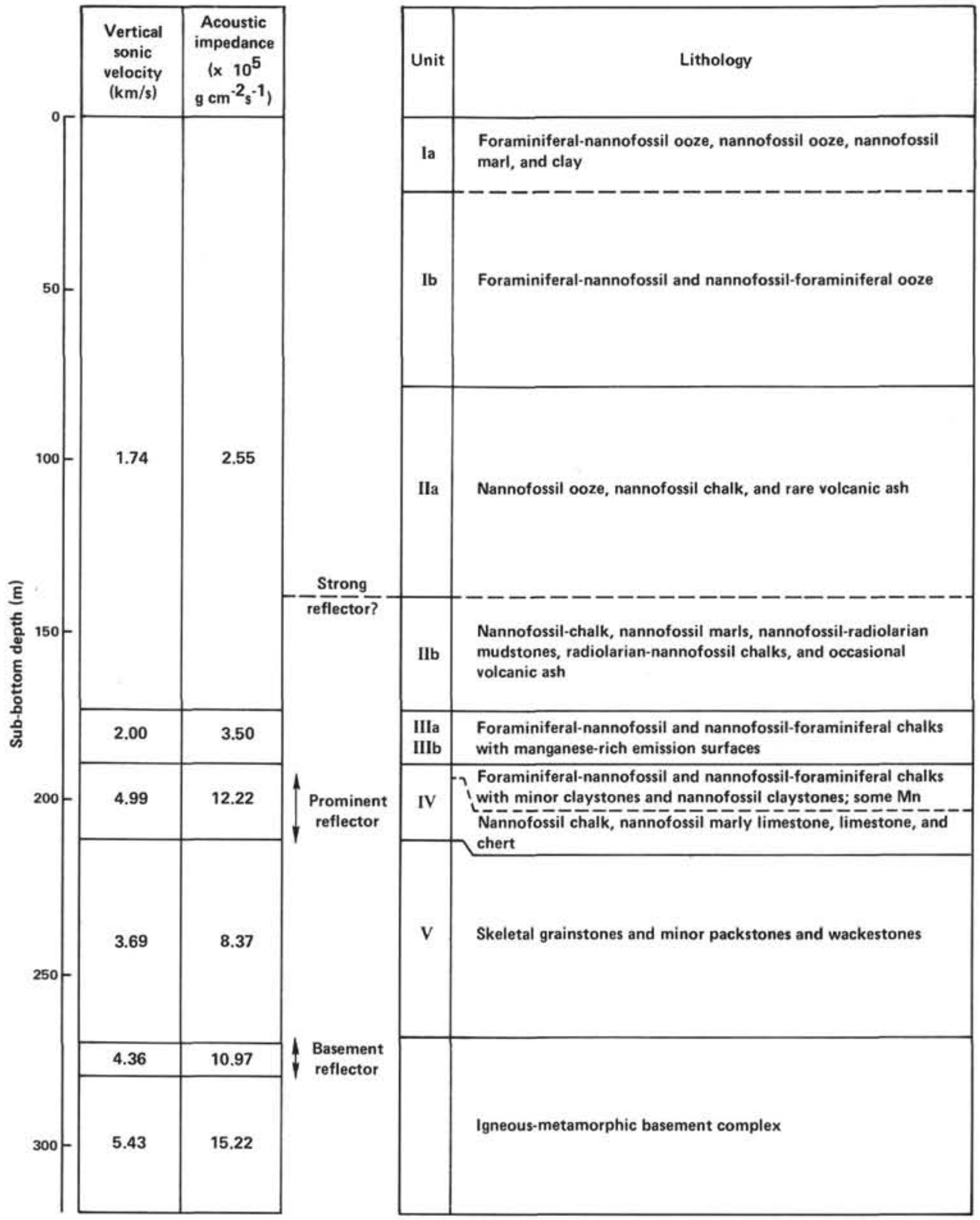

Figure 16. Relation between velocity, acoustic impedance, and lithologic boundaries at Site 538.

SITE 538 HOLE CORE 1 CORED INTERVAL 0.0–6.0 m

TIME – ROCK UNIT: late Pliocene; early Pliocene; late Oligocene

BIOSTRATIGRAPHIC ZONE: CN12a MPL4 (F); *Ceratolithus rugosus* CN10c; *Ceratolithus* MPL2 (F); *Ceratolithus acutus* MPL2 (F); *Sphenolithus ciperoensis* CP19 *Globigerina angulisuturalis* P22

FOSSIL CHARACTER: FORAMINIFERS: AG, AM, AM, CP, AG; NANNOFOSSILS: AG, AG

SECTION: 1, 2, 3, 4, CC

METERS: 0.5, 1.0

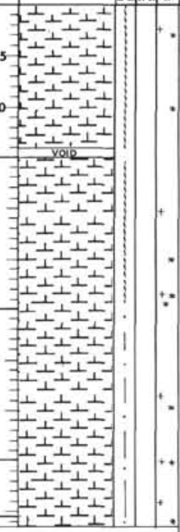

LITHOLOGIC DESCRIPTION

NANNOFOSSIL OOZE, variable colors with generally sharp changes — 1) light gray (2.5Y 7/2) to white (2.5Y 8/2) at 52 cm, Section 1; 2) white to light gray (2.5Y 7/0) at 130 cm, Section 2; 3) gradational change to pale blue green (5BG 7/2) at 145 cm, Section 2; 4) thin light gray interval at 60–72 cm, Section 3; and 5) sharp change of light gray (5Y 7/1) to white (2.5Y 8/0) at 10 cm, Section 4. Core intensely to moderately disturbed by drilling. Mottling common with some faint banding at ~60 cm, Section 3. Small ash-rich patch at 5 cm, Section 4.

SMEAR SLIDE SUMMARY (%):

	1, 30	1, 100	2, 100	2, 137
	D	D	D	D
Texture:				
Sand	6	2	2	7
Silt	86	88	83	78
Clay	8	10	10	15
Composition:				
Mica	–	–	–	3
Clay	8	10	10	15
Carbonate unspec.	5	5	5	5
Foraminifers	6	2	2	7
Calc. nannofossils	81	83	83	67
Dolomite	–	–	–	1

	2, 148	3, 100	4, 5	CC, 5
	M	D	D	D
Texture:				
Sand	10	5	5	1
Silt	–	60	60	89
Clay	35	35	35	10
Composition:				
Mica	–	–	–	–
Clay	35	35	75	10
Volcanic glass	–	–	10	–
Carbonate unspec.	5	5	5	5
Foraminifers	10	5	5	1
Calc. nannofossils	50	50	50	84
Dolomite	Tr	–	–	–

ORGANIC CARBON AND CARBONATE (%):

	1, 25	2, 51	2, 137	3, 88
Organic carbon	–	–	–	–
Carbonate	82	83	78	76

	4, 4	4, 40
Organic carbon	–	–
Carbonate	60	84

SITE 538 HOLE A CORE 1 CORED INTERVAL 0.0–2.5 m

TIME – ROCK UNIT: late Miocene; middle Miocene

BIOSTRATIGRAPHIC ZONE: CN9; *Catinaster calyculus* CN7b; *Catinaster coalitus* CN6 (F)?

FOSSIL CHARACTER: FORAMINIFERS: AM; NANNOFOSSILS: AG, AG, AG, AG

SECTION: 1, 2, CC

METERS: 0.5, 1.0

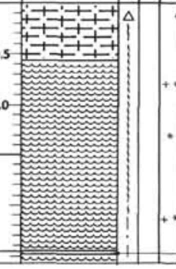

VOID

LITHOLOGIC DESCRIPTION

FORAMINIFERAL-NANNOFOSSIL OOZE and NANNOFOSSIL MARL. Foraminiferal-nannofossil ooze is yellowish gray (5Y 8/1) with slight green and brown tints. Top 20 cm of core contains white (N9) to very light gray (N8) chalk fragments in drilling breccia. Chalk has brownish black spots and yellowish streaky surfaces. Nannofossil marl is yellowish gray (5Y 7/2) to light olive gray (5Y 5/2) changing to greenish gray (5G 6/1) at 50 cm, Section 2. Intense drilling deformation. Streaks of white foraminiferal-nannofossil ooze at 100–130 cm, Section 1.

SMEAR SLIDE SUMMARY (%):

	1, 15	1, 80	1, 131	2, 60
	M	D	D	D
Texture:				
Sand	15	20	10	4
Silt	75	70	80	85
Clay	10	10	10	11
Composition:				
Quartz	–	2	–	2
Feldspar	–	Tr	–	–
Clay	10	20	10	10
Glauconite	–	1	–	–
Foraminifers	15	7	10	2
Calc. nannofossils	75	70	80	85
Diatoms	–	–	Tr	–
Yellow green transparent mineral	–	–	–	1

ORGANIC CARBON AND CARBONATE (%):

	1, 80	2, 63
Organic carbon	–	–
Carbonate	43	53

SITE 538 HOLE A CORE 2 CORED INTERVAL 2.5–12.0 m

TIME – ROCK UNIT: middle Miocene; late Oligocene

BIOSTRATIGRAPHIC ZONE: *Discoaster exilis* CN5; P22 (F) *Triquetrorhabdulus carinatus* CN1 — *Sphenolithus ciperoensis* CP19

FOSSIL CHARACTER: FORAMINIFERS: AG; NANNOFOSSILS: AG

SECTION: 1, 2, 3, CC

METERS: 0.5, 1.0

VOID

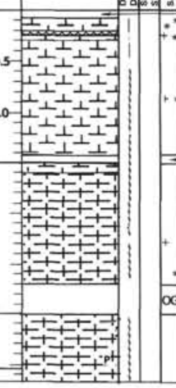

IW

OG

LITHOLOGIC DESCRIPTION

NANNOFOSSIL OOZE and FORAMINIFERAL-NANNOFOSSIL OOZE. Nannofossil ooze is white (N9), yellowish gray (5Y 7/2) to greenish gray (5G 6/1 and 5GY 6/1) and first occurs near top Section 1. Nannofossil ooze below 30 cm is greenish gray (5GY 6/1) changing downcore to very light gray (N8), light greenish gray (5G 8/1) with light to medium gray (N7–N6) streaks. Light–dark ooze contacts generally sharp. Foraminiferal-nannofossil ooze is bluish white (5B 9/1) with some medium gray pyrite streaks. Contact with nannofossil ooze at top Section 2 is mixed by drilling.

SMEAR SLIDE SUMMARY (%):

	1, 8	1, 15	1, 26	1, 89	2, 110
	M	M	M	D	M
Texture:					
Sand	–	Tr	20	5	20
Silt	100	90	60	65	70
Clay	–	10	20	30	10
Composition:					
Quartz	–	–	1	Tr	–
Clay	Tr	10	40	35	10
Carbonate unspec.	3	1	–	3	–
Foraminifers	1	–	–	2	20
Calc. nannofossils	96	89	59	60	70

ORGANIC CARBON AND CARBONATE (%):

	1, 24	1, 85	2, 80
Organic carbon	–	–	–
Carbonate	42	71	88

SITE 538 HOLE A CORE 3 CORED INTERVAL 12.0–21.5 m

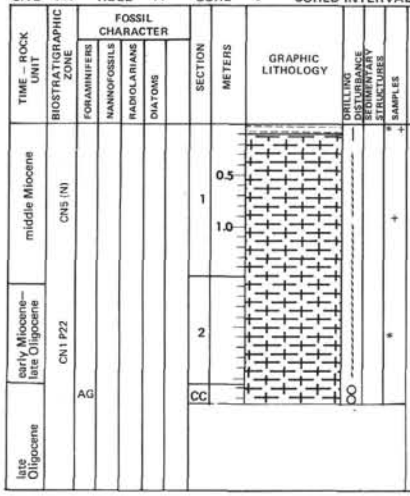

LITHOLOGIC DESCRIPTION

FORAMINIFERAL-NANNOFOSSIL OOZE, bluish white (5B 9/1) with some light gray (N7) streaks, intensely disturbed by drilling. Thin interval of greenish gray (5G 6/1) clay at top Section 1.

SMEAR SLIDE SUMMARY (%):

	1,1	2, 60
	M	D
Texture:		
Sand	1	20
Silt	74	70
Clay	25	10
Composition:		
Quartz	1	–
Clay	25	10
Foraminifers	–	20
Calc. nanno-fossils	70	70
Dolomite	Tr	–

ORGANIC CARBON AND CARBONATE (%):

	1, 3	1, 94
Organic carbon	–	–
Carbonate	17	90

SITE 538 HOLE A CORE 4 CORED INTERVAL 21.5–31.0 m

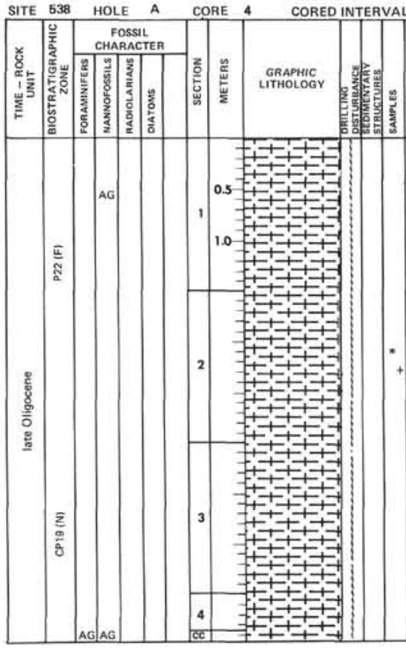

LITHOLOGIC DESCRIPTION

FORAMINIFERAL-NANNOFOSSIL OOZE, very pale blue (5B 8/2) to very light gray (N8), homogeneous, intense drilling deformation.

SMEAR SLIDE SUMMARY (%):

	2, 60
	D
Texture:	
Sand	15
Silt	85
Clay	–
Composition:	
Foraminifers	15
Calc. nannofossils	85
Dolomite	Tr

ORGANIC CARBON AND CARBONATE (%):

	2, 80
Organic carbon	–
Carbonate	90

SITE 538 HOLE A CORE 5 CORED INTERVAL 31.0–40.5 m

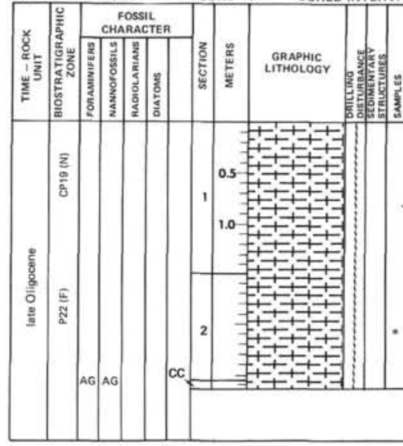

LITHOLOGIC DESCRIPTION

NANNOFOSSIL-FORAMINIFERAL OOZE, mixed very light gray (N8) and very pale blue (5B 8/2), homogeneous with intense drilling deformation.

SMEAR SLIDE SUMMARY (%):

	2, 60
	D
Texture:	
Sand	25
Silt	65
Clay	10
Composition:	
Clay	10
Foraminifers	25
Calc. nannofoossils	65

ORGANIC CARBON AND CARBONATE (%):

	1, 81
Organic carbon	–
Carbonate	90

SITE 538 HOLE A CORE 6 CORED INTERVAL 40.5–50.0 m

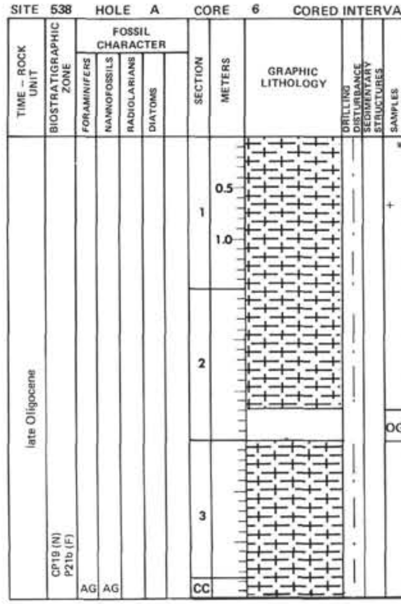

LITHOLOGIC DESCRIPTION

NANNOFOSSIL-FORAMINIFERAL OOZE, light greenish gray (5GY 8/1–5G 8/1) to white (N9) with very light gray (N8) tint at top Section 1. Core is partly lithified (e.g. 48–50 cm, Section 2). Homogeneous and moderate drilling deformation.

SMEAR SLIDE SUMMARY (%):

	1, 10
	D
Texture:	
Sand	40
Silt	60
Clay	–
Composition:	
Foraminifers	40
Calc. nannofossils	60
Diatoms	Tr
Radiolarians	Tr

ORGANIC CARBON AND CARBONATE (%):

	1, 70
Organic carbon	–
Carbonate	84

SITE 538 HOLE A CORE 7 CORED INTERVAL 50.0–59.5 m

TIME-ROCK UNIT: late Oligocene

BIOSTRATIGRAPHIC ZONE: P21b (F); CP19 (N)

FOSSIL CHARACTER: FORAMINIFERS AG; NANNOFOSSILS AG

SECTIONS: 1, 2, 3, 4, CC

SAMPLES: IW

LITHOLOGIC DESCRIPTION

NANNOFOSSIL-FORAMINIFERAL OOZE, white (N9) to light greenish gray (5GY 8/1), homogeneous, semi-lithified parts throughout.

SMEAR SLIDE SUMMARY (%):

	2, 80
	D
Texture:	
Sand	35
Silt	55
Clay	10
Composition:	
Clay	10
Foraminifers	35
Calc. nannofossils	55
Radiolarians	Tr

ORGANIC CARBON AND CARBONATE (%):

	2, 61
Organic carbon	–
Carbonate	86

SITE 538 HOLE A CORE 8 CORED INTERVAL 59.5–69.0 m

TIME-ROCK UNIT: late Oligocene

BIOSTRATIGRAPHIC ZONE: P21b (F); CP19 (N)

FOSSIL CHARACTER: FORAMINIFERS AG; NANNOFOSSILS AG, AG, AG, AG, AG, AG, AG

SECTIONS: 1, 2, 3, CC

LITHOLOGIC DESCRIPTION

NANNOFOSSIL-FORAMINIFERAL OOZE, white (N9) to light greenish gray (5GY 8/1), homogeneous with abundant semi-lithified (chalky) zones.

SMEAR SLIDE SUMMARY (%):

	2, 90
	D
Texture:	
Sand	35
Silt	60
Clay	5
Composition:	
Clay	5
Foraminifers	35
Calc. nannofossils	57
Radiolarians	2
Sponge spicules	1

ORGANIC CARBON AND CARBONATE (%):

	2, 60
Organic carbon	–
Carbonate	84

SITE 538 HOLE A CORE 9 CORED INTERVAL 69.0–78.5 m

TIME-ROCK UNIT: late Oligocene

BIOSTRATIGRAPHIC ZONE: CP19 (N); P21a (F)

FOSSIL CHARACTER: FORAMINIFERS AG; NANNOFOSSILS AG

SECTIONS: 1, 2, 3, 4, CC

SAMPLES: OG

LITHOLOGIC DESCRIPTION

FORAMINIFERAL-NANNOFOSSIL CHALK, white (N9) and light greenish gray (5GY 8/1) to bluish white (5B 9/1) with scattered, thin greenish gray (5G 6/1) and light olive gray (5Y 6/1) bands, homogeneous.

SMEAR SLIDE SUMMARY (%):

	1, 99	2, 5	2, 139
	D	D	D
Texture:			
Sand	10	17	15
Silt	90	83	85
Clay	–	–	–
Composition:			
Carbonate unspec.	–	2	–
Foraminifers	10	17	15
Calc. nannofossils	88	79	80
Sponge spicules	2	2	5
Pteropods	–	Tr	–

ORGANIC CARBON AND CARBONATE (%):

	2, 5	2, 60
Organic carbon	–	–
Carbonate	81	88

SITE 538 HOLE A CORE 10 CORED INTERVAL 78.5–88.0 m

TIME – ROCK UNIT	BIOSTRATIGRAPHIC ZONE	FORAMINIFERS	NANNOFOSSILS	RADIOLARIANS	DIATOMS	SECTION	METERS
late Oligocene	CP18 (N)		AG			1	0.5, 1.0
			AG			2	
			AG			3	
	P21a (F)		AG/M			4	
late–early Oligocene	CP17 (N)		AG/M, AG			5	
		AG	AG			CC	

GRAPHIC LITHOLOGY

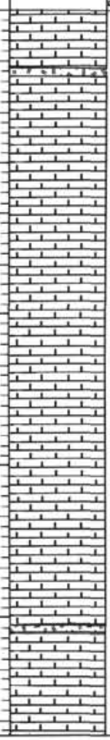

DRILLING DISTURBANCE / SEDIMENTARY STRUCTURES / SAMPLES

LITHOLOGIC DESCRIPTION

NANNOFOSSIL CHALK, white (N9) to bluish white (5B 9/1) with one light greenish gray (5G 8/1) laminated interval at 56 cm, Section 4 and several medium gray (N5) layers of ASH. Upper ash layer is mixed with chalk, lower ash layer has a sharp base and gradational, burrowed top. Chalk is homogeneous.

SMEAR SLIDE SUMMARY (%):

	1, 103	2, 69	3, 69	4, 50	5, 11
	D	D	D	D	M
Texture:					
Sand	2	1	5	2	–
Silt	98	99	95	98	100
Composition:					
Volcanic glass	–	Tr	–	5	96
Carbonate unspec.	2	3	2	4	–
Foraminifers	2	1	5	2	–
Calc. nannofossils	95	96	91	86	Tr
Diatoms	–	Tr	–	–	2
Sponge spicules	1	1	2	3	–
Dolomite	–	–	–	Tr	–

SITE 538 HOLE A CORE 11 CORED INTERVAL 88.0–97.5 m

TIME – ROCK UNIT	BIOSTRATIGRAPHIC ZONE	FORAMINIFERS	NANNOFOSSILS	RADIOLARIANS	DIATOMS	SECTION	METERS
late–early Oligocene	P21a (F)					1	0.5, 1.0
	CP17 (N)					2	
		AG	AG			CC	

GRAPHIC LITHOLOGY

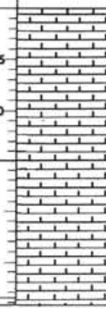

DRILLING DISTURBANCE / SEDIMENTARY STRUCTURES / SAMPLES

LITHOLOGIC DESCRIPTION

NANNOFOSSIL CHALK, white (N9) to bluish white (5B 9/1) with some light greenish gray (5G 8/1) zones and light gray (N7) to very light gray (N8) laminations.

SMEAR SLIDE SUMMARY (%):

	1, 57	2, 65
	D	D
Texture:		
Sand	5	10
Silt	95	90
Composition:		
Volcanic glass	Tr	–
Carbonate unspec.	3	2
Foraminifers	5	10
Calc. nannofossils	90	83
Diatoms	–	Tr
Radiolarians	–	1
Sponge spicules	2	4
Holothurian spines	Tr	–

ORGANIC CARBON AND CARBONATE (%):

	2, 60
Organic carbon	–
Carbonate	82

SITE 538 HOLE A CORE 12 CORED INTERVAL 97.5–107.0 m

TIME-ROCK UNIT: early Oligocene
BIOSTRATIGRAPHIC ZONE: CP17 (N); P20 (F)
FOSSIL CHARACTER: AG AM (CC)
SECTIONS: 1, 2, 3, 4, 5, CC

LITHOLOGIC DESCRIPTION

NANNOFOSSIL CHALK, bluish white (5B 9/1) to very light gray (N8) with scattered light greenish gray (5G 8/1) intervals. Thin medium gray (N5) VOLCANIC ASH with sharp base and gradational, burrowed top in Section 1. Ash also fills burrows in Section 1 and perhaps in Section 5.

SMEAR SLIDE SUMMARY (%):

	4, 50	5, 12
	D	D
Texture:		
Sand	5	7
Silt	95	93
Composition:		
Carbonate unspec.	5	10
Foraminifers	5	7
Calc. nannofossils	88	80
Diatoms	–	Tr
Radiolarians	1	1
Sponge spicules	1	2

ORGANIC CARBON AND CARBONATE (%):

	2, 60
Organic carbon	–
Carbonate	86

SITE 538 HOLE A CORE 13 CORED INTERVAL 107.0–116.5 m

TIME-ROCK UNIT: early Oligocene; late Eocene?
BIOSTRATIGRAPHIC ZONE: P20 (F), CP17 (N); (F) P19?, (F) CP16 (N)
FOSSIL CHARACTER: AG AG
SECTIONS: 1, 2, 3, CC

LITHOLOGIC DESCRIPTION

NANNOFOSSIL CHALK, white (N9) to very light gray (N8), fractured by drilling. Small patch of medium gray (N5) VOLCANIC ASH at 42 cm, Section 3.

SMEAR SLIDE SUMMARY (%):

	2, 119	2, 122	3, 42
	D	D	M
Texture:			
Sand	5	10	3
Silt	95	90	97
Composition:			
Volcanic glass	Tr	Tr	40
Carbonate unspec.	30	45	27
Foraminifers	5	10	3
Calc. nannofossils	65	45	27
Radiolarians	–	–	1
Sponge spicules	–	Tr	2

ORGANIC CARBON AND CARBONATE (%):

	2, 60
Organic carbon	–
Carbonate	86

SITE 538 HOLE A CORE 14 CORED INTERVAL 116.5–126.0 m

TIME-ROCK UNIT: early Oligocene late Eocene; late Eocene
BIOSTRATIGRAPHIC ZONE: P19 (F), CP16 (N); CP15 (N), P17–18 (F)
FOSSIL CHARACTER: FM AG; AG; AM AG
SECTIONS: 1, CC

LITHOLOGIC DESCRIPTION

NANNOFOSSIL CHALK, very light gray (N8), indistinctly or faintly laminated in upper 35 cm, homogeneous. Core-Catcher is RADIOLARIAN-NANNOFOSSIL LIMESTONE with irregular CHERT lenses or nodules ~1 cm across. Core fractured by drilling.

SITE 538 HOLE A CORE 15 CORED INTERVAL 126.0–135.5 m

TIME – ROCK UNIT	BIOSTRATIGRAPHIC ZONE	FORAMINIFERS	NANNOFOSSILS	RADIOLARIANS	DIATOMS	SECTION	METERS
middle Eocene	P14 (F) CP14 (N)	AM	AG			1, CC	

GRAPHIC LITHOLOGY / DRILLING DISTURBANCE / SEDIMENTARY STRUCTURES / SAMPLES

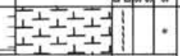

LITHOLOGIC DESCRIPTION

NANNOFOSSIL OOZE/CHALK, bluish white (5B 9/1), homogeneous.

SMEAR SLIDE SUMMARY (%):

	1, 25 D
Texture:	
Sand	5
Silt	95
Composition:	
Volcanic glass	Tr
Carbonate unspec.	44
Foraminifers	5
Calc. nannofossils	45
Radiolarians	3
Sponge spicules	3

SITE 538 HOLE A CORE 16 CORED INTERVAL 135.5–145.0 m

TIME – ROCK UNIT	BIOSTRATIGRAPHIC ZONE	FORAMINIFERS	NANNOFOSSILS	RADIOLARIANS	DIATOMS	SECTION	METERS
middle Eocene	CP14 (N); middle Eocene P13 (F)	AG	AM			1, 2, 3, 4, 5, 6, CC	0.5, 1.0

GRAPHIC LITHOLOGY / DRILLING DISTURBANCE / SEDIMENTARY STRUCTURES / SAMPLES

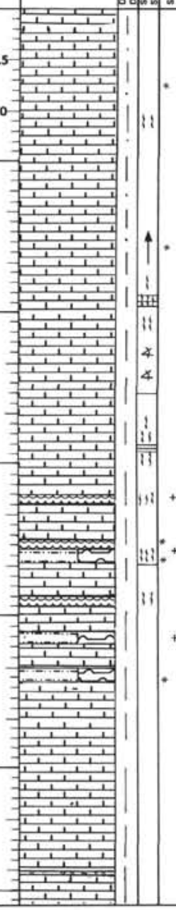

LITHOLOGIC DESCRIPTION

Interbedded NANNOFOSSIL CHALK, NANNOFOSSIL MARL and NANNOFOSSIL-RADIOLARIAN MUDSTONE. Chalk is bluish white (5B 9/1) to light greenish gray (5G 8/1) and pale green (5G 7/2) with scattered burrowed zones and faint laminations. Inclined layering occurs in Section 3. Marls are pale green (10G 6/2) with common chondrites and planolites type burrows filled with lighter chalk. Common light gray layers at base of marls in Section 3 are VOLCANIC ASH. Mudstone is dark yellowish brown (10YR 4/2) and dusky yellowish brown (10YR 2/2) to black (N1), radiolarian-rich, indistinctly laminated with common burrows (planolites type) filled with lighter marl and chalk. Generally sharp contacts between mudstone and marl/chalk, gradational between marl and ooze. Medium light gray (N5) VOLCANIC ASH layer in Section 6. Sharp basal contact, gradational top.

Thin Section:

5, 61: Phosphatic radiolarian mudstone – laminated dark brown mudstone composed of dark, deformed, and discontinuous wispy layers (~30–40 μm; iron-rich?) and lighter clayey layers containing common radiolaria molds filled with microcrystalline to cryptocrystalline quartz. Microcrystalline quartz also fills lenses. Yellow brown to reddish brown phosphatic concretions are common around quartz lenses and replaced radiolaria. Other phosphatic "grains" are irregular and aligned with bedding. A dark band (iron-concentration) ~100 μm to 2 mm occurs in this section.

SMEAR SILDE SUMMARY (%):

	1, 77 D	2, 85 D	4, 79 M	4, 95 M
Texture:				
Sand	1	1	–	–
Silt	99	99	80	85
Clay	–	–	20	15
Composition:				
Clay	–	–	20	15
Volcanic glass	1	1	1	1
Glauconite	–	–	1	Tr
Carbonate unspec.	53	79	58	6
Foraminifers	1	1	–	–
Calc. nannofossils	31	16	10	25
Radiolarians	–	–	5	30
Sponge spicules	5	3	5	10
Organic matter	–	–	–	3

ORGANIC CARBON AND CARBONATE (%):

	4, 32	4, 89	5, 23	5, 25	5, 60
Organic carbon	–	–	–	3	2
Carbonate	30(?)	38(?)	53	52	12

SITE 538 HOLE A CORE 17 CORED INTERVAL 145.0–154.5 m

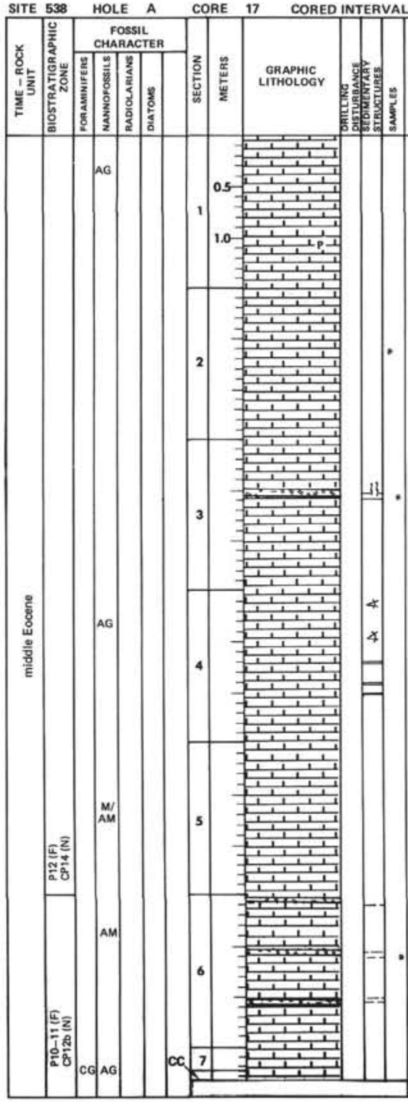

LITHOLOGIC DESCRIPTION

NANNOFOSSIL CHALK with thin layers of VOLCANIC ASH. Chalk is light greenish gray (5G 8/1) to white (N9) with sparse very pale green (10G 8/2) layering or laminations; these dip ~25° in top Section 4. Otherwise chalk is homogeneous with no obvious burrowing. Ash is medium gray (N5) and soft. Several layers have sharp bases and burrowed tops. Core fairly intact but broken by drilling.

SMEAR SLIDE SUMMARY (%):

	2, 66 D	3, 57 D	6, 61 M
Texture:			
Sand	1	–	–
Silt	99	100	99
Clay	–	–	1
Composition:			
Heavy minerals	–	Tr	–
Clay	Tr	5	–
Volcanic glass	–	92	–
Palagonite	–	Tr	–
Carbonate unspec.	84	2	24
Foraminifers	1	–	Tr
Calc. nannofossils	12	1	62
Diatoms	–	–	Tr
Radiolarians	2	Tr	10
Sponge spicules	1	Tr	4
Tunicate spicules	–	–	Tr

SITE 538 HOLE A CORE 18 CORED INTERVAL 154.5–164.0 m

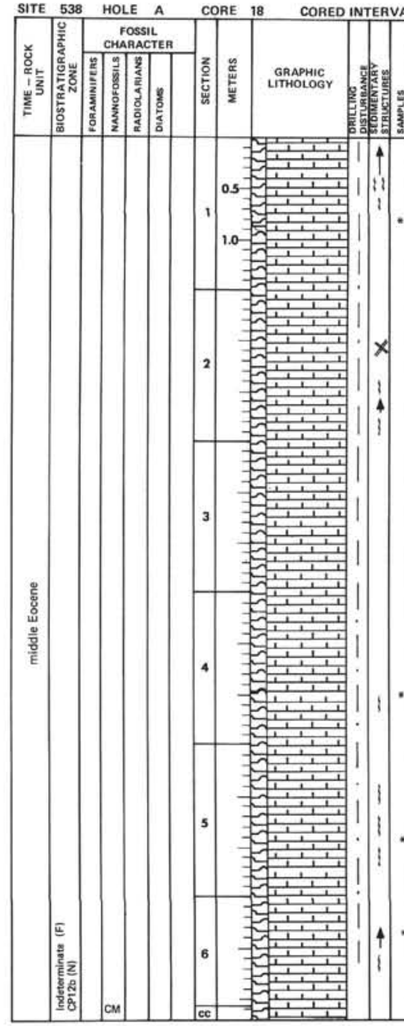

LITHOLOGIC DESCRIPTION

RADIOLARIAN-NANNOFOSSIL CHALK, light greenish gray (5G 8/1) and white (N9) to yellowish gray (5Y 8/1), colors alternating for variable lengths of core. Burrows are sparse as marked. An asphalt filled fracture ~2 mm wide occurs at 65 cm in Section 2. Moderate drilling disturbance.

SMEAR SLIDE SUMMARY (%):

	1, 80 D	4, 100 D	5, 93 D	6, 36 D
Texture:				
Sand	3	–	–	–
Silt	97	100	95	95
Clay	–	–	5	5
Composition:				
Clay	Tr	–	5	5
Carbonate unspec.	57	54	58	60
Foraminifers	3	–	–	–
Calc. nannofossils	21	21	12	11
Diatoms	Tr	Tr	–	Tr
Radiolarians	15	20	20	20
Sponge spicules	3	5	5	4

SITE 538 HOLE A CORE 19 CORED INTERVAL 164.0–173.5 m

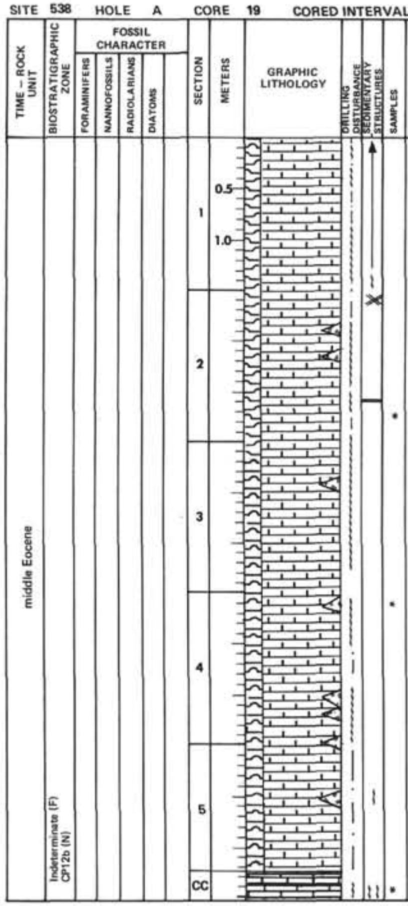

LITHOLOGIC DESCRIPTION

RADIOLARIAN-NANNOFOSSIL CHALK, yellowish gray (5Y 8/1) with common patches of medium gray (N5) VOLCANIC ASH scattered throughout. An asphalt-filled fracture ~1 mm across occurs at 16 cm, Section 2. Dark spots (asphalt?) are scattered through core at 30–50 cm, Section 2 and below 87 cm in Section 3 to top Section 4. Core-Catcher contains several pieces of yellowish gray to light greenish gray limestone with a prominent greenish gray (5G 6/1) patch. Limestone is burrowed. No radiolaria noted in smear slide from chalk in Core-Catcher.

SMEAR SLIDE SUMMARY (%):

	2, 125	4, 12	CC, 19
	D	M	M
Texture:			
Silt	90	90	100
Clay	10	10	–
Composition:			
Clay	10	10	–
Volcanic glass	–	88	–
Pyrite	–	2	–
Carbonate unspec.	40	–	90
Calc. nannofossils	20	–	10
Radiolarians	30	–	–

SITE 538 HOLE A CORE 20 CORED INTERVAL 173.5–183.0 m

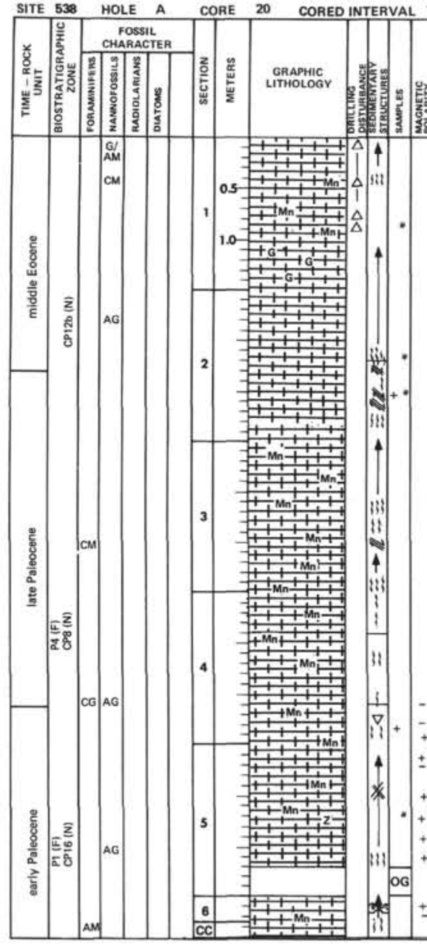

LITHOLOGIC DESCRIPTION

NANNOFOSSIL-FORAMINIFERAL and FORAMINIFERAL NANNOFOSSIL CHALK, variable colors ranging from yellowish gray (5Y 8/1), very pale orange (5Y 8/1) and light gray (N7) to 111 cm Section 4. Below this, chalk is mottled grayish orange pink (5YR 7/2) to pinkish gray (5YR 8/1). Black manganese oxide patches and spots scattered throughout. At least two sharp boundaries occur: 1) Surface at 75 cm, Section 2 is highly irregular and bored, borings filled with light foraminiferal nannofossil ooze. Several large (1 cm) bulls-eye shaped, light burrows (cylindrichus?) and small faults occur below this surface. 2) Irregular surface at 111 cm, Section 4 coated with ~0.5 cm of black manganese oxide crust and brown iron-oxides. Burrows common below crust and sand-size Mn fragments decrease in abundance downcore below the crust. Pinkish gray chalk below this surface is mottled with faint suggestions of bedding. An unidentified zeolite(?) occurs in this chalk.

SMEAR SLIDE SUMMARY (%):

	1, 89	2, 68	2, 102	5, 70
	M	D	D	D
Texture:				
Sand	50	20	15	Tr
Silt	45	75	80	90
Clay	5	5	5	10
Composition:				
Quartz	–	–	–	1
Clay	5	5	5	10
Zeolite(?)	–	–	–	10
Carbonate unspec.	30	15	5	30
Foraminifers	50	20	15	15
Calc. nannofossils	15	60	75	35
Dolomite	–	Tr	–	Tr

ORGANIC CARBON AND CARBONATE (%):

	2, 105	4, 138
Organic carbon	–	–
Carbonate	88	78

SITE 538 HOLE A CORE 21 CORED INTERVAL 183.0–192.5 m

TIME – ROCK UNIT	BIOSTRATIGRAPHIC ZONE	FOSSIL CHARACTER: FORAMINIFERS	NANNOFOSSILS	RADIOLARIANS	DIATOMS	SECTION	METERS
early Eocene	CP11 P8	AG, AM, AM				1	0.5, 1.0
late Campanian–early Maastrichtian	*Tetralithus trifidus*, *Globotruncana tricarinata*	AG, AG				2, 3	
middle-late Campanian	*T. aculeus*, *G. elevata*	FP	AG, AG, AG			4	
Santonian/Conacian	*M. furcatus*, *D. conc.*	CM, CM, FM	AG			4	
latest Albian	*E. turriseiffeli*, *P. buxtorfi*	FP, AM	AG			5, CC	

GRAPHIC LITHOLOGY / DRILLING DISTURBANCE / SEDIMENTARY STRUCTURES / SAMPLES

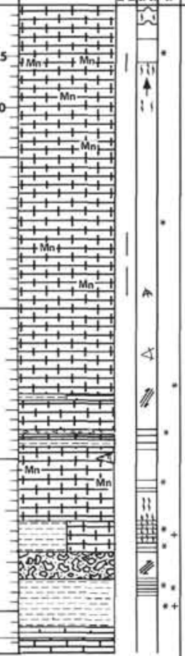

LITHOLOGIC DESCRIPTION

Complex association of lithologies and structures:

Section 1:

0–32 cm: grayish orange pink (5YR 7/2) FORAMINIFERAL-NANNOFOSSIL CHALK, similar to base of Core 20 but with brecciated layers and slump folds.

32–57 cm: white (N9) to yellowish gray (5Y 8/1) FORAMINIFERAL-NANNOFOSSIL CHALK with light gray streaks and irregular band. Top contact sharp. Basal contact irregular, marked by burrowed Mn-crust.

57–150 cm: light gray to yellowish gray FORAMINIFERAL-NANNOFOSSIL CHALK. Four cm thick brown-black manganese-oxide crust at top over irregular chalk surface. Chalk below crust has large burrows filled with white chalk; others filled with sand-size MnO_2 fragments. These decrease downcore.

Sections 2 and 3:

Principally FORAMINIFERAL-NANNOFOSSIL CHALK, white (N9) to very light gray (N8). MnO_2 spots scattered throughout. A large burrow at 90 cm (Section 2). Clayey intervals near base Section 3 and a brecciated VOLCANIC ASH layer at 122–125 cm, Section 3. Inclined and offset layering in Section 2.

Section 4:

0–62 cm: white (N9) to yellowish gray FORAMINIFERAL-NANNOFOSSIL CHALK with streaky dark yellowish orange (10YR 6/6) staining. Burrowed, with one irregular burrowed surface (omission surface?) at ~20 cm.

62–77 cm: a series of interlayered olive gray (5Y 3/2) to olive black (5Y 2/1) CLAYSTONES and white and yellowish gray to pinkish gray (5YR 8/1) CHALK. Claystones are bored and borings filled with chalk. Angular claystone fragments occur in overlying chalk layers.

77–94 cm: white, very light gray (N8) to very pale orange (10YR 8/2) FORAMINIFERAL-NANNOFOSSIL CHALK and light gray (N7) altered VOLCANIC ASH *separated by thin breccia included pieces of ash, chalk,* and claystone.

94–110 cm: breccia consisting of several dark CLAYSTONE layers in a matrix of CHALK and claystone fragments. Broken pieces of claystone layers can be reconstructed. Base of breccia is a fault dipping ~45° to core axis (apparent dip). Pieces of greenish claystone occur just above fault.

110–150 cm: CLAYSTONE, dusky yellow (5Y 6/4), light olive brown (5Y 5/6) to dark yellowish orange (10YR 6/6) and laminated grading downcore to less well-laminated; pale green (10G 6/2) claystone.

Section 5:

0–18 cm: pale green CLAYSTONE as at base Section 4. Some brecciated thin layers within.

18–25 cm: light brownish gray (5YR 6/1) NANNOFOSSIL CHALK with platy, dark brown fish scales and phosphatic debris aligned parallel to bedding.

25 cm–Core-Catcher: light brownish gray (5GY 8/1) LIMESTONE with porosity and common wispy, greenish zones. Variously lithified; some drilling paste.

SMEAR SLIDE SUMMARY (%):

	1, 49 D	2, 63 D	3, 87 M	3, 125 M	3, 132 M	4, 23 M	4, 69 M	4, 88 M	4, 124 D	4, 126 D	4, 144 M
Texture:											
Sand	20	15	–	–	–	15	–	–	–	–	–
Silt	75	80	20	95	40	80	10	100	15	1	1
Clay	5	5	80	5	60	5	90	–	85	99	99
Composition:											
Quartz	–	–	–	–	–	–	Tr	1	Tr	Tr	–
Feldspar	–	–	–	–	–	–	–	1	Tr	Tr	–
Clay	5	5	80	5	60	5	90	–	85	99	99
Volcanic glass	–	–	–	95	20	–	–	98	–	–	–
Zeolite	–	–	–	–	15	–	–	–	–	–	–
Carbonate unspec.	10	–	–	–	–	20	–	–	5	–	Tr
Foraminifers	20	15	Tr	–	–	15	Tr	–	–	Tr	–
Calc. nannofossils	65	80	20	–	5	60	10	–	10	Tr	Tr
Dolomite	Tr	–	–	–	–	–	–	–	–	–	–

ORGANIC CARBON AND CARBONATE (%):

	4, 76	4, 146
Organic carbon	–	–
Carbonate	4	6

SITE 538 HOLE A CORE 22 CORED INTERVAL 192.5–202.0 m

TIME – ROCK UNIT	BIOSTRATIGRAPHIC ZONE	FOSSIL CHARACTER: FORAMINIFERS	NANNOFOSSILS	RADIOLARIANS	DIATOMS	SECTION	METERS
latest Albian	*E. turriseiffeli*, *P. buxtorfi*	FP	AG			1	0.5

GRAPHIC LITHOLOGY / DRILLING DISTURBANCE / SEDIMENTARY STRUCTURES / SAMPLES

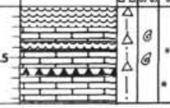

LITHOLOGIC DESCRIPTION

Interbedded(?) NANNOFOSSIL-MARLY LIMESTONE, LIMESTONE, and CHERT. Marly limestone is olive gray (5Y 4/1) and massive. Limestone is light olive gray (5Y 6/1) to light gray (N7) and medium light gray (N6) and contains abundant ammonite molds (parallel to bedding) and pores, many of which are shell molds. Chert is black and vitreous; no structures noted. Several small pieces of pale green (5G 7/2) CLAYSTONE occur at top of core and in Core-Catcher. Core is broken into drilling fragments.

Thin Section:

1, 78: radiolarian limestone (wackestone) — principally radiolaria and foraminifer empty and calcite-filled molds in a micritic matrix.

SMEAR SLIDE SUMMARY (%):

	1, 1 M	1, 40 D
Texture:		
Silt	20	65
Clay	80	35
Composition:		
Clay	80	35
Carbonate unspec.	10	10
Calc. nannofossils	10	50
Dolomite	Tr	–

SITE 538 HOLE A CORE 23 CORED INTERVAL 202.0–211.5 m

TIME – ROCK UNIT	BIOSTRATIGRAPHIC ZONE	FOSSIL CHARACTER: FORAMINIFERS	NANNOFOSSILS	RADIOLARIANS	DIATOMS	SECTION	METERS
latest Albian	*P. buxtorfi*	CP, CG	AM			1	0.5

GRAPHIC LITHOLOGY / DRILLING DISTURBANCE / SEDIMENTARY STRUCTURES / SAMPLES

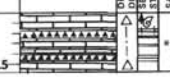

LITHOLOGIC DESCRIPTION

Interbedded(?) LIMESTONE, CHERT, and NANNOFOSSIL CHALK. Limestone is yellowish gray (5Y 7/2) to light olive gray (5Y 6/1), indistinctly layered with common, small round pores and shell molds. Ammonite molds common along bedding planes at 10–20 and 25–30 cm. Chert includes two varieties: 1) upper piece is black and vitreous with a thin layer across the center and common milky replaced radiolaria; and 2) lower piece is mottled dark yellowish brown (10YR 4/2), banded and indistinctly layered with blotchy light olive gray (5Y 6/1) and yellowish gray (5Y 8/1) patches and partial laminations. Nannofossil chalk is white (N9) and homogeneous. Core broken into fragments by drilling. No contacts between lithologies preserved.

Thin Section:

1, 30: foraminifer-radiolarian limestone (mudstone) — foraminifer and radiolaria empty and calcite-filled molds in a micritic matrix. Abundant irregular voids which may be leached shell debris.

SMEAR SLIDE SUMMARY (%):

	1, 36 M
Texture:	
Sand	5
Silt	90
Clay	5
Composition:	
Clay	5
Foraminifers	5
Calc. nannofossils	89
Dolomite	Tr

SITE 538 HOLE A CORE 24 CORED INTERVAL 211.5–221.0 m

TIME – ROCK UNIT	BIOSTRATIGRAPHIC ZONE	FORAMINIFERS	NANNOFOSSILS	RADIOLARIANS	DIATOMS	SECTION	METERS	GRAPHIC LITHOLOGY	DRILLING DISTURBANCE	SEDIMENTARY STRUCTURES	SAMPLES
? late Albian	*P. buxtorfi*	FP RP FP				1	0.5		△ △ △		* * * *

LITHOLOGIC DESCRIPTION

LIMESTONE (oolitic grainstone), white (10YR 8/3) to very pale brown (10YR 8/3–10YR 8/4). Principally grainstones that are moderately well sorted. Grain types include coated grains, foraminifers, molluscs, coral, bryozoans, and gastropods(?). One piece has well-preserved red algae. Another is encrusted with coral/bryozoans. Some boundstones present. Porosity is high.

(Core length exaggerated by addition of spacers in half-liner.)

Thin Sections:

1, 5: Limestone (oolitic grainstone) – ~90% ooids with some trocolina, echinoderm fragments, and traces of dolomite as rhombs in ooid cotecies, with marine cement. Both ooids and cement cut by borings (clast edges?).

1, 15: Limestone (oolitic grainstone) – ~95% ooids, one coral fragment, echinoderms and molluscs as nuclei, marine cement. One echinoid spine. Peloids common in cement. Many ooids are composite grains. Some oncolites or ooids with bored rims.

1, 33: Limestone (packstone-grainstone) – two-thirds of this slide includes a single coral fragment; remainder is peloidal packstone-wackestone with common encrusters, probable marine cement. Several borings in coral skeleton. Moldic porosity.

1, 55: Limestone (oolitic packstone) – ~80% ooids, some trocolina as nuclei. Echinoderm fragments common in ooids and as grains. Some patches of micrite and minor marine cement(?). Good primary and secondary porosity.

SITE 538 HOLE A CORE 25 CORED INTERVAL 221.0–230.5 m

TIME – ROCK UNIT	BIOSTRATIGRAPHIC ZONE	FORAMINIFERS	NANNOFOSSILS	RADIOLARIANS	DIATOMS	SECTION	METERS	GRAPHIC LITHOLOGY	DRILLING DISTURBANCE	SEDIMENTARY STRUCTURES	SAMPLES
Valanginian	*Calpionellid* D3	FP VM FP				1			△		* *

LITHOLOGIC DESCRIPTION

LIMESTONE (oncolitic grainstone), white (N9) to grayish orange (10YR 6/6). Most pieces are moderately well-sorted grainstones. Peloids and/or coated grains of coarse sand-size are most common grain types. Mollusc fragments also common with several algal fragments. Good primary and secondary moldic porosity. Core is drilling breccia.

Thin Sections:

1, 3: Limestone (oncolitic-grainstone) – grainstone containing oncolites (40%), peloids (25%), oolites (10%), foraminifers (10%), echinoderm fragments and spines (8%), and leached mollusc fragments (5%). Oncolites ~0.5–3.0 mm in diameter. Trocohind foraminifers common; some in oncolites. Primary porosity ~20%, secondary ~5%. Some encrusting foraminifers and marine cement. Scattered 40–50 μm dolomite rhombs.

1, 7: Limestone (oncolitic grainstone) – similar to Sample at Section 1, 3 cm. Grain distribution is oncolites (50%), peloids (25%), ooids (20%), foraminifers (2%), echinoderm fragments (2%), and molluscs (1%). Oncolites up to 4 mm in diameter. Trocolinid foraminifers common and some possible *calpionellids*. Encrusting foraminifers, scattered dolomite rhombs, and some calcite cement. Porosity ~25%, mostly primary. Erosional horizon in thin section.

1, 10: Limestone (oncolitic grainstone) – same as Section 1, 7 cm with following grain percentages: oncolites (40%), peloids (25%), oolites (10%), foraminifers (10%), echinoderm fragments (3%), mollusc fragments (10%). Primary porosity 15% and secondary porosity ~10%. Leached mollusc fragments account for part of latter.

SITE 538 HOLE A CORE 26 CORED INTERVAL 230.5–240.0 m

TIME – ROCK UNIT	BIOSTRATIGRAPHIC ZONE	FORAMINIFERS	NANNOFOSSILS	RADIOLARIANS	DIATOMS	SECTION	METERS	GRAPHIC LITHOLOGY	DRILLING DISTURBANCE	SEDIMENTARY STRUCTURES	SAMPLES
Valanginian	*Calpionellid* D3	FP				CC			△		* * *

LITHOLOGIC DESCRIPTION

LIMESTONE (oncolitic grainstone-packstone), white (N9) to yellowish gray (5Y 8/1). Predominantly grainstones, poorly to moderately well sorted. Common fragments include molluscs, foraminifers, corals, coated grains, and gastropods. Secondary moldic porosity is well-developed. Core is drilling breccia.

Thin Sections:

1, 4: Limestone (oolitic-oncolitic grainstone) – grain type distribution is: oncolites (50%), ooids (40%), peloids (10%), foraminifers (3%), echinoderm fragments (3%), and mollusc fragments (3%). Some calcite (marine) cement and scattered 20–40 μm dolomite rhombs. Porosity ≅ 15%, half primary and half secondary. Many leached grains comprise latter.

1, 7: Limestone (oncolitic grainstone-packstone) – contains coated grains (oncolites and composite grains ~60%), peloids (20%), foraminifers (5%), echinoderm fragments (2%), unidentified grains (10%), and a large surpulid worm tube. *Calpionellids* and *trochilina* sp. also present. Peloids occur in some graded pockets. Spar cement and borings also present. Primary porosity fair with some secondary porosity.

1, 10: Limestone (oncolitic grainstone-packstone) – grain type distribution is oncolites (50%), ooids – coated grains and composite grains (30%), mollusc fragments (5%), echinoderm pieces (5%), and foraminifers (3%), some *trocolinid* foraminifers; no *calpionellids*. Some calcite cement and rare dolomite. Porosity ≃ 10%, mostly secondary. Some leached mollusc grains.

SITE 538 HOLE A CORE 27 CORED INTERVAL 240.0–249.5 m

TIME – ROCK UNIT	BIOSTRATIGRAPHIC ZONE	FORAMINIFERS	NANNOFOSSILS	RADIOLARIANS	DIATOMS	SECTION	METERS	GRAPHIC LITHOLOGY	DRILLING DISTURBANCE	SEDIMENTARY STRUCTURES	SAMPLES
Berriasian	*Calpionellid* D2 Berriasian	FP FP				CC			△		* *

LITHOLOGIC DESCRIPTION

LIMESTONE (oncolitic grainstone), white (N9) to yellowish gray (5Y 8/1). Moderately well-sorted to poorly sorted grainstones and packstones composed mostly of peloids and coated grains, foraminifers, and some mollusc fragments. Small (1 cm) pelecypod preserved in one piece. Core is drilling breccia. Fair moldic porosity. Core is drilling breccia.

Thin Sections:

1, 3: Limestone (peloidal-oncolitic grainstone) – grain population is: oncolites (40%), peloids and coated grains (40%), foraminifers (5%), and echinoderm fragments (5%). Scattered patches of micrite and 50 μm dolomite rhombs. Minor cement. Porosity ~20%, half primary and half secondary.

1, 12: Limestone (peloidal mudstone-wackestone) – consists of scattered silt and fine sand-size carbonate grains in micrites and of patchy grainstone or packstone areas. Grains are mainly peloids with several composite grains or oncolites. Rare possible *calpionellids*. Scattered 40–50 μm dolomite rhombs and some calcite cement. Primary porosity 10% and secondary porosity (moldic) 10%.

SITE 538 HOLE A CORE 28 CORED INTERVAL 249.5–259.0 m

TIME – ROCK UNIT	BIOSTRATIGRAPHIC ZONE	FOSSIL CHARACTER: FORAMINIFERS	FOSSIL CHARACTER: NANNOFOSSILS	FOSSIL CHARACTER: RADIOLARIANS	FOSSIL CHARACTER: DIATOMS	SECTION	METERS	GRAPHIC LITHOLOGY	DRILLING DISTURBANCE	SEDIMENTARY STRUCTURES	SAMPLES
Berriasian	*Calpionellid* D2	FP FP				1			△ △		*

LITHOLOGIC DESCRIPTION

LIMESTONE (oncolitic packstone), white (N9) to yellowish gray (5Y 8/1). Poorly sorted grainstones and packstones. Grains include peloids/coated grains, foraminifers, gastropods, and molluscs. Good second moldic porosity. Core is drilling breccia.

Thin Section:

1, 3: Limestone (oncolitic packstone) – consists almost exclusively of oncolites (80^{+}%), with some peloids(?) (10%), and rare *trochalina* foraminifers and possible sponge fragments. Dolomite rhombs (50 μm) scattered throughout micritic matrix. Primary porosity 20%.

SITE 538 HOLE A CORE 29 CORED INTERVAL 259.0–268.5 m

TIME – ROCK UNIT	BIOSTRATIGRAPHIC ZONE	FOSSIL CHARACTER: FORAMINIFERS	FOSSIL CHARACTER: NANNOFOSSILS	FOSSIL CHARACTER: RADIOLARIANS	FOSSIL CHARACTER: DIATOMS	SECTION	METERS	GRAPHIC LITHOLOGY	DRILLING DISTURBANCE	SEDIMENTARY STRUCTURES	SAMPLES
early? Berriasian	*Calpionellid* D1?	FP FP				1			△		* *

LITHOLOGIC DESCRIPTION

LIMESTONE (oolitic and oncolitic grainstones), white (N9) to yellowish gray (5Y 8/1). Poorly sorted grainstones and packstones. Grain types include peloids/coated grains, of medium to coarse sand-size, mollusc fragments and some calcite-lined tubes (filled borings or serpulids?).

Thin Sections:

1, 4: Limestone (oolitic grainstone) – oolite containing 80% ooids, 10% peloids and rare *trocholina* foraminifers and echinoderm fragments. Scattered dolomite rhombs; some in ooid cortices. Minor micritic matrix and some (marine) calcite cement. Primary porosity 10–15%. Several erosional or truncation horizons.

1, 11: Limestone (oncolitic grainstone) – grain population includes oncolites (40%), oolites (40%), peloids (10%), and foraminifers. Rare *calpionellids* and scattered dolomite rhombs. Several generations of calcite cement. Porosity (~25%) is mostly primary.

SITE 538 HOLE A CORE 30 CORED INTERVAL 268.5–278.0 m

TIME – ROCK UNIT	BIOSTRATIGRAPHIC ZONE	FOSSIL CHARACTER: FORAMINIFERS	FOSSIL CHARACTER: NANNOFOSSILS	FOSSIL CHARACTER: RADIOLARIANS	FOSSIL CHARACTER: DIATOMS	SECTION	METERS	GRAPHIC LITHOLOGY	DRILLING DISTURBANCE	SEDIMENTARY STRUCTURES	SAMPLES
early Berriasian?	*Retecapsa angustiforata* *Calpionellid* D2	FM	RP CP			1	0.5 1.0	Metamorphic Rocks (see igneous/ metamorphic description forms)			* *
						2					

LITHOLOGIC DESCRIPTION

LIMESTONE (oncolitic grainstone-packstone) and GNEISS. Limestone is white (N9) to yellowish gray (5Y 8/1), poorly sorted grainstone-packstone. Recovery is only few pieces above gneiss. (Gneiss described on following igneous/metamorphic description forms.)

Thin Sections:

1, 1: Limestone (grainstone-packstone) – grain population includes coated grains (50%), composite grains and lithoclasts (20%), mollusc fragments (10%), echinoderm fragments and spines (10%), and foraminifers (5%). Some pentagonal gastropods and *trochilina* foraminifers as well. Well-developed (marine) cement which predates micritic fill. Some primary porosity.

1, 2: Limestone (oncolitic grainstone) – grain population includes coated grains and oncolites (50%), echinoderm fragments and spines (20%), peloids (20%), foraminifers (5%), and mollusc fragments (2%). Many coated grains are composite. Distinct biomodal grain distribution with peloids very small (~50 μm), reversely graded and enclosed in (marine) calcite cement. Some *trocholina* foraminifers present and rare possible sponges. Moderate primary porosity.

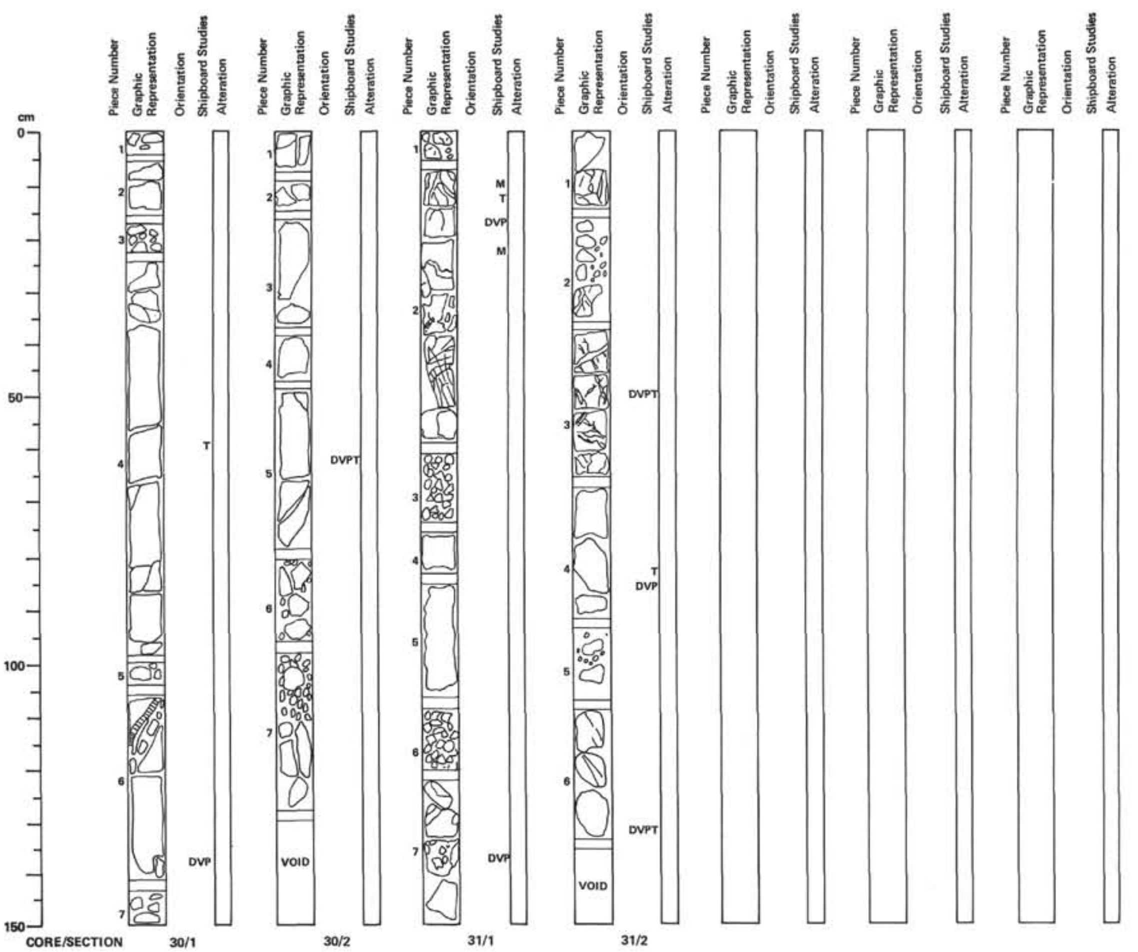

HOLE 538A, CORE 30, SECTIONS 1–2, 268.5–271.3 m

MAJOR ROCK TYPE – GNEISS

MINOR ROCK TYPE – LIMESTONE

Macroscopic Description:

Gneiss – dark gray, fine- to coarse-grained with a porphyroblastic to slightly mylonitic texture and a steeply dipping schistose or gneissose fabric. Porphyroblasts are mostly white, pink, and less commonly greenish feldspars up to 10 mm across. Thin, steeply dipping fractures lined with reddish material (clay? or biotite?) and parallel to the schistose fabric are pervasive. Coarsely crystalline white to pinkish calcite veins occur in Piece 6, Section 1 and Piece 7, Section 2. Piece 2 of Section 1 consists of several fractured, brecciated, and calcite-veined gneiss fragments with thin coatings of yellowish brown to white chalkly nannofossil limestone.

Limestone – Piece 1, Section 1, consists of several fragments of white to rusty yellowish gray bioclastic limestone (see description on sediments description form).

Thin Section Summaries:

Section 1, Piece 4 at 58 cm and Section 2, Piece 5 at 60 cm: both pieces are fine- to coarse-grained gneiss with a porphyroblastic to slightly mylonitic texture. Quartz is most abundant mineral (~50%) forming irregular and elongate stained crystals up to 2 mm long with sutured contacts and moderate c-axis orientation. Feldspars (~20%) mostly large (up to 3 mm) porphyroblasts of orthoclase and perthitic orthoclase-albite; smaller (0.1–0.5 mm) granular, twinned albite(?) crystals common. Biotite (~5%) occurs as greenish brown, pleochroic platy crystals (~0.1–0.5 mm) aligned parallel to shear zones. Sphene (<1%) is 0.1–0.3 mm (but up to 1 mm), has rhombohedral or drop-like form, rhombohedral cleavage; some have opaque mineral cores. Opaque minerals (<1%; magnetite) are cubic or subhedral (~0.1–0.5 mm).
Section 2, Piece 7 at 107 cm: coarsely crystal calcite vein material.

Paleomagnetics/Physical Properties:

Sample	D	P	V (⊥)	V (∥)	Int.	Incl.	S. I.	Q.
Section 1, Piece 6	2.58	10	4.57	4.74	–	–		–
Section 2, Piece 5	2.48	14	3.73	4.34	–	–	–	–

HOLE 538A, CORE 31, SECTIONS 1–2, 278.0–280.8 m

MAJOR ROCK TYPES – DIABASE, GNEISS AND GNEISS BRECCIA AMPHIBOLITE

Macroscopic Description:

Diabase – Piece 1 and Piece 2 down to ~30 cm is dark green, very fine-grained to aphyric diabase. Rusty brown concentric alteration occurs between ~15–30 cm. Calcite veins are common. Diabase is altered downcore to dark green clay (30–120 cm, Section 1). The altered diabase contains some calcite veins and is highly fractured. White feldspar crystals up to 2 mm across and partly altered to green clay occur sporadically. Pieces 4–6 are highly fractured (some well-developed slickensides), have a soap feel and are easily scratched with a fingernail.

Gneiss and Gneiss Breccia – Piece 7 and fragments of Piece 6 in Section 1 consists of angular fragments of pinkish gray gneiss (and perhaps some finer grained amphibolite) up to 3 cm across cemented together by calcite. Pieces 4 and 5 in Section 2 are dark gray, fine- to coarse-grained gneiss with distinct porphyroblastic to slightly mylonitic texture and a steeply dipping schistose to gneissose fabric (~70° from perpendicular to core axis). Rusty weathered and irregular shear surfaces with common green and yellowish alterations are subparallel to this fabric. Gneiss is darker colored and has more pronounced fabric than that in Core 30.

Amphibolite – Pieces 1–3 and Piece 6 in Section 2 are dark gray to grayish green fine- to medium-grained amphibolite. White calcite veins common in upper part above gneiss; pink feldspar veins occur in Piece 6 and top of Piece 1, both in Section 2. Faint steeply dipping gneissose fabric in Piece 6, Section 2. Excellent transition from gneiss to amphibolite between 50–70 cm in Section 2; amphibolite has relic gneissose fabric in this interval.

Thin Section Summaries:

Section 1, Piece 2 at 15 cm: fine-grained, altered diabase containing small (0.01–0.02 mm) plagioclase laths (~An_{45-55}) and apparent subophitic to intersertal intergrowths of pyroxene and interstitial glass, the latter two completely altered to green clay. Skeletal and cubic magnetite(?) (~0.01–0.1 mm) occur along edges of plagioclase.

Section 2, Piece 4 at 78 cm – gneiss that is texturally and compositionally similar to gneiss in Core 3 but with a slightly stronger or better developed fabric (see Thin Section Description, Core 30). Biotite crystals bend and "flow" more around porphyroblasts; some biotite is altered to green clay.

Section 2, Piece 3 at 45 cm and Piece 6 at 126 cm – amphibolite with aphitic to subophitic texture and consisting of about equal proportions of idioblastic green hornblende and xenoblastic plagioclase with minor sphene (<1%) and no opaque minerals. Hornblende (0.1–0.4 mm) is strongly pleochroic (light to deep green), has good cleavage, with extinction angle of ~46°. Plagioclases (~An_{40}) are slightly larger than hornblende and partly sericitized. Sphene occurs as small (~0.2 mm) xenoblastic crystals associated with hornblende. Faint lineation of hornblende and plagioclase in these thin sections.

Paleomagnetics/Physical Properties:

Sample	D	P	V (⊥)	V (∥)	Int.	Incl.	S. I.	Q.
Section 1, Piece 2, 12 cm	2.54	17	4.08	4.19	–	–	–	–
Section 1, Piece 2, 23 cm	–	–	–	–	231	21.1	−21.2	2.81
Section 1, Piece 7	2.52	16	4.55	5.05	–	–	–	–
Section 2, Piece 3	2.51	17	4.64	3.95	–	–	–	–
Section 2, Piece 4	2.48	18	4.57	5.06	–	–	–	–
Section 2, Piece 6	2.86	4	6.39	6.58	–	–	–	–

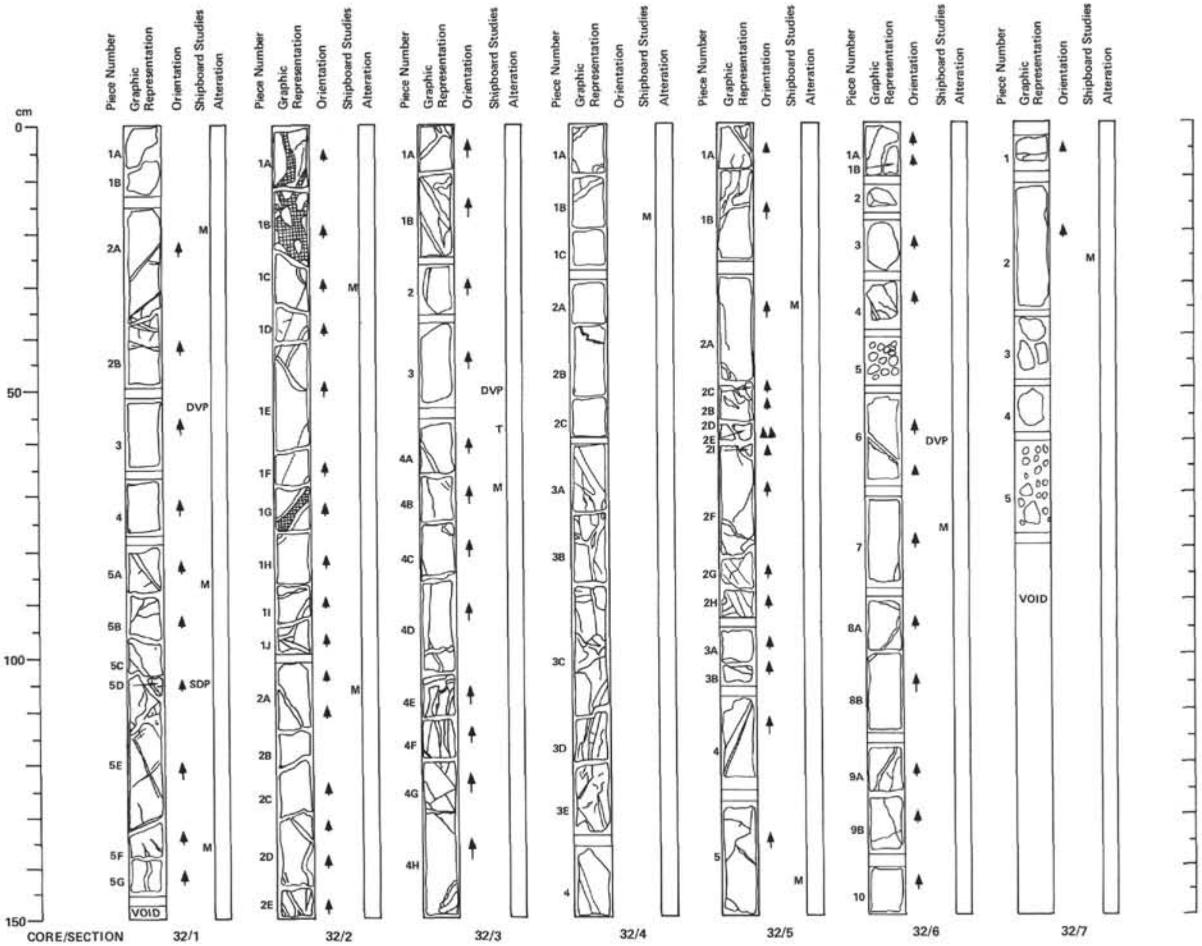

HOLE 538A, CORE 32, SECTIONS 1–7, 287.5–296.5 m

MAJOR ROCK TYPE – DIABASE

Macroscopic Description:

Diabase – medium gray, medium grained and generally homogeneous. Piece 1A in Section 1 is slightly finer grained than rest of core; contains some phenocrystic feldspar. Calcite veins, some including angular diabase fragments, common throughout as marked. Some fractures have green clay coating with later calcite fill. Alteration is moderate to slight, usually greenish and moderate yellowish brown colors around calcite vein. Thin fractures occur throughout diabase but no distinct or strong fabric as in associated metamorphic rocks.

Thin Section Summary:

Section 3, Piece 4A – medium grained diabase with ophitic to subophitic texture composed of plagioclase (55%), pyroxene (40%), green clay (alteration of interstitial glass; 5%), biotite (<1%), and opaque minerals (5%). Plagioclases ($\sim An_{30-65}$) zoned, lath-shaped, about 1–2 mm long with common Carlsbad and albite twins. Pyroxene mostly normal euhedral augite (0.2–1.2 mm) with extinction angle ~4.0°, +2V ≅ 60°, and some (100) twins. Green clay in interstices between plagioclase and augite crystals. Biotites are small, green-brown pleochroic platy crystals associated with interstitial green clay. Opaques (magnetite?) are skeletal and interstitial, granular crystals up to 0.5 mm across.

Paleomagnetics/Physical Properties:

Sample	D	P	V (↓)	V (↕)	Int.	Incl.	S. I.	Q.
Section 1, Piece 2A, 21 cm	–	–	–	–	733	3.3	–23.0	5.60
Section 1, Piece 3	2.96	4	6.37	6.40	–	–	–	–
Section 1, Piece 5A, 85 cm	–	–	–	–	770	– 7.0	–27.0	7.03
Section 1, Piece 5F, 132 cm	–	–	–	–	967	– 2.2	–33.4	7.63
Section 2, Piece 1C, 30 cm	–	–	–	–	672	11.2	–19.6	5.19
Section 2, Piece 2A, 106 cm	–	–	–	–	842	–18.3	–25.4	6.94
Section 3, Piece 3	2.93	5	6.01	6.15	–	–	–	–
Section 3, Piece 4B, 70 cm	–	–	–	–	583	5.4	–22.4	4.62
Section 4, Piece 1B, 16 cm	–	–	–	–	933	28.5	–	7.34
Section 5, Piece 2A, 33 cm	–	–	–	–	707	–10.9	–19.9	6.10
Section 5, Piece 5, 141 cm	–	–	–	–	630	17.9	–21.4	7.88
Section 6, Piece 6	2.95	4	6.18	6.16	–	–	–	–
Section 6, Piece 7, 77 cm	–	–	–	–	703	5.5	–25.3	5.15
Section 7, Piece 2, 25 cm	–	–	–	–	850	3.3	–17.4	6.17

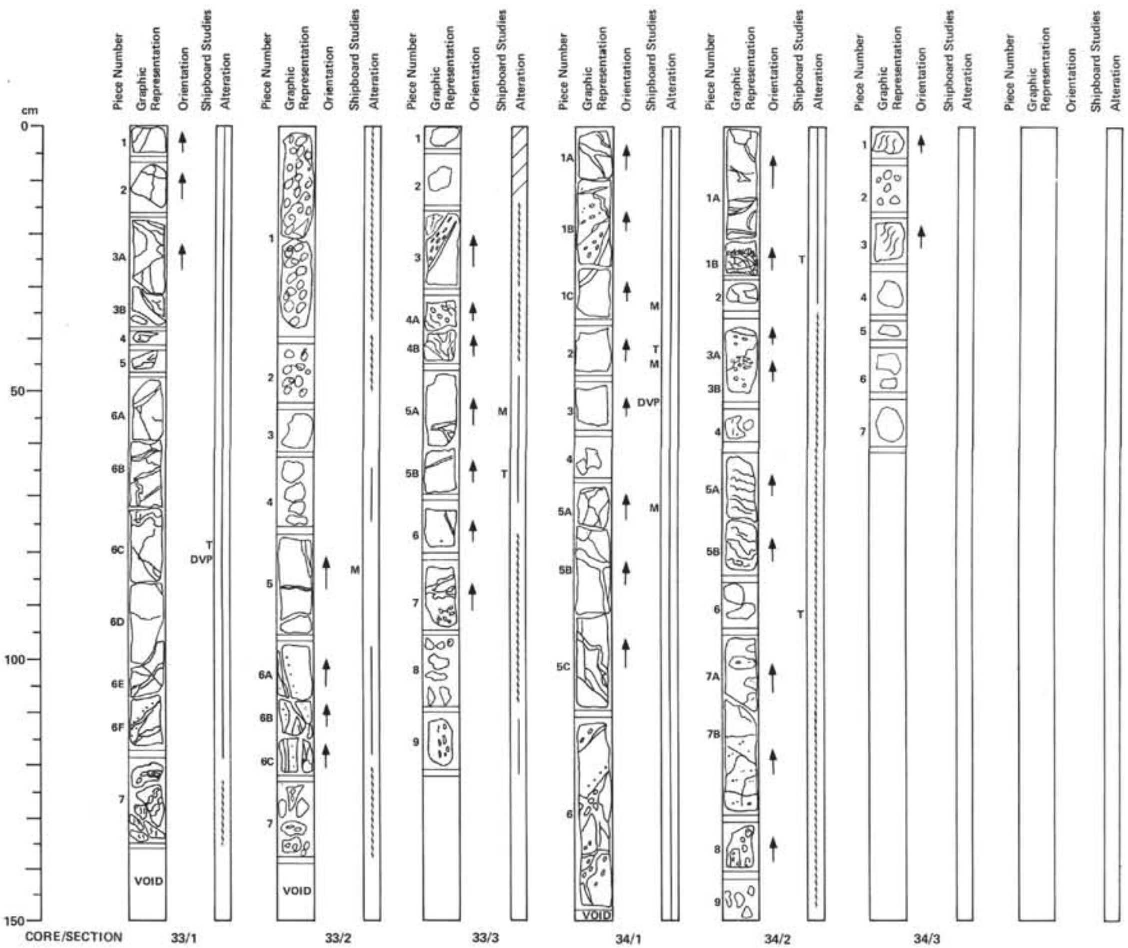

HOLE 538A, CORE 33, SECTIONS 1–3, 296.5–300.4 m

MAJOR ROCK TYPES – DIABASE, AMPHIBOLITE

Macroscopic Description:

Diabase – Pieces 1–6F, Section 1 are dark gray to greenish gray, medium grained diabase. White plagioclase clusters give rock an apparent porphyritic texture. Abundant white calcite veins throughout, many lined on outside edges with green clay. Basal part of Piece 6F below large calcite vein has pink feldspar remnants and relic gneissose fabric. Dark green to dark reddish brown, brecciated altered amphibolite makes up Pieces 1 and 2 of Section 2, and the lower fragments of Piece 7, Section 1. Slickensides common on many fragments. Some fragments in Piece 1, Section 2 appear to have a relic gneissose fabric.

Amphibolite – part of Piece 7, Section 1; Pieces 3–7, Section 2; and all of Section 3 are dark gray amphibolite. Texture varies from finely crystalline (e.g. Pieces 3, 4, and 7 in Section 3) to faintly relic porphyroblastic (remaining pieces) with very indistinct gneissose fabric. Some pieces are partly serpentinized. Topmost fragment in Piece 7, Section 1, has a large "lense" of pink feldspar. Piece 3, Section 3 has a high angle (shear?) zone where gneissose fabric is well-preserved.

Thin Section Summaries:

Section 1, Piece 6C – altered diabase containing some relic plagioclase laths and patches of glomerocrystic(?) opaques and biotite. Most of the rock is calcite, apparently pseudomorphed after pyroxene(?), and clay and an alteration of biotite, feldspars and mafic minerals.

Section 3, Piece 5B – amphibolite, texturally, and compositionally similar to those described for Pieces 3 and 6 in Section 2 of Core 31 with several important differences: 1) hornblende is somewhat more altered to clay, and 2) 2% opaque minerals (0.3 mm) are present, usually associated with the hornblende crystals. Texture is ophitic to subophitic.

Paleomagnetics/Physical Properties:

Sample	D	P	V (l)	V (s)	Int.	Incl.	S. I.	Q.
Section 1, Piece 6C	2.40	23	3.39	3.62	–	–	–	–
Section 2, Piece 5, 81 cm	–	–	–	–	1.37	4.2	–15.0	0.52
Section 3, Piece 5A, 52 cm	–	–	–	–	13.7	25.9	3.0	2.65

HOLE 538A, CORE 34, SECTIONS 1–3, 305.5–309.0 m

MAJOR ROCK TYPES – GNEISS, AMPHIBOLITE, ALTERED AMPHIBOLITE, and GNEISS

Macroscopic Description:

Amphibolite – all pieces of Section 1 and Piece 1A of Section 2 and Pieces 4, 5, and 7 of Section 3 are dark gray to greenish gray, very fine-grained amphibolite with common calcite veins throughout. Some large intersecting calcite veins contain angular amphibolite fragments. Relic feldspar porphyroblasts in Pieces 1A, 1B, and 6 in Section 1. Piece 1A in Section 2 is highly altered.

Altered Amphibolite and Gneiss – a complex association of xenolithic gneiss in amphibolite highly altered to green clay in places occurs from Piece 1B, Section 2 through Piece 3, Section 3. In Section 2, Piece 1B contains a large gneiss xenolith (~3 cm across) in fine-grained amphibolite. Pieces 3 and 5 are altered amphibolites with relic feldspar porphyroblasts and gneissose fabric and calcite veins; faint outlines of a gneiss xenolith occur in Piece 3. Piece 6 is a strongly mylonitized gneiss. Piece 7 is amphibolite with relic feldspar porphyroblasts and gneissose texture that is altered to clay and apparently brecciated in Piece 7A and somewhat less altered and more intact in Piece 7B. Pieces 8 and 9 in this section (Section 2) and Pieces 1–3 in Section 3 are yellowish gray to reddish altered gneisses and amphibolites with xenoliths or subrounded gneiss fragments. These rocks have breccia-like textures.

Thin Section Summaries:

Section 1, Piece 2 – amphibolite with ~40% hornblende, 55% plagioclase and 5% opaque minerals. Hornblende is green, and strongly pleochroic occurring in subophitic growth with feldspar and as inclusions (sieve structure) in several large plagioclases. Plagioclase crystals (~An_{30-45}) are ~0.2–0.4 mm across and twinned (albite mostly, but Carlsbad for larger crystals). Opaques irreulgar to subhedral (0.1–0.2 mm), mostly as cores in hornblende crystals. Plagioclase and hornblende show strong linear fabric.

Section 2, Piece 1B – amphibolite with gneiss xenolith. Gneiss is mostly large strained and sutured quartz grains (~0.1–2.0 mm) and sericitized orthoclase (~0.5–2 mm) and some microcline with common pale green pleochroic mica (altered biotite?) along anastomosing "rifted" shear fractures. Amphibolite host contains about equal proportions of green pleochroic hornblende and plagioclase, both in size range 0.2–0.5 mm. Hornblende extinction angle is ~10–20°; some alteration(?) to green clay(?) mineral having abnormal bluish gray birefringence. Plagioclases are sericitized. Sharp contact between amphibolite host and gneiss xenolith; epidote (<1%; 0.2–0.5 mm) occurs along contact. Alteration along shear fractures in gneiss fragment.

Section 2, Piece 6 – mylonitized gneiss consisting of large (1–2 mm) feldspar porphyroblasts that have been rolled and broken. Quartz (~70%) occurs as small (0.2–0.4 mm) grains and larger (1.0–1.5 mm) stained grains with sutured contacts. Grains occur between anastomosing subparallel shear surfaces; also as wispy "tails" of feldspar porphyroblasts. Feldspars both Carlsbad-twinned orthoclase and perthitic albite-orthoclase mostly sericitized. Porphyroblasts surrounded by swirling patterns of quartz and biotite; some have abraded edges and oval cross sections. Biotites (1–5%) are small (0.1 mm) platy grains aligned parallel to shear surfaces and plastered around porphyroblasts. Epidote (<1%) occurs as small (0.1 mm), broken grains along shear planes.

Paleomagnetics/Physical Properties:

Sample	D	P	V (l)	V (s)	Int.	Incl.	S. I.	Q.
Section 1, Piece 1C, 31 cm	–	–	–	–	9.67	56.3	12.5	2.72
Section 1, Piece 2, 40 cm	–	–	–	–	11.1	47.9	19.6	2.68
Section 1, Piece 5A, 75 cm	–	–	–	–	16.9	35.3	6.1	3.61

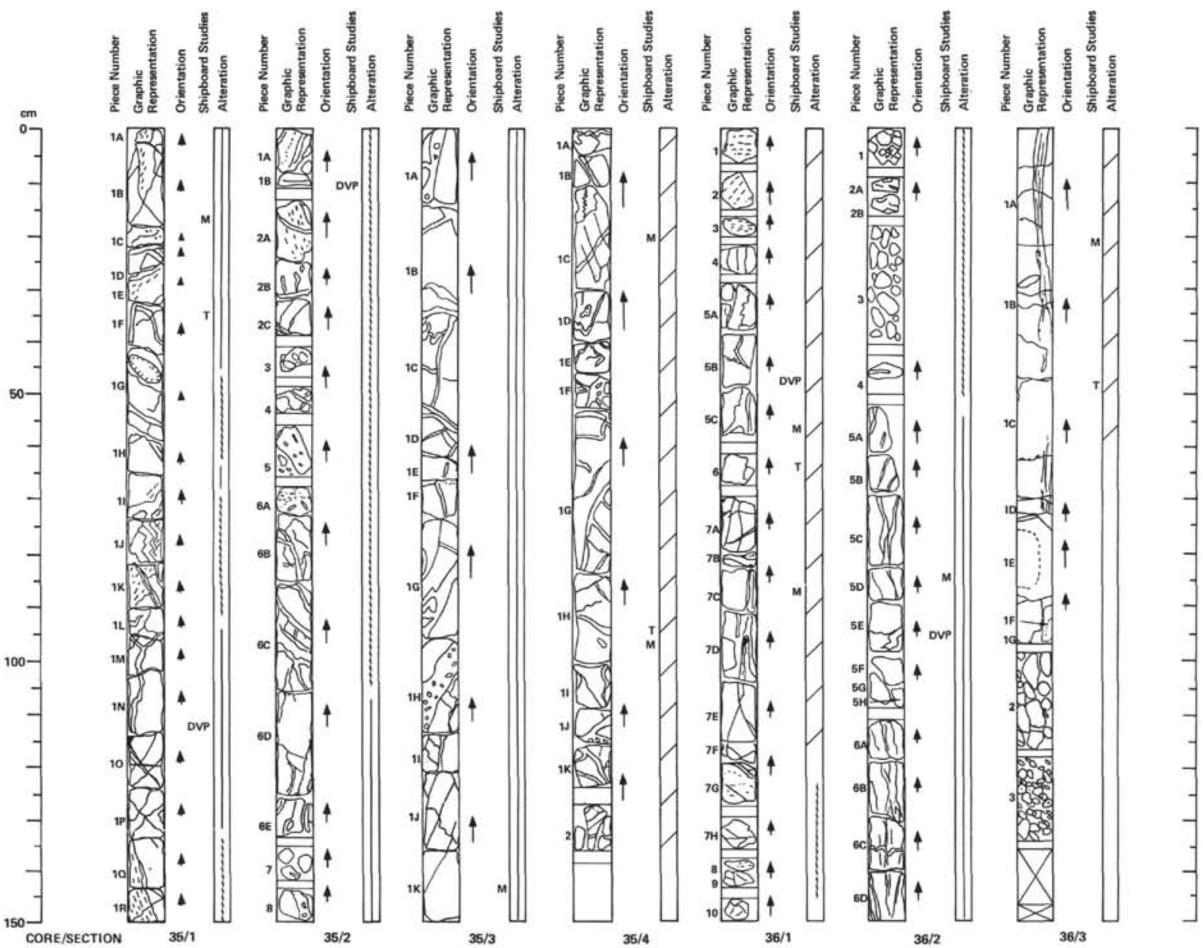

HOLE 538A, CORE 35, SECTIONS 1–4, 314.5–320.3 m

MAJOR ROCK TYPES – DIABASE AND AMPHIBOLITE

Macroscopic Description:

Diabase – all of Section 1 and from Piece 6A–base of Section 4 is diabase. Mostly fine- to medium-grained, greenish gray with abundant large calcite veins and yellowish orange alteration patches. Greenish cast to less altered-looking rock may be pervasive alteration to green clay. Piece 1G, Section 1 has a large pink feldspar lense similar to the pink feldspar veins in the amphibolites. Pieces 6A–6E, Section 2, represent gradational change from calcite veined contact between "overlying" amphibolite and fine-grained diabase. Piece 8 in Section 2 has a pinkish quartz or feldspar late-stage vein fill. Large calcite veins in Piece 1H, Section 3, have brecciated fragments of diabase.

Amphibolite – dark greenish gray, highly altered with some relic medium- to coarse-grained fabric and a hint of lineation occurs from top Section 2 through Piece 6A, Section 2. Contacts with diabase complex and extensively veined with calcite.

Thin Section Summaries:

Section 1, Piece 1F – altered medium-grained diabase with intersertal to subaphitic texture. Plagioclase (~An_{38-46}) makes up about 30% of rock; mostly laths up to 0.4 mm long. Pyroxenes (~10%) are stubby, corroded normal augite with +2V=60° and are extinction angle of ~50°. Most of sample (30%) is dusky brown augite-size clay(?) and/or calcite. Green clay (~ 5%) is interstitial between plagioclase laths. Opaques (~ 5%) are cubic and skeletal intergrowth with pyroxene; crystals 0.1–0.2 mm across.

Section 4, Piece 1H – diabase, intersertal to subophitic texture with ~40% plagioclase, 15% augite, 20% green clay, rare biotite (1%) and opaques (5%). Plagioclase (~ An_{33-42}) in zoned laths ~0.2–0.4 mm long. Pyroxene is normal augite, ~0.3 mm. Green clay is interstitial as is biotite. Opaques are skeletal and cubic grain (0.2 mm) mostly around plagioclase.

Paleomagnetics/Physical Properties:

Sample	D	P	V (⊥)	V (∥)	Int.	Incl.	S. I.	Q.
Section 1, Piece 1B, 14 cm	–	–	–	–	388	18.8	11.8	6.91
Section 1, Piece 1N	2.70	13	4.80	4.72	–	–	–	–
Section 2, Piece 1A	2.65	16	4.95	5.00	–	–	–	–
Section 3, Piece 1K, 146 cm	–	–	–	–	1730	53.6	37.2	14.11
Section 4, Piece 1C, 18 cm	–	–	–	–	1790	45.3	37.2	12.42
Section 4, Piece 1H, 94 cm	–	–	–	–	3100	46.1	38.1	21.31

HOLE 538A, CORE 36, SECTIONS 1–3, 323.5–327.8 m

MAJOR ROCK TYPES – DIABASE, AMPHIBOLITE, GNEISS, and GNEISS BRECCIA

Macroscopic Description:

Diabase – fine grained in Section 1, coarsening to medium grained in Sections 2 and 3. Calcite veins common throughout. Blotching white coarse grained mica mineralization in Pieces 1B and 1C in Section 3.

Amphibolite – dark greenish gray fine-grained with relic feldspar porphyroblasts and faint gneissose texture. Only Pieces 1 and 2 in Section 1 are amphibolites; contact with underlying diabase is a drilling break.

Gneiss, Gneiss-Diabase Breccia – These rock types occur between Pieces 7H, Section 1 and Piece 4A, Section 2. Breccias are calcite-cemented, variably altered to clay and contain angular fragments of fine-grained diabase, altered gneiss and fragments of green rock (altered amphibolites) with brick-red inclusions and alterations. Piece 8, Section 1 is a gneiss with a strong metamorphic fabric. Piece 3 in Section 2 contains fragments of dark green altered gneiss or amphibolite.

Thin Section Summaries:

Section 1, Piece 6 – Diabase with intersertal to subophitic texture. Consists of zone plagioclase laths (~40%; ~ An_{38-45}) up to 1 mm long, augite (~ 15%; extinction angle ≈30°; 0.3–0.5 mm), interstitial green clay (20%), small biotite crystals (1%), and scattered skeletal and cubic opaques (0.2 mm) mostly around plagioclase.

Section 3, Piece 1C – altered diabase consisting mostly of large (0.5–1 mm) crystals of white mica, green clay and augite. Mica is probably muscovite despite low-2V (-15°); too hard for talc and wrong paragenesis for philogopite. No feldspars remain in sample.

Paleomagnetics/Physical Properties:

Sample	D	P	V (⊥)	V (∥)	Int.	Incl.	S. I.	Q.
Section 1, Piece 5B	2.83	9	5.21	5.08	–	–	–	–
Section 1, Piece 5C, 57 cm	–	–	–	–	2370	24.8	15.5	14.00
Section 1, Piece 7C, 89 cm	–	–	–	–	2220	8.7	– 4.1	13.83
Section 2, Piece 5D, 86 cm	–	–	–	–	686	– 1.2	–20.8	4.58
Section 2, Piece 5E	2.69	14	4.84	4.48	–	–		–
Section 3, Piece 1A, 21 cm	–	–	–	–	221	46.1	18.0	4.92

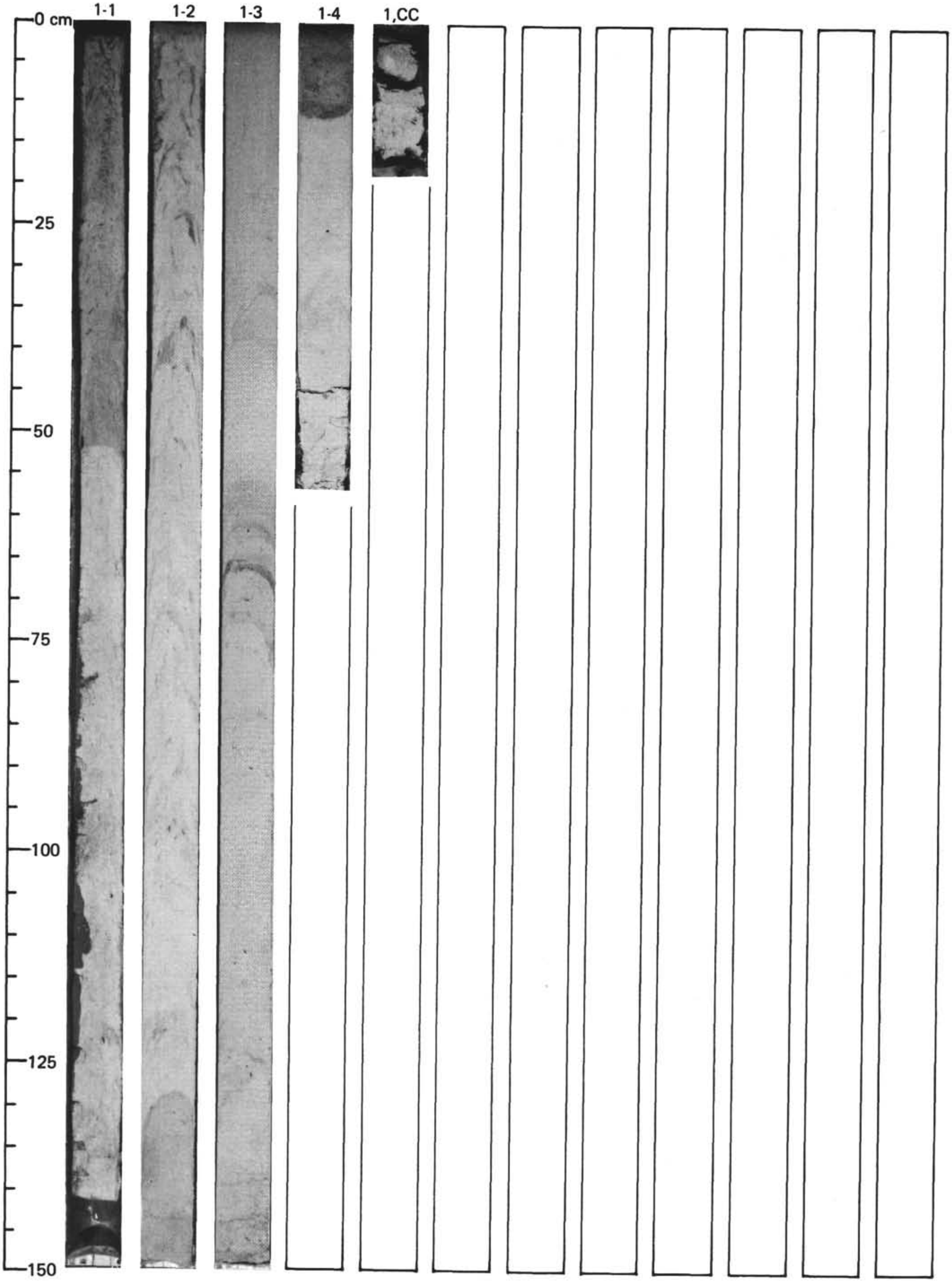
0 cm
25
50
75
100
125
150
1-1
1-2
1-3
1-4
1,CC

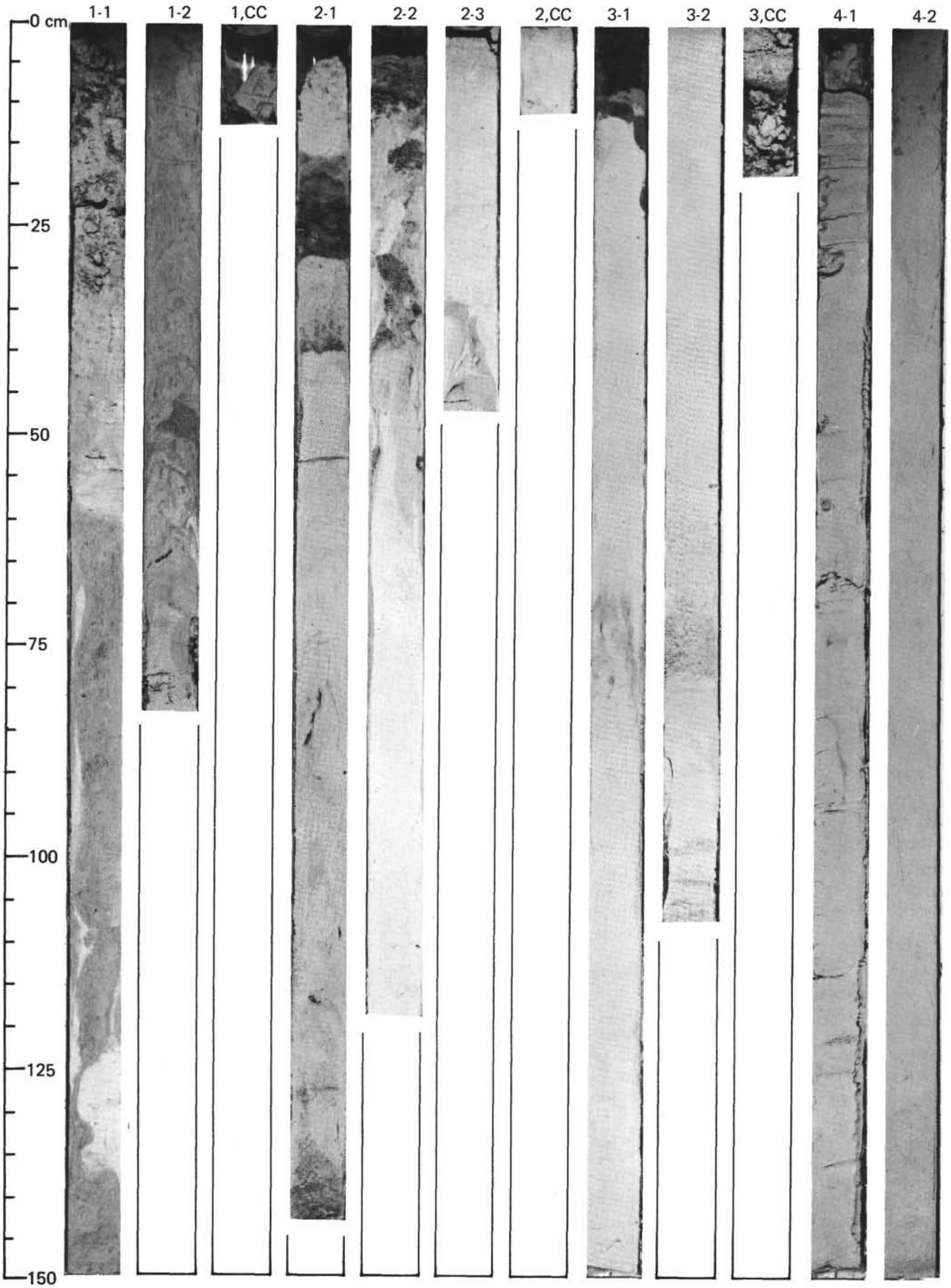

0 cm
25
50
75
100
125
150
1-1
1-2
1,CC
2-1
2-2
2-3
2,CC
3-1
3-2
3,CC
4-1
4-2

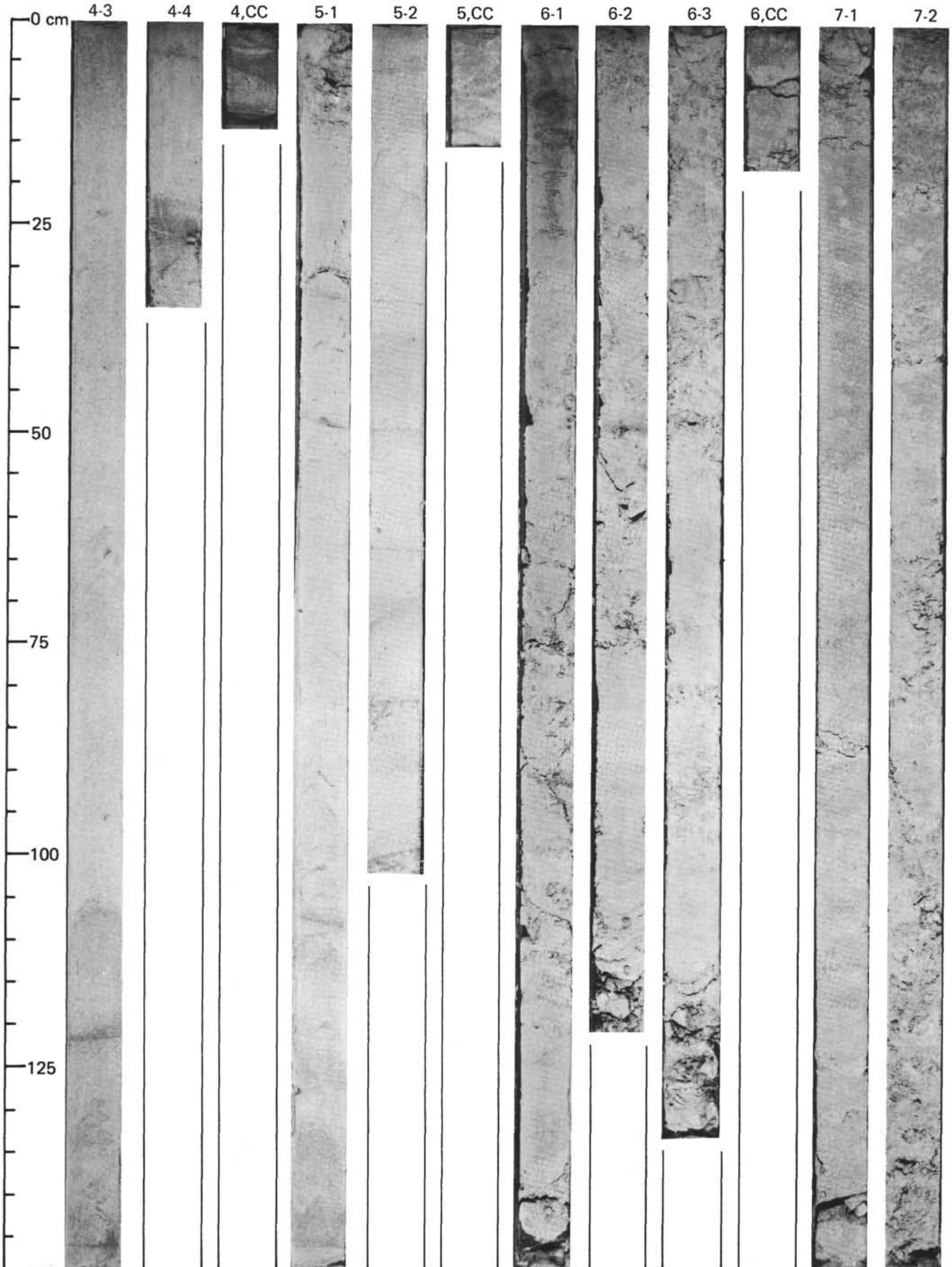
0 cm
25
50
75
100
125
150
4-3
4-4
4,CC
5-1
5-2
5,CC
6-1
6-2
6-3
6,CC
7-1
7-2

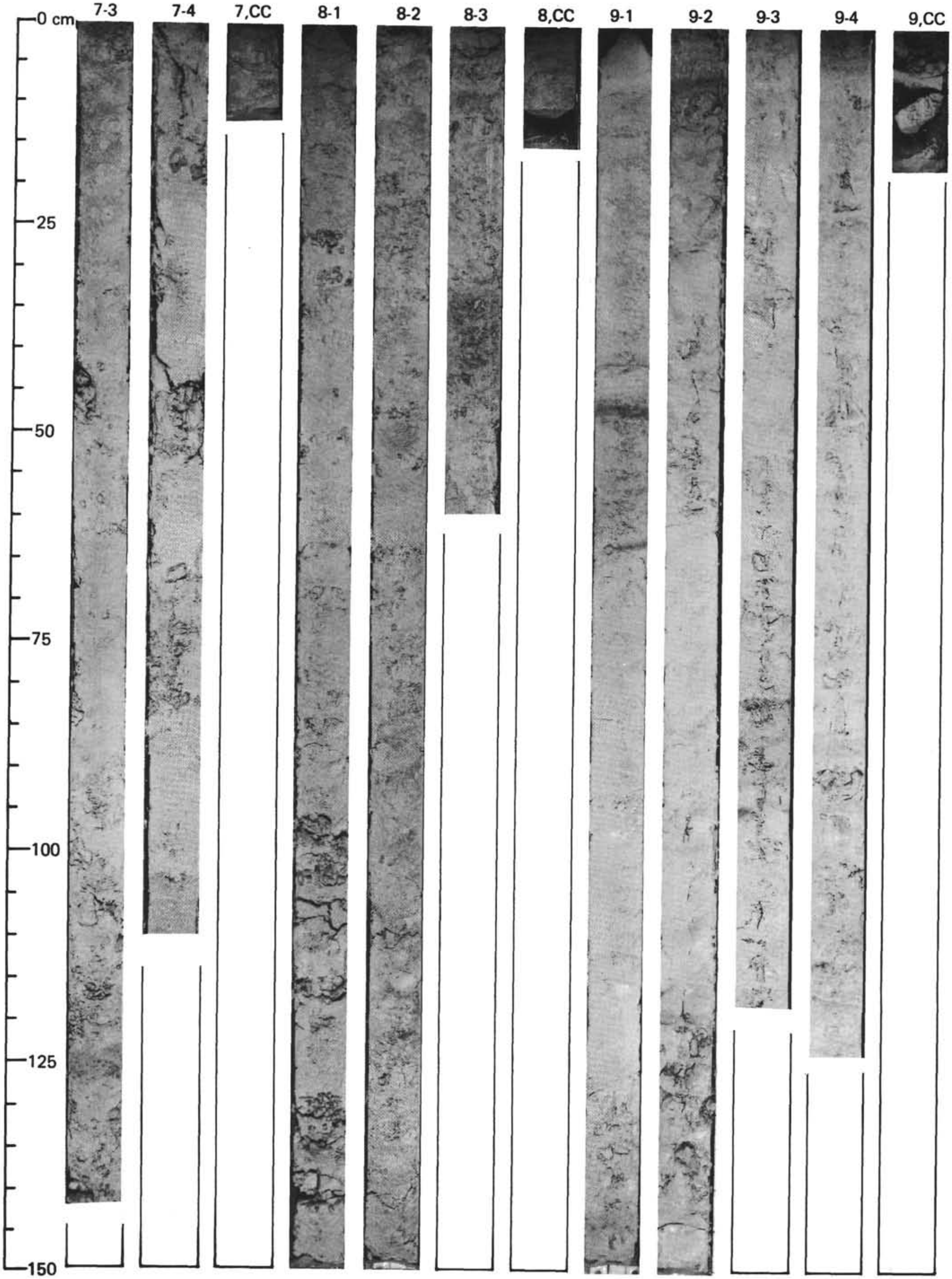
0 cm
25
50
75
100
125
150
7-3
7-4
7,CC
8-1
8-2
8-3
8,CC
9-1
9-2
9-3
9-4
9,CC

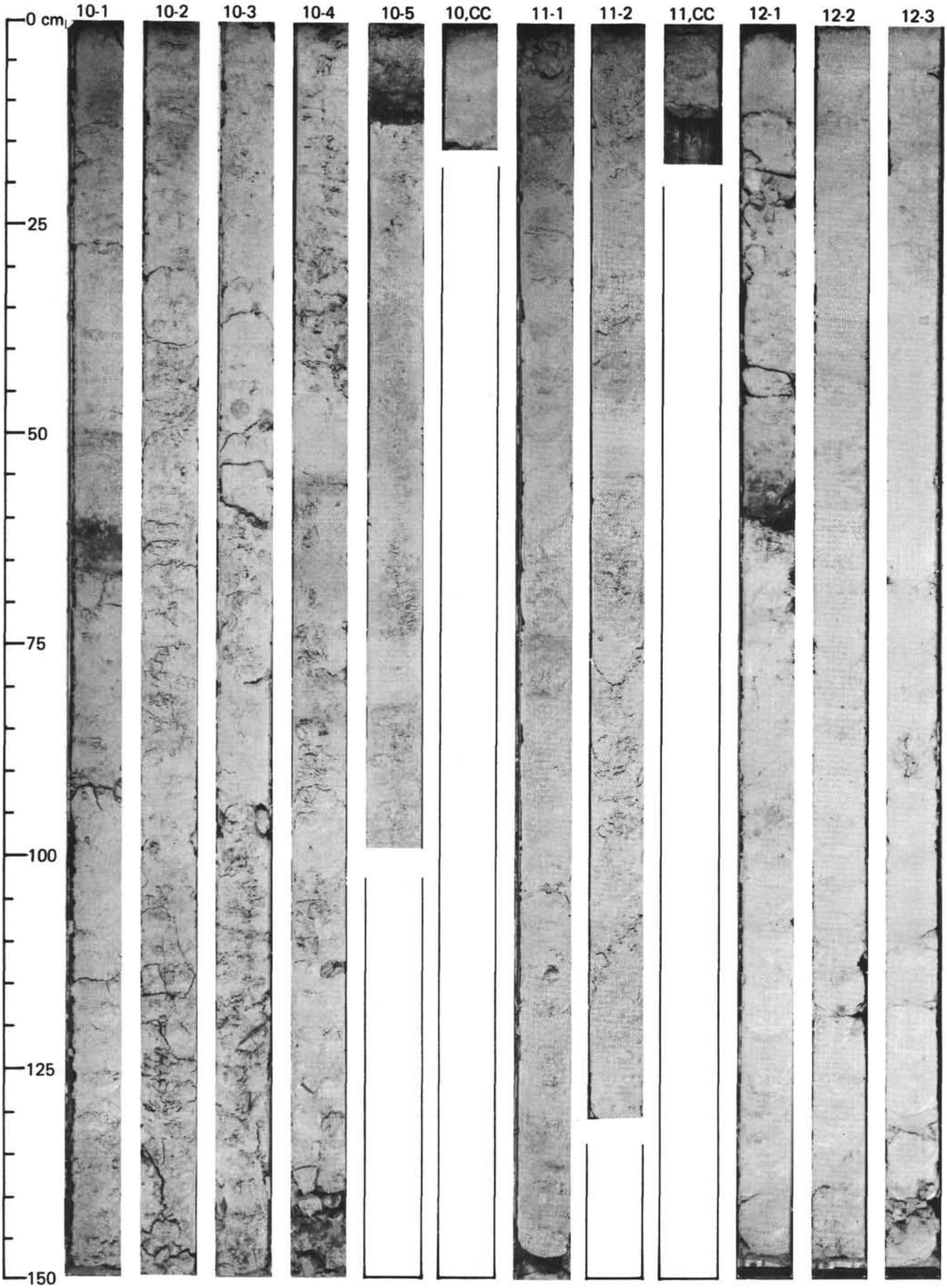
0 cm
25
50
75
100
125
150
10-1
10-2
10-3
10-4
10-5
10,CC
11-1
11-2
11,CC
12-1
12-2
12-3

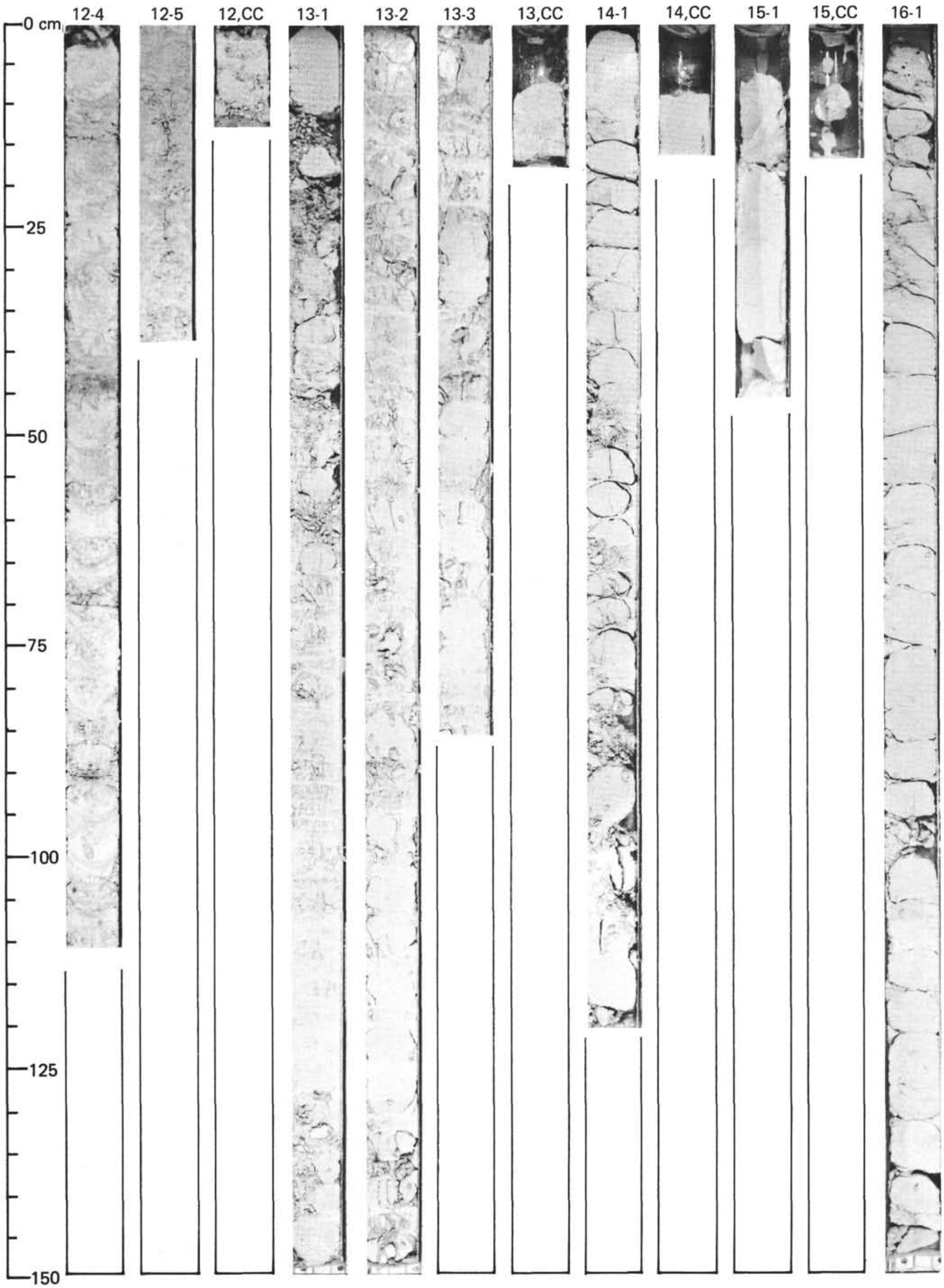
12-4
12-5
12,CC
13-1
13-2
13-3
13,CC
14-1
14,CC
15-1
15,CC
16-1
0 cm
25
50
75
100
125
150

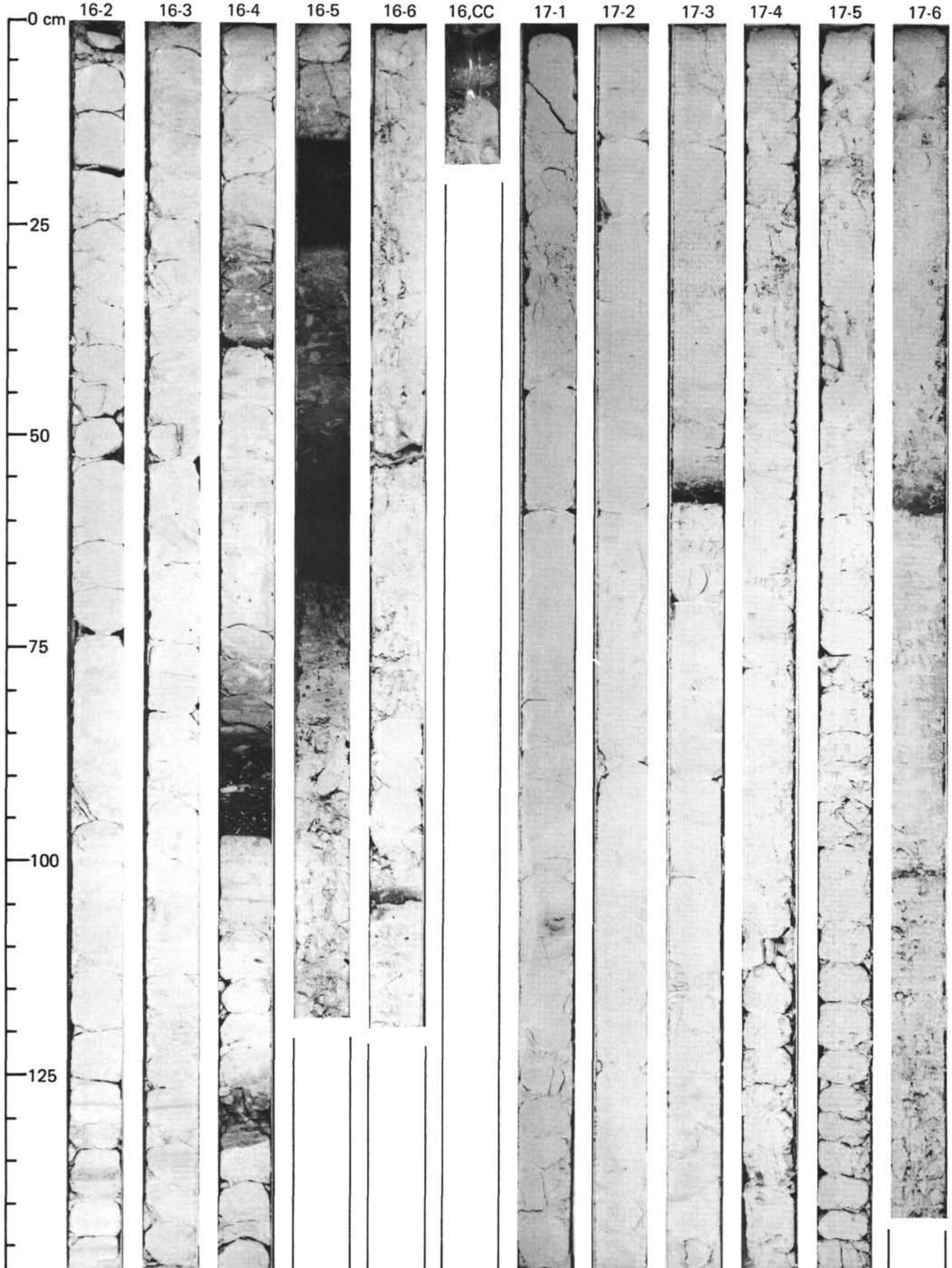
0 cm
25
50
75
100
125
150
16-2
16-3
16-4
16-5
16-6
16,CC
17-1
17-2
17-3
17-4
17-5
17-6

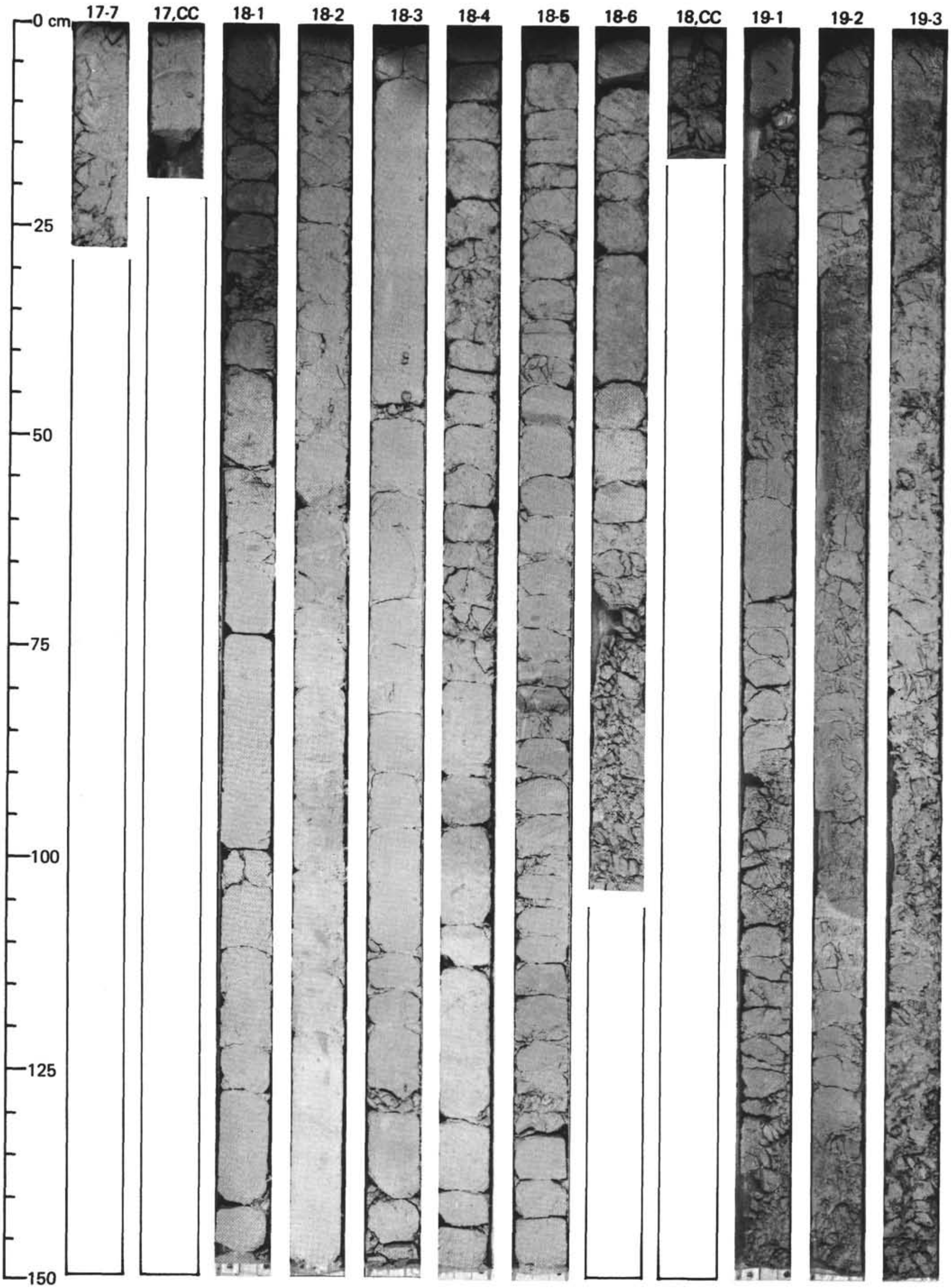
0 cm
25
50
75
100
125
150
17-7
17,CC
18-1
18-2
18-3
18-4
18-5
18-6
18,CC
19-1
19-2
19-3

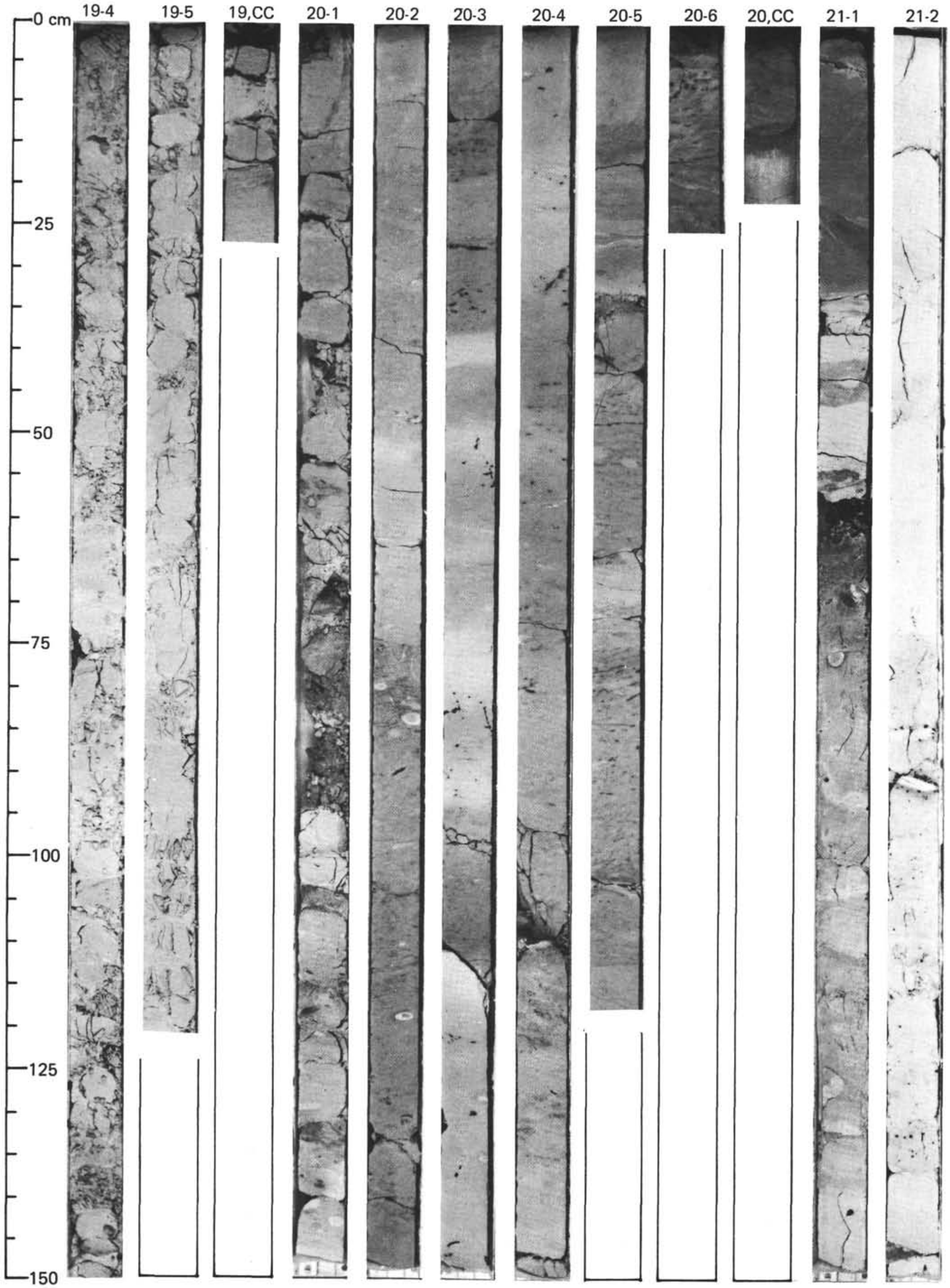
0 cm
25
50
75
100
125
150
19-4
19-5
19,CC
20-1
20-2
20-3
20-4
20-5
20-6
20,CC
21-1
21-2

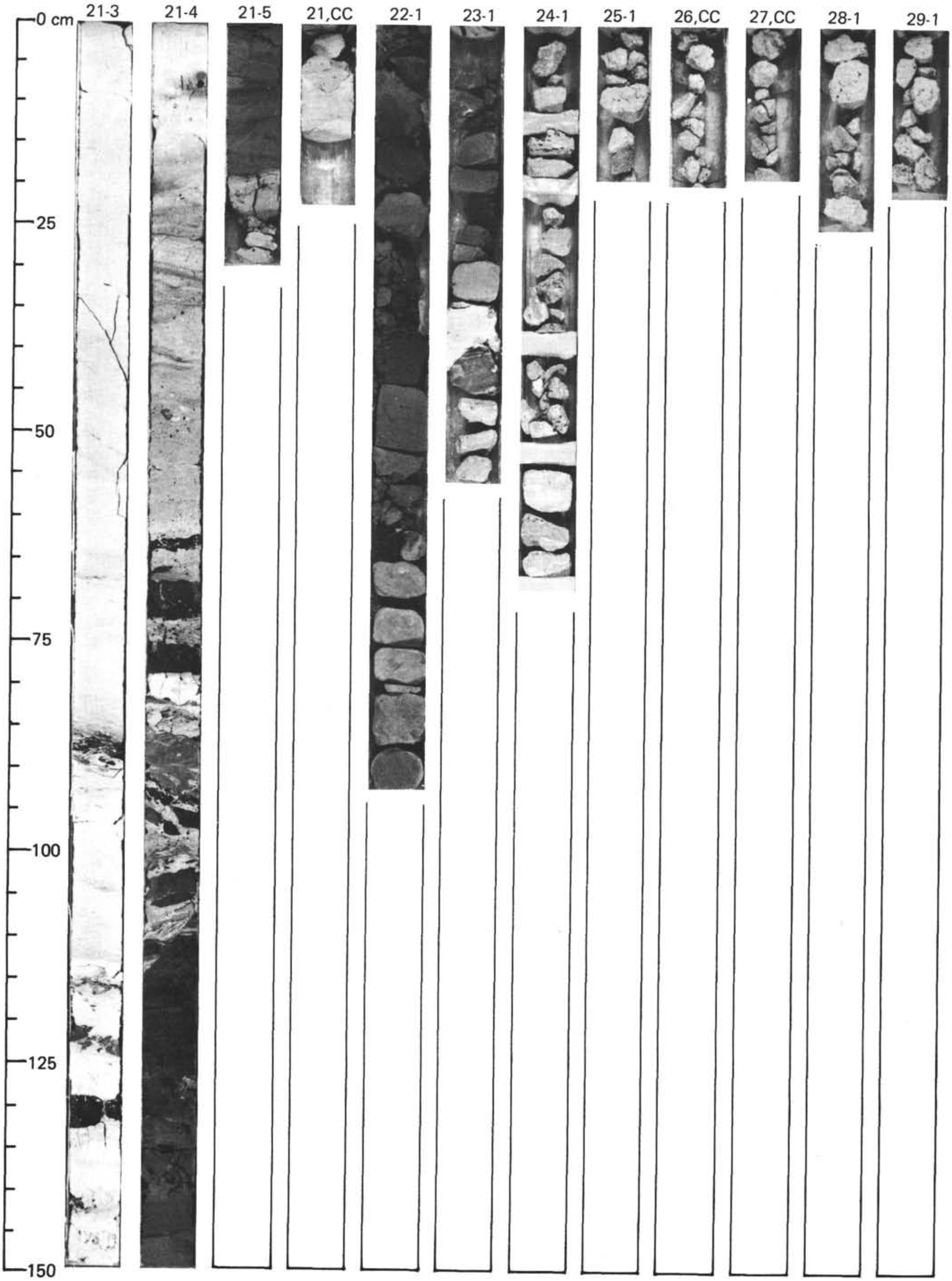
0 cm
25
50
75
100
125
150
21-3
21-4
21-5
21,CC
22-1
23-1
24-1
25-1
26,CC
27,CC
28-1
29-1

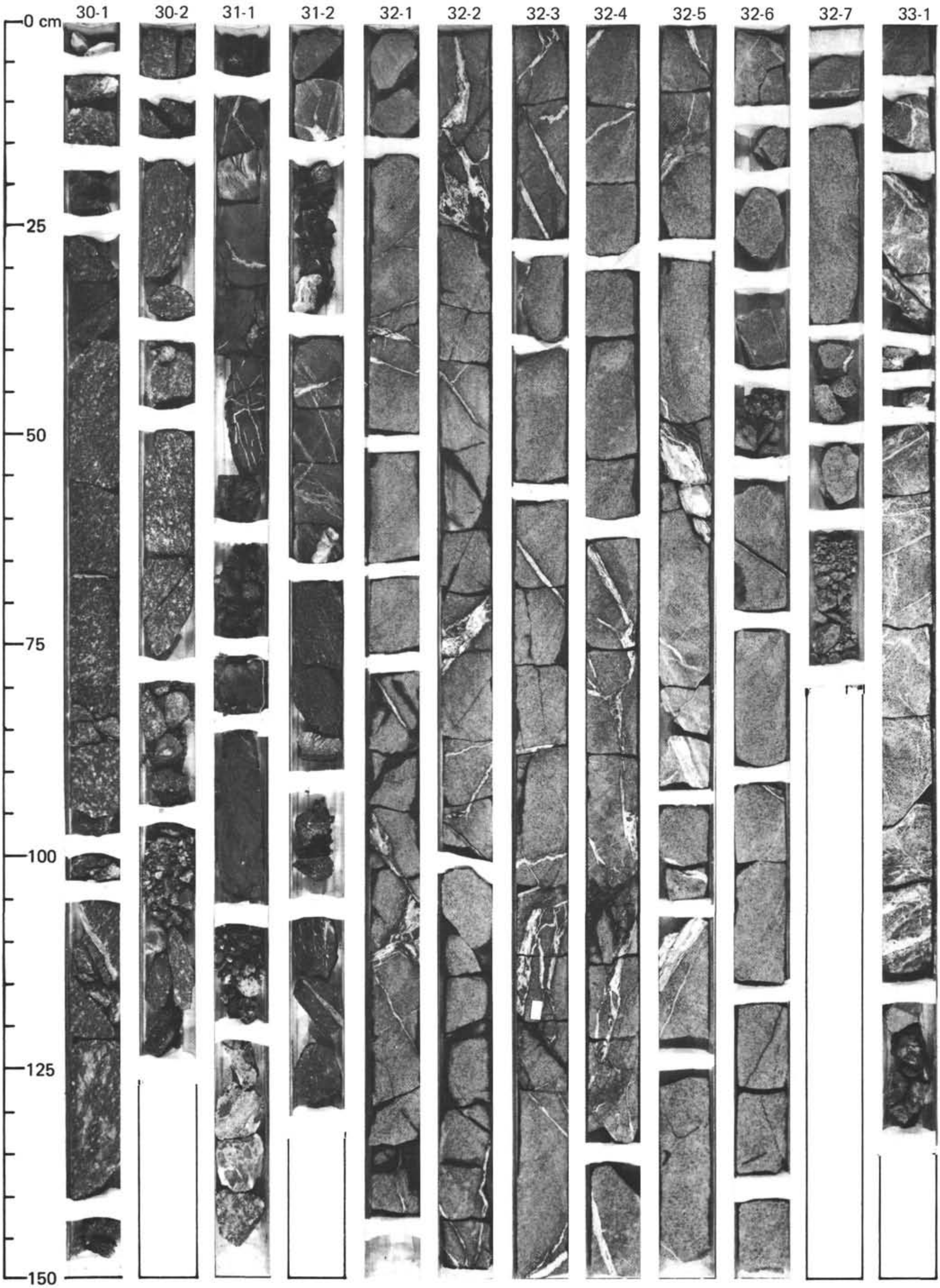

0 cm
25
50
75
100
125
150
30-1
30-2
31-1
31-2
32-1
32-2
32-3
32-4
32-5
32-6
32-7
33-1

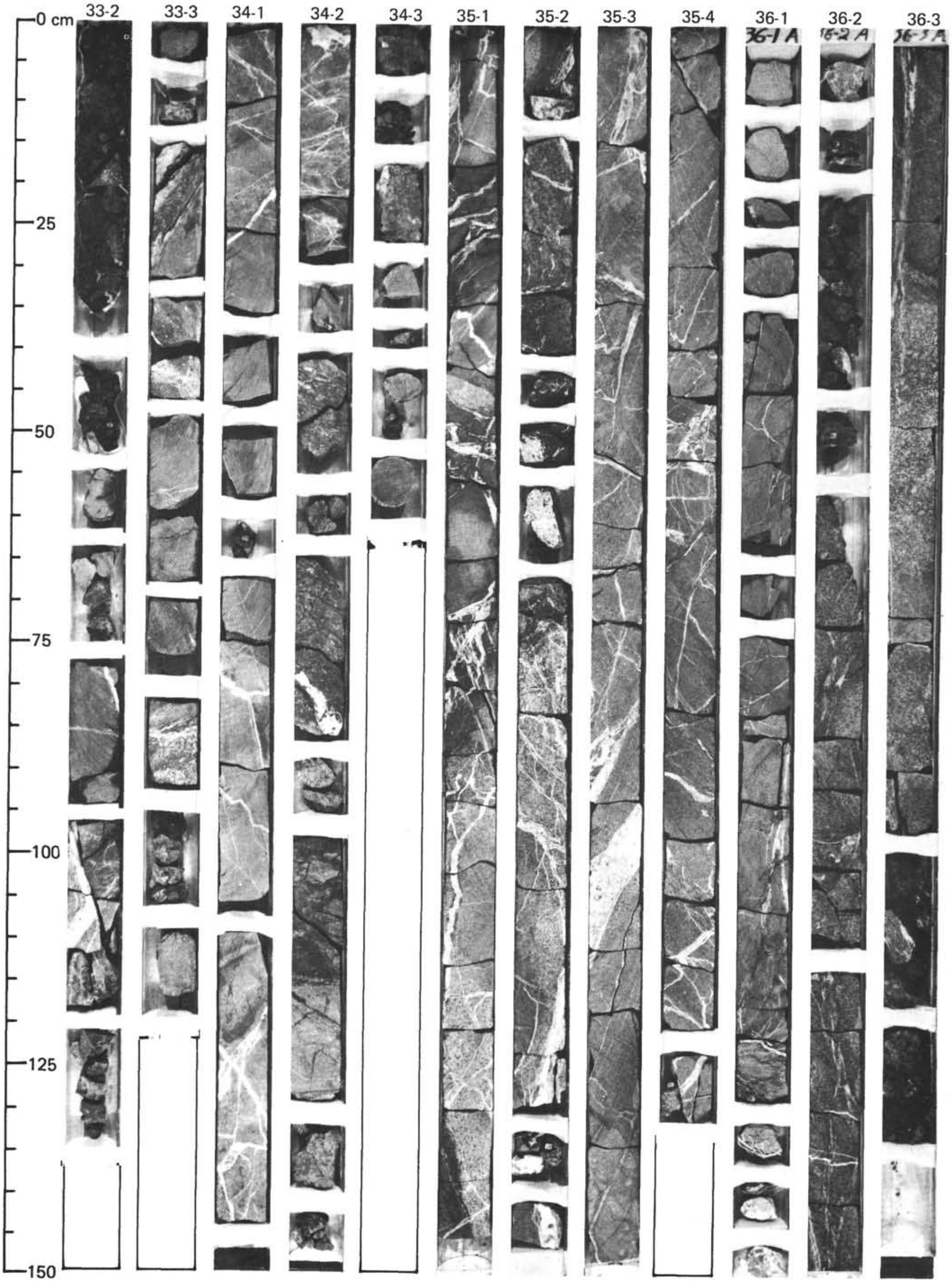
0 cm
25
50
75
100
125
150
33-2
33-3
34-1
34-2
34-3
35-1
35-2
35-3
35-4
36-1
36-2
36-3